Nitrogen Loadings in Stormwater and Snowmelt from Cold-region Urban Catchments in 1991 – 2018 and Prediction for Year 2050

by

Xiaoyu Zhang

A thesis submitted in partial fulfillment of the requirements for the degree of

Master of Science

in

Water Resources Engineering

Department of Civil and Environmental Engineering

University of Alberta

ABSTRACT

Urban stormwater and snowmelt runoff has become a primary source of pollution in receiving water bodies (e.g., rivers, lakes and oceans), causing eutrophication, harmful algae blooms and hypoxia and many other environmental issues. It is therefore imperative to study pollutant loadings from urban surface runoff, examine their spatiotemporal variabilities and predict future loadings to improve the stormwater/snowmelt management for federal, provincial and municipal governments. This thesis focused on nitrogen loadings, and was written in paper-based format that includes two parts: Part I "*Nitrogen Loadings in Stormwater and Snowmelt from a Major, Cold Region, North American City in the Past 30 years*"; and Part II "*Predicting Stormwater Nitrogen Loadings from an Urban Catchment in Cold-region in Year 2050*". Part I and Part II explored nitrogen loadings in the past and predicted loadings in the future, respectively.

Long-term monitoring on pollutant loadings in urban surface runoff is scarce in the literature. In Part I of the thesis, nitrogen loadings were examined in storm/snowmelt runoff from four urban catchments of a major North America city (Edmonton, Canada) located in cold-region in the past almost 30 years (1991 to 2018), with a focus on both spatial and temporal variabilities. The TN loading exhibited a pronounced inter-annual variability, with an increasing trend from 1991 to 2011 due to the increases of annual precipitation, and a decreasing trend afterwards as a result of discharging stormwater into creeks. The ratios of monthly loadings in wet season (April – October) to dry season (November – March) for TN, TON and NO_x-N were 2.26, 2.77 and 2.93, respectively, whereas the ratio was 1.17 for the NH_4-N loading. The maximum monthly fluctuation appeared in March/April and July due to

the high frequency of snowmelt and storm events, respectively. Event mean concentrations (EMCs) of TN in snowmelt was slightly higher than in storm runoffs from 2007 to 2018. We further used Mann-Kendall test, Pettitt test and Rescaled Range Analysis to detect the abrupt change time. The results showed that climatic condition, catchment characteristics and urban drainage infrastructure had substantial impacts to the loading variability. Moreover, we compared the EMCs and loadings with those reported worldwide.

Modeling and predicting stormwater nitrogen loadings in urban catchments of cold regions have been much less reported. In Part II of the thesis, a build-up and wash-off model was developed in MIKE Urban to assess the impacts of climate change and urban densification on stormwater nitrogen loadings (TN, TKN, NO_x-N and NH_4-N) of an urban catchment (the 30th Ave Catchment in Edmonton) in Canada. The model was calibrated and validated against the observed loadings and event mean concentrations (EMCs) in 2010 - 2016. Based on the model, important factors for the nitrogen loadings were found as rainfall intensity and duration and antecedent dry days. The model also showed that first flush effect was clear for storm events, with 32.1 - 59.8% of the nitrogen loadings transported by the first 30% of runoff volume. Based on projections of future precipitation and population, the model predicted that the loading of TN, TKN, NO_x-N and NH_4-N in 2050 will increase by 33.7%, 39.4%, 27.1%, and 31.1% for months from May to September, compared to those of 2010 - 2016.

Finally, general conclusions and future directions were provided at the end of this thesis based on the above two (Part I and II) studies.

PREFACE

The dissertation is original work by Xiaoyu Zhang. The descriptions of the study area and data sources presented are contributed by Ross Bulat in EPCOR Drainage Service. Their data were used for analyzing long-term variation of nitrogen loading in the past 28 years in Chapter 2 and for model calibration and validation in Chapter 3.

The MIKE Urban model in Chapter 3 was obtained from Mohamed Gaafar. The MIKE Urban model was originally from City of Edmonton and used to simulate nitrogen loading under the climate change effect and urban densification in the future.

All of the other parts of the thesis are my original work with the assistance of Dr. Wenming Zhang, including the introduction in Chapter 1, the literature reviews in Chapter 2 and 3, and the conclusions in Chapter 4. Chapter 2 and Chapter 3 include two papers expected to be published in 2022.

ACKNOWLEDGEMENTS

Undertaking this M.Sc has been a truly challenging time for me due to the covid situation and I would not have been possible to finish these works without the help and guidance that I received from many people.

I would like to first express my great appreciation to my supervisor Dr. Wenming (William) Zhang for all the support and encouragement he gave me. Without his guidance on my work, I would not have been achieving this M.Sc.

The first part of my work could not have been possible without the corporation of EPCOR drainage service. I am grateful to Ross Bulat for providing me the data. Furthermore, I would also like to say a very big thank you to Dr. Evan Davies and Mohamed Gaafar for sharing me the original MIKE Urban model, without their help I cannot finish my second part work.

Meanwhile, I would like to thank you to my parents for supporting me and believing in me. Finally, I thank every person who helped me, offered me advice and gave me encouragements.

Table of Contents

List of Tables

List of Figures

Chapter 1 Introduction

1.1 Background

Rivers, lakes and oceans are precious water resources that receive, carry and degrade pollutants from stormwater and wastewater (Sharma et al., 2020) and are hotspots of nutrient pollution (Zhang et al., 2015; Zhang et al., 2017). Urban stormwater and snowmelt runoff are an important non-point source that cause the nutrient pollution (Hu and Huang 2014; Chen et al., 2018), for instance, in the United States, it has been identified as the primary source (Tomasko et al., 2001; Jani et al., 2020). As one of the essential nutrients, nitrogen is important for aquatic ecosystem, but excessive inputs to receiving water bodies has become a serious problem, causing nitrogen pollution (Refgaard et al., 2014; Wang et al., 2016). Nitrogen species include total organic nitrogen (TON), ammonium-N (NH_4-N), nitrite-N (NO_2-N) and nitrate-N (NO_3-N), and nitrogen pollution have a direct impact on the water quality (Jani et al., 2020). For example, elevated ammonium and nitrate can lead to excessive growth of algae (algal bloom) and macrophytes, which may alter the composition of aquatic communities and substantially reduce dissolved oxygen concentrations when they die (Turner, 2002; Smith, 2003). Similarly, elevated ammonia inputs can increase the pH of the waterbody and result in direct toxicological impairment of aquatic biota (Camargo and Alonso, 2006).

For nitrogen loadings in stormflow and snowmelt runoff, climatic conditions (e.g., precipitation, temperature and humidity) (Gobel et al., 2006; Clark and Pitt, 2012) and catchment characteristics (e.g., stormwater infrastructure, land use and land cover) are important factors (Causse et al., 2015). Precipitation variables (e.g., rainfall/snowfall amount,

duration, intensity and antecedent dry periods) have significant relationships with nitrogen transported by surface runoff (Lewis and Grimm, 2007; Liu et al., 2011; Schiff et al., 2016). Catchments with different land use, road texture and traffic volume have different influences on accumulated nitrogen on urban surface (Chow et al., 2015).

In addition to climate change and catchment properties, urban densification also needs to take into account for stormwater/snowmelt nitrogen loadings in urban areas. Increases of population and impervious area are typical results of urban densification. In Canada, more than 27 million people (72% of the total population) lived in metropolitan area in 2020, and it is projected to reach 49 million people by 2050 under the medium-growth scenario (Dimmell, 2021; Statistical Canada, 2021). In the City of Edmonton, population will grow from 1 million people in 2020 to 1.50 – 1.71 million in 2050 (City of Edmonton Sustainable Development, 2018). During the urban densification process, raw lands are replaced by impervious areas, which alters urban hydrological cycle, affect the quantity and quality of surface runoff (Goonetilleke et al., 2005; Poelmeans, 2010) and increases stormwater and snowmelt nitrogen loadings (Zhang et al., 2015). Moreover, more impervious urban surfaces means that the accumulation of nitrogen due to atmospheric deposition, litter, and other sources can be more easily flushed by surface runoff into receiving water bodies (Bhaduri et al., 2000).

The variability of nitrogen loading in urban stormwater/snowmelt runoff mainly because of (1) multiple complex factors as mentioned above; (2) highly variability with precipitation (both rainfall & snow); (3) anthropogenic influence (stormwater management policies). These variability causes the challenges to quantify the loadings. Currently, numerous studies have worked on nitrogen loading in surface runoff (Alvarez-Cobelas et al., 2008; Yang et al., 2016),

but fewer researches focused on urban catchments, particularly in cold region urban catchments. Evaluating nitrogen loadings from snowmelt and projections of future nitrogen loading based on build-up and wash-off models are even less.

Numerous models have been used to study stormwater nitrogen loadings from urban catchments. Available models include: (1) GWLF and PLOAD, which estimate pollutant loadings from a catchment outlet into receiving water (Schneiderman et al., 2010; Gurung et al., 2013) and (2) HSPF, SWAT, STORM, Wallingford, SWMM, and DHI's MIKE Urban, which combine the capacities of simulating pollutant loadings in catchment (Zoppou, 2001; Borah et al., 2006).

SWMM and MIKE Urban are two typical stormwater quality models rely on pollutant build-up and wash-off processes. Nitrogen build-up process is the accumulation of nitrogen mass during the interval of storm/snow events, then stormwater or snowmelt runoff flows on surface and wash off sediments attached with nitrogen in its path, and then flows into receiving waters, causing a deterioration of water quality (Carey et al., 2013; Long et al., 2014). Thus, simulations on nitrogen loading by build-up and wash-off models in urban stormwater are important.

1.2 Knowledge Gaps

Based on a thorough literature review on urban stormwater/snowmelt nitrogen loadings, the following knowledge gaps are identified as follows:

- Long-term monitoring and evaluation of pollutant loadings (including nitrogen loadings) in stormwater/snowmelt runoff have been rarely reported. Not to mention their temporal

(e.g., seasonal, annual, multi-years and decades) and spatial (e.g., from different land uses) variabilities of the loading.

- In cold regions, there is a substantial lack of studies on pollutant loadings (including nitrogen loadings) in snowmelt runoff, where the loadings are further complicated by freeze-thaw cycles, snow and the use of deicing salts and/or sands. Comparison of pollutant loadings in stormwater and snowmelt are even more scarce.
- Comparison of nitrogen loadings in urban surface runoff in different cities worldwide has not been reported.
- Modeling of stormwater nitrogen loadings is limited for an urban catchment. In particular, predicting the loadings for the future using build-up and wash-off models in the context of climate change and urban densification.

1.3 Research Goal and Objectives

The overall goal of this research is to explore the four knowledge gaps stated above. Specifically, this research is to **(1)** examine nitrogen loadings in stormwater and snowmelt and their spatiotemporal variabilities in the past 28 years from four urban catchments in major North American city (Edmonton, Alberta, Canada) located in cold region; and **(2)** predict nitrogen loadings in stormwater in one of the four catchments in Year 2050 in the context of climate change and urban densification.

In the first part of the thesis (Chapter 2), the detailed objectives are:

- To evaluate the dynamics of nitrogen loadings (TN, TON, NO_x-N and NH_4-N) in 1991-2018 (28 years) at four major stormwater outfalls that collect surface runoff from four

urban catchments in Edmonton, Canada.

- To examine the temporal (annually, monthly and seasonally) and spatial (from different catchments) variations of nitrogen loadings and explore the possible reasons. In particular, Mann-Kendall, Pettitt and Rescaled Range methods will be used to elucidate the trend of nitrogen loadings and detect the abrupt change time.
- To assess the nitrogen event-mean-concentrations (EMCs) and loadings in snowmelt runoff, and compare them with those in stormwater runoff in the four catchments, as well as with those in other catchments reported in the literature.
- To compare the TN and NO_3-N EMCs and annual loadings per unit area from this study with those reported in other catchments worldwide.

In the second part of the thesis (Chapter 3), the detailed objectives are:

- To develop build-up and wash-off models for stormwater runoff from an urban catchment (the 30^{th} Ave catchment) in Edmonton. The models will be calibrated and validated against the data in 2010-2016 in terms of EMCs and loadings of nitrogen species (TKN, NO_x-N and NH_4-N).
- To investigate rainfall characteristics (rainfall intensity, peak rainfall intensity, rainfall duration) on nitrogen loadings. To assess the impacts of antecedent dry days and population on the accumulation of build-up mass of total suspended solids (TSS).
- To predict the nitrogen loadings in the study catchment in the year of 2050 by using the projection of climate (rainfall intensity, rainfall precipitation) and urban densification (population, TSS loading), and compare the results of 2010 to 2016.

1.4 Thesis Layout

The thesis is a paper-based thesis, which mainly includes two parts (papers): **Part I** "Nitrogen Loadings in Stormwater and Snowmelt from a Major North American City in Cold Region in the Past 30 years" (Chapter 2 of the thesis); and **Part II** "Predicting Stormwater Nitrogen Loadings from an Urban Catchment in Cold-region in Year 2050" (Chapter 3).

The thesis is organized into four chapters. In addition to the main body of the thesis (Chapters 2 and 3 mentioned above), Chapter 1 gives a brief background, knowledge gaps and objectives of the research; and Chapter 4 summarizes the general conclusions from this research and provides suggestions on future research directions.

Chapter 2 Nitrogen Loadings in Stormwater and Snowmelt from a Major North American City in Cold Region in the Past 30 years

2.1 Introduction

Water bodies such as rivers, lakes and oceans receive stormwater and wastewater (Sharma et al., 2020) and are hotspots of pollution (Zhang et al., 2015; Zhang et al., 2017). With rapid urbanization, more than 60% of the global population will live in urban area by 2030 (FAO, 2018), making urban runoff an even more important pollution source (Carpenter et al., 2011; Balter, 2013). For nitrogen that is the focus of this study, sources in urban areas include atmospheric deposition, anthropogenic sources (e.g., vehicle exhausted, fertilizers, pet waste), and natural sources (e.g., tree canopy, leaf litter, grass clippings) (Divers et al., 2014; Yang and Lusk, 2018). During storm (or snowmelt) events, nitrogen will be flushed to storm sewers and eventually to downstream receiving water bodies, affecting the water quality. Nitrogen is an essential nutrient for aquatic ecosystem (Wang et al., 2019); however, persistence of high concentration is toxic to aquatic life (Camargo and Alonso, 2006) and could result in long-term harms to aquatic ecosystem and human (Refgaard et al., 2014; Wang et al., 2016). Consequences include eutrophication (Howarth et al., 2006; Smith et al., 2006), harmful algae blooms (Wang, 2006; Li et al., 2014), hypoxia (Tian et al., 2020) and change of pH in water bodies (Camargo and Alonso, 2006). To date, only a few studies have investigated nitrogen loadings from stormwater and snowmelt from an urban catchment.

Climate change (e.g., changes in precipitation and temperature) combined with urban densification (e.g., city expansion, land use change) will influence urban stormwater runoff

and thus the nitrogen loadings to receiving water. Rainfall variables such as rainfall depth (Liu et al., 2011a), duration (Schiff et al., 2016), intensity and antecedent dry periods (Lewis and Grimm, 2007) have strong correlations with nitrogen transported by stormwater runoff. Rapid population growth with the increase of impervious urban areas, typical phenomena of urbanization, increase urban stormwater nitrogen loading (Van Drecht et al., 2009; Zhang et al., 2015).

Total organic nitrogen (TON), ammonium-N (NH_4-N), nitrate-N (NO_3-N) and nitrite-N (NO_2-N) are nitrogen-based nutrients in water (Jani et al., 2020). In urban areas, TON is mainly from human and pet wastes (Wall, 2013), NH_4-N is mainly from industrial wastes and animal/human wastes discharge (Wall, 2013), and NO_3-N is mainly from fertilizers (Groffman et al., 2004; Mueller et al., 2016; Yi et al., 2017) as well as the transform from other nitrogen forms. Bratt et al. (2017) estimated that 50% of annual nitrogen export from surface runoff was contributed by leaf litter during winter snowmelt events in an urban residential area in St. Paul, Minnesota, USA. Recent studies have shown that organic nitrogen can be a large proportion of nitrogen in urban stormwater (Janke et al., 2017). The US Geological Survey reported that a large portion of TN and NO_3-N were contributed by lawns (Waschbusch et al., 1999; Hobbie et al., 2017).

A few studies on nitrogen loadings from urban runoff have been reported (Alvarez-Cobelas et al., 2008; Yang et al., 2016), but fewer have considered the loadings of different forms of nitrogen, the loadings from stormwater and snowmelt, as well as their annual, monthly and seasonal variations. In addition, existing studies seldom conducted long-term monitoring, and examined the spatio-temporal variabilities and their mechanisms. McLeod et al. (2006) found that total Kjeldahl nitrogen (TKN) loading in urban stormwater runoff was larger than that from

wastewater treatment plant in Saskatoon, SK, Canada. Janke et al. (2014) found that the contributions of nitrogen loading of baseflow was similar to stormflow in St. Paul, MN, USA. Jani et al. (2020) reported that dissolved organic nitrogen (DON) was the dominant nitrogen species in stormwater runoff (47%) followed by particulate organic nitrogen (PON, 22%), nitrite and nitrate nitrogen (NO_x-N, 17%), and NH_4-N (14%) in Bradenton, Florida, USA. Studies on nitrogen in snowmelt were mostly in cold regions. Valtanen et al. (2014) evaluated the TN loading in three urban catchments in Lahti, Finland, and pointed out that the TN loading generated from cold seasons accounted for 60-90% of annual total loading. Galfi et al. (2016) reported that the TN loading was higher in snowmelt, although the flow rate was about three times smaller than those during storms in Ostursund, Sweden. Chen et al. (2018) demonstrated that loadings of NO_3-N and NH_4-N were higher in snowmelt than stormwater because surface snow more easily adsorbs nitrogen from air.

Quantifying urban stormwater pollutant loadings remains challenging due to high uncertainties and dynamics of storms, limited understanding of pollutant build-up and wash-off processes on urban surfaces, and lack of field monitoring data (Littlewood and Marsh, 2005; Salles et al., 2008; Cha et al., 2010; Ullrich and Volk, 2010). As a result, there is a lack of long-term evaluation of nitrogen loadings as well as their temporal (within a rainfall event, seasonal, annual, multi-years and decades) and spatial (e.g., from different land uses) variabilities. Especially in cold regions (Bratt et al., 2017), these variabilities are further complicated by freeze-thaw cycles, snowfalls and the use of deicing salts and/or sands, all of which have been much less studied. Moreover, climate variables (e.g., rainfall frequency and intensity) and anthropogenic conditions (e.g., stormwater management) are seldom evaluated on their

impacts to the loadings. These issues are even worsening in the contexts of climate change and urbanization.

In this study, we collected the monitoring data of nitrogen loadings (TON, NH_4-N and NO_x-N) at four major storm outfalls from a major North American City located in cold region, for a period of 28 years (1991-2018). Our study aims at evaluating (1) the loading dynamics under spatial and temporal scales; (2) the loading contributions in dry and wet seasons, and from snowmelt and stormflow; (3) the trend based on Mann-Kendall, Pettitt and Rescaled Range methods. This study is useful in understanding the long-term variation of nitrogen loadings from urban stormwater (and snowmelt) in cold regions.

2.2 Methods and materials

2.2.1 Study area

The study area is in the City of Edmonton, Alberta, Canada (53°27′-53°24′N, 113°21′-113°36′ W; Figure 2.1), which is a major Canadian city with one million population (1/40 of the Canada's total population) and located in cold region (Plant Hardiness Zone: 3b) with an annual mean temperature of 2.8°C. The annual mean precipitation is 456 mm, comprised of snow in November to March and rainfall in April to October. The study area has four urban catchments (the 30th Avenue, Groat road, Quesnell and Kennedale), where surface runoff is collected by storm sewers (separate sewer systems) and discharged via four major storm outfalls (Figure 2.1b) into the North Saskatchewan River that flows through the city. The four catchments account for about 30% of the city's population, and generates about 60% of the city's total storm sewer discharge. The four catchments have different land uses, population and

imperviousness ratios (Table 2.1). Residential area has a large fraction of all the four catchments with the range from 44.5% to 72.7%. The range of industrial area is 3.2 % to 22.6%, with the largest fraction appears in Quesnell. The Groat Road catchment has the largest imperviousness with the value of 85%, due to a relative higher fraction of commercial area (38.7%). The imperviousness of other three catchments is around 60%. Population in the four catchments has a range of 23.9 thousand to 136.2 thousand, with maximum and minimum in Kennedale and Groat Road, respectively.

Table 2.1 Characteristics of the four study catchments.

Catchment	Area (ha)	Residential (%)	Commercial (%)	Industrial (%)	Park/Greenland (%)	Imperviousness (%)	Population (Year 2019)
30th Ave	6,051	72.7%	8.2%	9.9%	9.1%	65	163,216
Groat Road	1,589	44.5%	38.7%	3.2%	14.6%	85	23,932
Quesnell	7,134	57.1%	11.3%	22.6%	3.8%	57	37,226
Kennedale	7,881	68.5%	5.7%	16.9%	8.9%	51	136,232

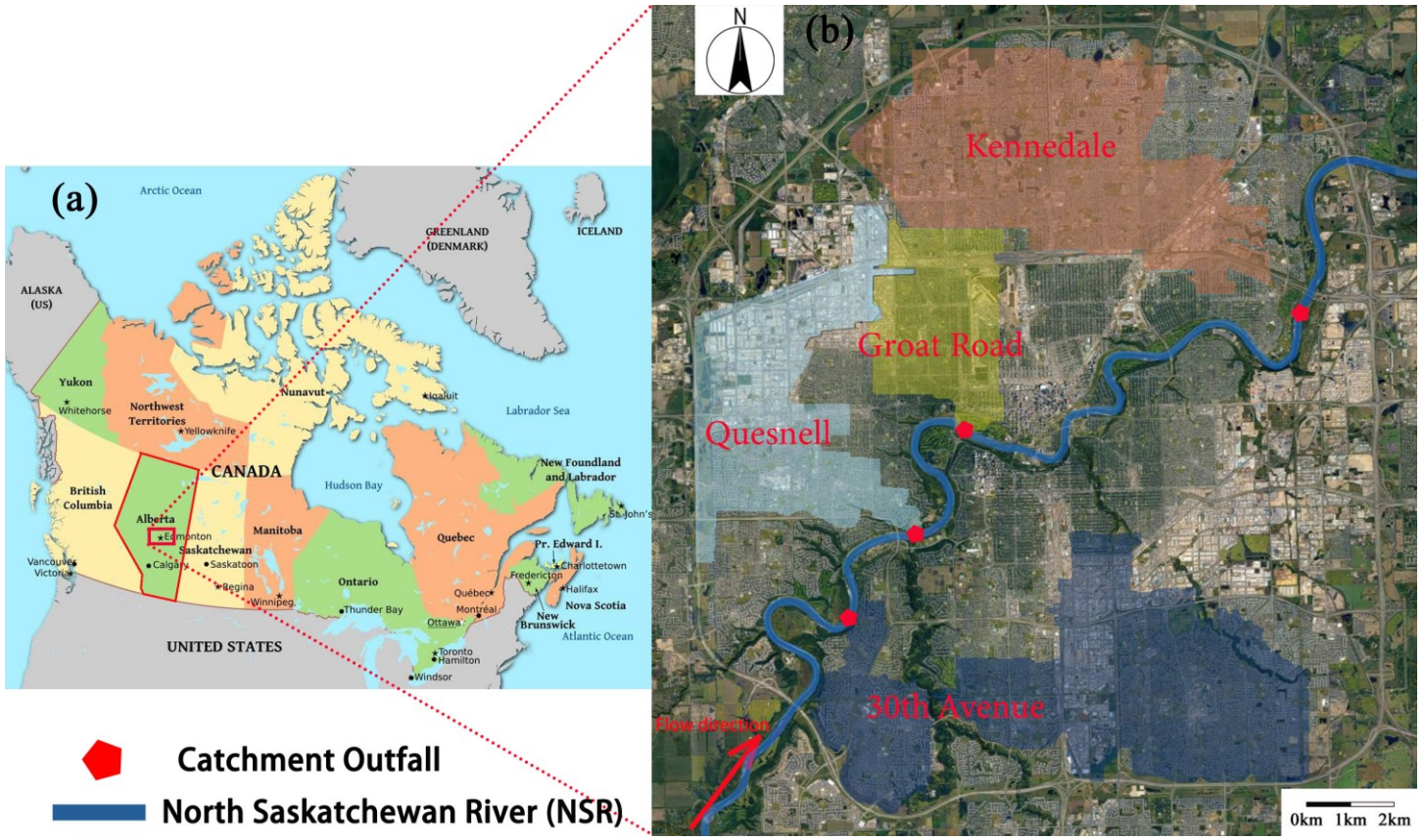

Figure 2.1 (a) Location of the study area; and **(b)** the four urban stormwater catchments - boundaries and outfalls (red dots)

2.2.2 Monitoring data

The raw data were collected from the City of Edmonton and EPCOR Drainage Services (Labatiuk et al., 2000 – 2005; Bulat et al., 2006 – 2018), who conducted field monitoring from 1991 to 2018 at three outfalls (30th Avenue, Quesnell and Groat road), and from 2004 to 2018 at the Kennedale outfall. The discharges at the outfalls were measured using continuous monitoring equipment. Water quality samples for the base flows at the outfalls were collected as grab samples once every two weeks. Storm or snowmelt water quality samples were collected using auto-samplers (American Sigma Model 1600 and Campbell Scientific CR10, USA) with a 30-minute interval. Samples were collected and measured for event mean concentrations (EMCs) of TKN, NH_4-N, and NO_x-N. In this study, we also calculated the concentration and loading of TON by subtracting NH_4-N from TKN (David et al., 2012) to better compare the contribution of each nitrogen species to TN loading.

2.2.3 Nitrogen loadings

Nitrogen loadings from the storm outfalls were divided into stormflow loading and snowmelt loading in this study. Baseflow loading was included in the loading from storm and snowmelt, which meant our monitored stormflow and snowmelt loadings represent the loading due to storm and snowmelt events and the baseflow loading at the corresponding time of storm/snowmelt events. The nitrogen loadings with various temporal scales (daily, monthly, seasonal and annual) were also calculated in this study to examine their temporal variabilities.

2.2.4 Trend analysis

2.2.4.1 Mann-Kendall and Pettitt tests

Mann-Kendall (M-K) (Mann, 1945; Kendall, 1975) test and the Pettitt test (Pettitt, 1979) were used in this study to examine the time series of monthly nitrogen loadings (TN, TON, NH_4-N and NO_x-N) at the four storm outfalls. The M-K trend analysis and Pettitt test have been used in hydrology, meteorology and sedimentology to identify significant trend and discern change points, and recommended by the World Meteorological Organization (Zhang et al., 2015; Shi et al., 2017).

The advantages of non-parametric M-K test are: no assumption is needed on the probability distribution of data samples, the result will not be affected by a few outliers (Zhou et al., 2020), and the calculation is relatively simple (Fu et al., 2018). For a given time series x_n, which has n random samples, a rank-based procedure is constructed:

$$S_k = \sum_{i=1}^{k} r_i \ \ (k = 2, 3, \dots, n) \tag{2-1}$$

$$r_i = \begin{cases} +1 & if \ \ x_i > x_j \\ 0 & if \ \ x_i \ll x_j \end{cases} \tag{2-2}$$

$$(j = 1, 2, \dots, i)$$

S_k is the sum of the number of values when the value at moment i is greater than the value at moment j. Under the hypothesis that the time series is random, the test statistic is defined as:

$$UF_k = \frac{[S_k - E(S)_k]}{\sqrt{Var(S_k)}} \ \ (k = 1, 2, \dots, n) \tag{2-3}$$

In Eq. (2-3), $UF_1 = 0$, $E(S_k)$ and $\mathrm{Var}(S_k)$ are the average and variance of S_k. When the $x_1, x_2, \ldots, x_n$ are independent of each other and have the same continuous distribution, $E(S_k)$ and $\mathrm{Var}(S_k)$ could be calculated as follows (Yin et al., 2015; Duan et al., 2016):

$$E(S_k) = \frac{n(n+1)}{4} \tag{2-4}$$

$$Var(S_k) = \frac{n(n-1)(2n+5)}{72} \tag{2-5}$$

In this method, UF_k is the standard normal distribution which was calculated from the forward sequence. UB_k repeated the above process in backward sequence of the time series data. The significant level was taken as 0.05, and the critical level of $U_{0.05} = \pm 1.96$. $UF_k > 0$ represents an increasing trend, while $UF_k < 0$ means a decreasing trend. When the value of UF_k exceeded the critical line, it indicated a significant upward or downward trend. If there was only one obvious intersection point between UF_k and UB_k within the significance lines, this intersection was the abrupt change point (Liu et al., 2020). However, if the intersection was beyond the reliable lines or there were several intersections within the reliable lines, the abrupt change time cannot be determined, and the Pettitt test needs to be applied.

The Pettitt test is also a non-parametric method to identify a change point of a time series. It can be briefly described as follows: Given a sequence of the dataset $x_1, x_2, \ldots, x_T$. Once the abrupt change point is detected, then the time series dataset is divided into two intervals at time t, i.e., $(x_1, x_2, \ldots, x_t)$, and $(x_{t+1}, x_{t+2}, \ldots, x_T)$. The most significant change point is where the Pettitt statistic (K_T) value is max (Zhang et al., 2009). The non-parametric statistic $U_{t,T}$ is used for identification of change point, which is given by:

$$U_{t,T} = \sum_{i=1}^{t} \sum_{j=i+1}^{T} sgn(x_i - x_j) \tag{2-6}$$

$$K_T = max\left|U_{t,T}\right| \tag{2-7}$$

where *sgn* = 1 if $x_i - x_j > 0$, -1 if $x_i - x_j < 0$, and 0 if $x_i and\ x_j$ are identical.

The approximate significance probability (p) for a change-point is defined as:

$$p = 1 - exp\left(\frac{-6K_T^2}{T^3+T^2}\right) \tag{2-8}$$

Three percentile levels (99, 95 and 50 percentiles) were selected to evaluate the significance of the abrupt change point. Here, the probability should exceed these levels for change point to be statistically significant.

2.2.4.2 Rescaled range analysis

Rescaled range analysis (R/S) is used to analyze the fractal features and long-term memory process of a given time series of data (Mandelbrot and Wallis, 1969; Zhang et al., 2012), which has been widely used in hydrometeorology (Tatli, 2015). Main steps are as follows: (1) divide the time series $\{X_i\}$ into sub-intervals of length *n*, and determine the mean value of each sub-interval; (2) calculate the cumulative deviation of each sub-interval and determine the range *R* of each sub-interval; (3) draw a graph of the range *R* and standard deviation *S* of each sub-interval, carry out a linear regression analysis of them, and calculate the slope *H* (Hurst index) of the regression equation (Hurst, 1951).

H ($0 \leq H < 1$) is an effective statistic of R/S analysis (Zhou et al., 2020), which can help predict the persistency of the trend in the four outfalls. When $H = 0.5$, it indicates that the time series is a random sequence with independent distribution, i.e., the current change has no impact to the future. When $0 \leq H < 0.5$, it means that the process has anti-sustainability, i.e., the future change will be contrary to the general trend in the past. The closer *H* is to 0, the stronger the

anti-sustainability will be. When $0.5 < H \leq 1$, the time series has a long-term dependence, i.e., the future has the same changing trend as the past. The closer H is to 1, the stronger the persistency of the time-series (Tong et al., 2018).

2.3 Results

2.3.1 Spatiotemporal characteristics of TN loadings to the river

2.3.1.1 Annual scale analysis

The annual TN loadings from the four storm outfalls were rather dynamic for the monitoring period of 1991 - 2018 (2004 - 2018 for the Kennedale outfall) (Figure 2.2). The maximum loading occurred in 2011 at three outfalls (Quesnell, Groat road and Kennedale, with the values of 84.5 tons, 17.8 tons and 46.9 tons, respectively), and in 2011 and 2012 at the 30th Ave outfall (94.5 tons). In 2011, June and July had the largest monthly precipitation over the 28 years (Bulat et al, 2011), the total accumulated snow on the ground was also the highest (52 cm), and the annual precipitation (466 mm) was the third largest. These factors resulted the largest annual discharge (45.8 Mm^3) over the 28 years and contributed to the maximum TN loadings in 2011, indicating the importance of climatic conditions on the loading. Moreover, in 2011 in Quesnell catchment, a breach of the sanitary line into storm sewer was found, which also possibly increased the loading at that outfall. The minimum annual TN loading occurred in 1992 at three outfalls (30th Ave, Quesnell and Groat road, with 13.4 tons, 2.4 tons and 9.5 tons, respectively) due to the minimum rainfall precipitation during wet season (180 mm), and in 2009 at the Kennedale outfall (14.4 tons).

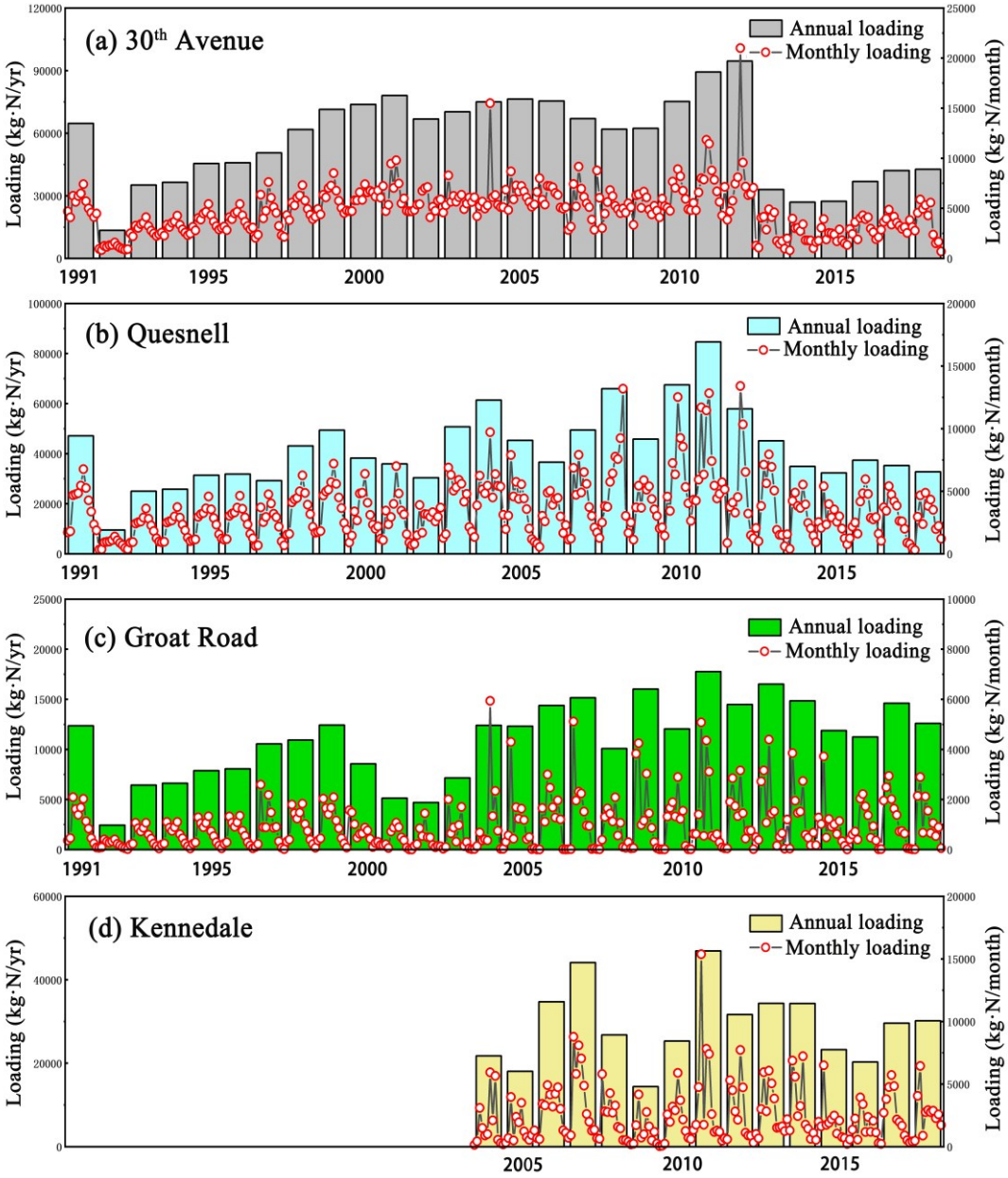

Figure 2.2 Annual and monthly total nitrogen (TN) loadings at the four storm outfalls: **(a)** the 30th avenue outfall; **(b)** the Quesnell outfall; **(c)** the Groat Road outfall; **(d)** the Kennedale outfall.

The changing trends of annual TN loading were similar for the four outfalls: an increasing trend from 1992 to 2011, then a decreasing trend from 2011 to 2015, and finally a small rise from 2015 to 2018. After 2011, the four outfalls had a lower loading in around 2014/15, 2015, 2016 and 2016, respectively. The lower values were attributed to the fact that the city began to discharge stormwater into creeks (i.e., Wedgewood, Mill, Whitemud, and Horsehills Creeks) within the city (Bulat et al, 2013). This change led a decrease in the discharges (e.g., the discharge in the 30th Ave outfall dropped from 9.4 Mm^3 to 7.4 Mm^3) and thus the loadings. From 2016 to 2018, there were cross-connections between sanitary and storm sewer lines in 30th Ave outfall, which caused a small-scale rise of the loadings. These results suggest that stormwater management policies, practices and infrastructure also play important roles in TN loading, in addition to the climatic condition.

The annual TN loadings were tried to correlate with various influencing factors. From 1980 to 2005, the population increasing rate was 1.1%, whereas it was 2.5% after 2005. We used Pearson coefficient of determination (R^2) to describe the correlation between annual TN loading to the catchment population for each of the four outfalls and found the relationships were weak, with $R^2 < 0.3$ (Figure A2.1). In general, the annual TN loading had a weak correlation with annual precipitation, with $R^2 \leq 0.2$; and also weakly correlated with annual mean temperature, with $R^2 < 0.1$. The weak correlations are because the TN loading is simultaneously affected by multiple and complex factors (climate such as temperature, rainfall and snow characteristics, and antecedent dry days, population, sewer systems, stormwater management, land covers, land uses, etc.). Correlation to a single factor is expected to be low.

2.3.1.2 Monthly scale analysis

Based on the 336-month data (180-month for Kennedale) as shown in Figure 2.2, the monthly statistics (maximum, minimum, mean and median) of TN loadings at the four outfalls are shown in Figure 2.3. Generally, the TN loadings had pronounced monthly variation. July or March was detected to have the statistically monthly loading peak, which corresponded to the highest monthly runoff volume of stormflow or snowmelt. For two outfalls (the 30th Ave and Quesnell), the sole peak was in July, with 6.8 ± 3.9 tons (monthly average ± standard deviation) and 6.1 ± 2.9 tons, respectively. This indicates storm events are the main drive for the maximum monthly loading in the two catchments. For the other two outfalls (Groat Road and Kennedale), there were two peaks (July and March) and they were rather close, e.g., at the Groat Road outfall, the peaks were 1.8 ± 1.1 tons (July) and 1.9 ± 1.2 tons (March). This indicates both snowmelt and storm flow were the major drives of the maximum monthly TN loading in those two catchments.

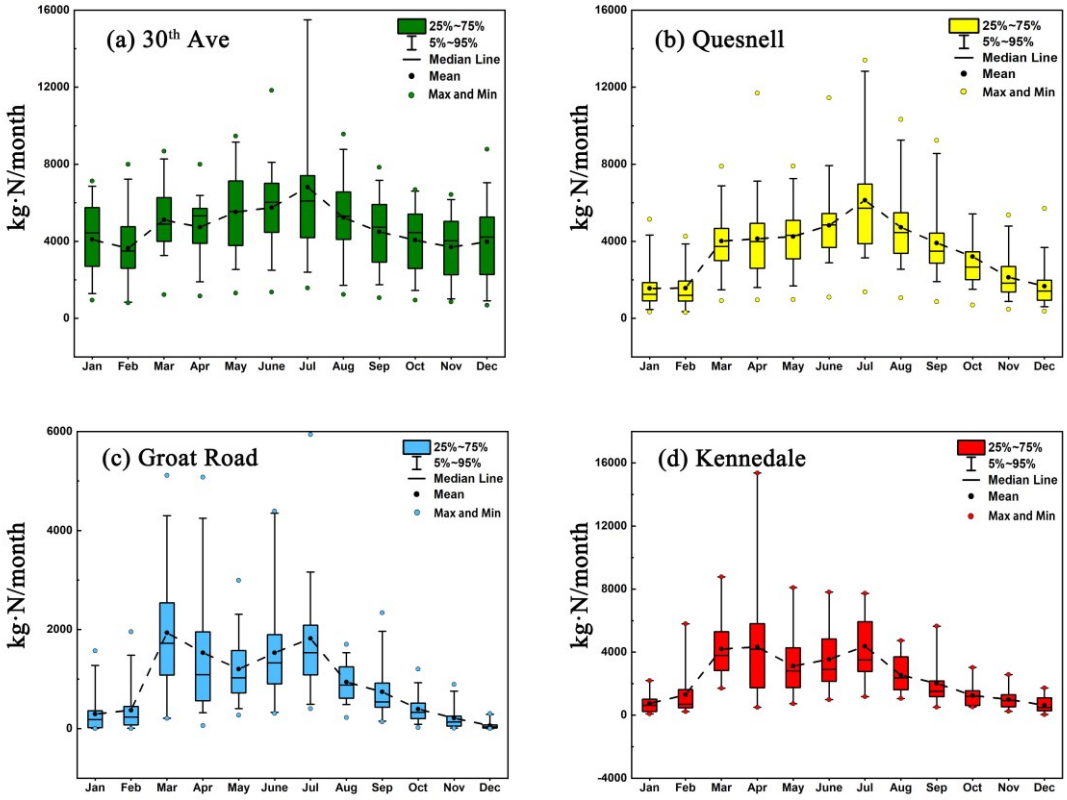

Figure 2.3 Monthly statistics of TN loadings at the four storm outfalls from 1991- 2018 (2004 - 2018 for Kennedale), including the maximum, minimum, median and mean, as well as the 5%-95% percentiles. **(a)** the 30th avenue outfall; **(b)** the Quesnell outfall; **(c)** the Groat Road outfall; **(d)** the Kennedale outfall.

The statistically lowest monthly TN loadings were all during the winter (December - February) at the four outfalls. Two outfalls (Groat Road and Kennedale) had the lowest monthly loading in December, with 0.1 tons and 0.6 tons, respectively. The other two outfalls (the 30th Ave and Quesnell) had its lowest monthly values in February and January, with 3.6 tons and 1.6 tons, respectively. The results suggest that lower TN loading always appeared in winter dry season, which has a strong correlation with the low temperature and there was small surface runoff in winter.

At all the four outfalls, the monthly TN loading had similar changing trend over a year. It was

low in January - February because of little snowmelt despite of snowfalls, and then a sharp increase in March due to the start of snowmelt. The loading kept steadily high or slowly increasing in March - July due to snowmelt and most rainfall of a year occurred within this period. Then, it decreased steadily in August - October, during which rainfalls were much less. The loading further decreased or remained low in November - December, similarly as in January - February.

For the 28-year monitoring period, the statistically maximum inter-annual variations of monthly TN loading occurred in July at two outfalls (the 30th Ave and Quesnell), and in March and/or April at the other outfalls (Groat road and Kennedale), as demonstrated by the high standard deviations (SD) and data range shown in Figure 2.3. Their corresponding SD values were 3.9, 2.9, 1.2 and 3.5 tons, respectively. Obviously, the high variability of rainfall or snowfall and snowmelt from year to year contributed to the high inter-annual variation of the loading in July or March/April. On the other hand, the minimum inter-annual variations were in December to February for the four outfalls, which were related to low snowmelt in these months.

2.3.2 Spatiotemporal characteristics of TON, NH_4-N and NO_x-N loadings

2.3.2.1 Monthly scale analysis

Loadings of TON, NH_4-N, and NO_x-N at the four storm outfalls varied with years (Figure A2.2-2.4) and months (Figure 2.4). The annual TON, NO_x-N and NH_4-N loadings had similar changing trends as the TN loading. Meanwhile, the monthly loadings also had similar trends (except NH_4-N loading in 30th Ave outfall): (a) low value in January - February; (b) a sharp

increase in March; (c) steadily high value or a small increase from March to July; (d) a continuous decrease from August to October; and (e) low value again in November - December. The trends appeared to be highly consistent with rainfall, snowfall and snowmelt patterns within a year, as stated earlier for the TN loading. NH_4-N loading in 30th Ave outfall had a high value during wet season (November to February), low value in dry season (March to October). Generally, the monthly variation of NH_4-N loading was much smaller within a year, i.e., the loading remained more or less stable values. For instance, at the Groat Road outfall, the NH_4-N loading varied between 19.1 kg·N/month (December) and 431.5 kg·N/month (March) due to the NH_4-N mainly from baseflow.

The largest inter-annual fluctuation and maximum SD values were detected in July for all the three nitrogen species at 30th Ave and Quesnell outfalls. For Quesnell and Kennedale outfalls, they were in March and April, respectively. The reason for the largest fluctuation possibly due to the timing of snowfall and rainfall events and the use of fertilizers, pet waste, tree canopy, leaf litter as well as grass clippings during storm seasons (Wall, 2013).

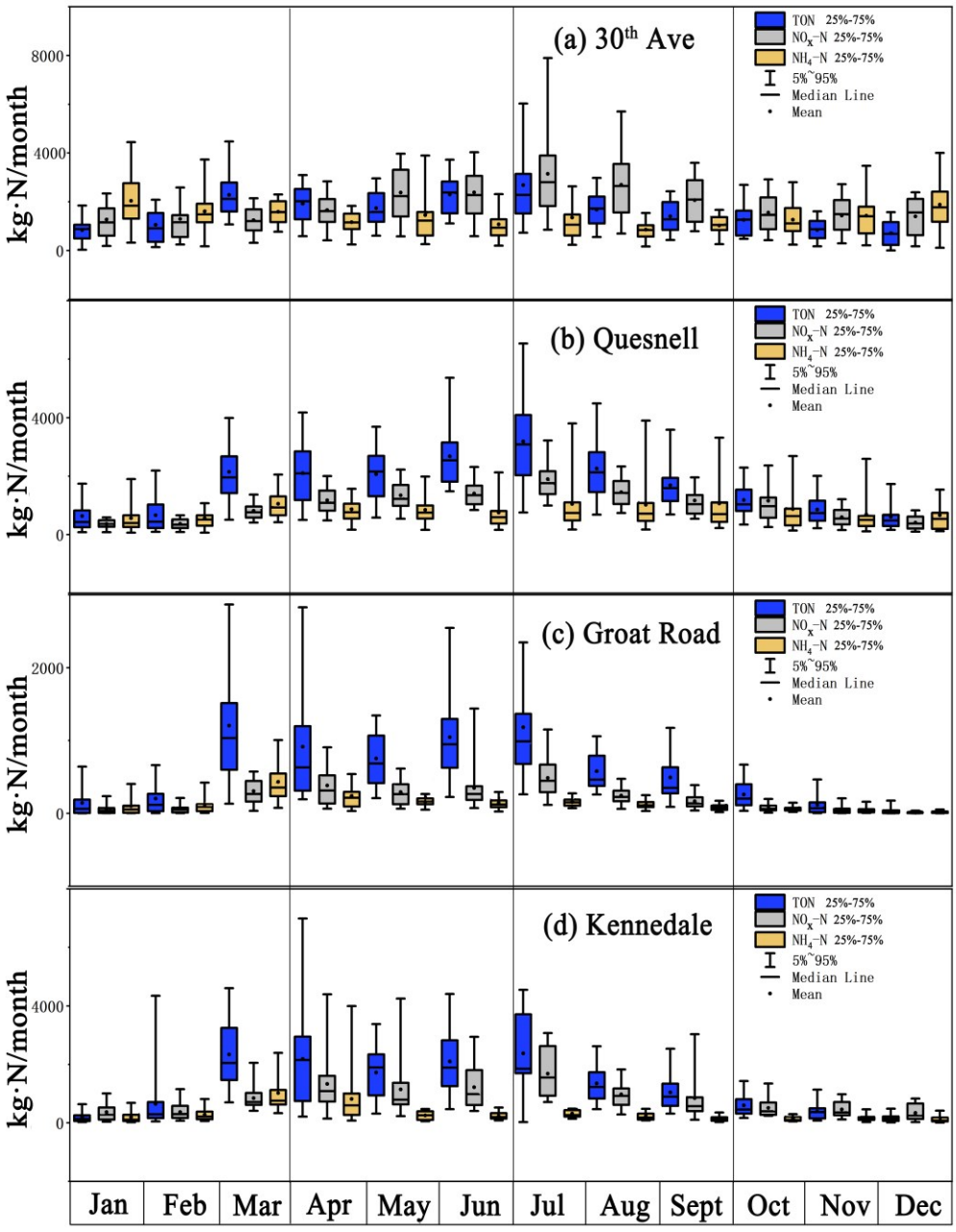

Figure 2.4 Loadings of TON, NH_4-N and NO_x-N at the four storm outfalls in different months from 1991- 2018 (2004 - 2018 for Kennedale). **(a)** the 30th Ave outfall; **(b)** the Quesnell outfall; **(c)** the Groat Road outfall; **(d)** the Kennedale outfall.

2.3.2.2 Contributions to TN loading

The averaged contribution of each nitrogen species to the TN loading in each month for the four outfalls are shown in Figure 2.5. TON contributed the largest portion (25.7 – 68.2 %) to the TN loading for three outfalls (Quesnell, Groat Road and Kennedale). TON includes both soluble form (e.g., from livestock manure and human wastes) and particulate form (e.g., from dead organisms and decaying plant materials) (Wall, 2013). At these three catchments, it was likely to the combined inputs of these sources. At the 30th Ave outfall, TON only accounted for a portion of 31.3 % to the TN loading. Inorganic nitrogen (NH_4-N and NO_x-N) contributed more (68.7 %), with NO_x-N contributed more than NH_4-N in wet seasons for all the four outfalls. This could be because that most of the industrial areas of the city were concentrated in 30th Ave catchment, and industrial waste is one of the common sources of inorganic nitrogen (Wall, 2013).

The ratios of monthly total inorganic nitrogen (TIN) to TON were also plotted for the four outfalls. High values appeared in dry season (November to February), which meant NH_4-N and NO_x-N mainly from baseflow. Ratios were relatively low when snowmelt and storm events began, which represented the increases of TON were more relative with the increases with the snowmelt runoff and stormflow.

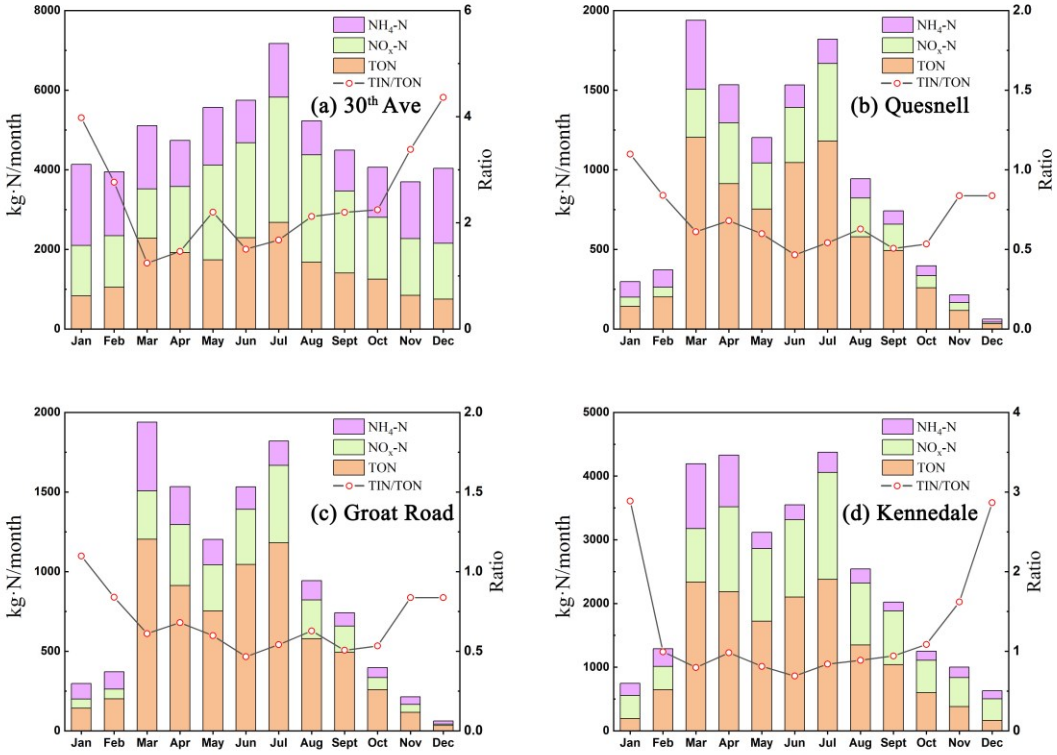

Figure 2.5 Average contribution of each nitrogen species to TN loading in each month at the four storm outfalls from 1991- 2018 (2004 - 2018 for Kennedale). **(a)** the 30th Ave outfall; **(b)** the Quesnell outfall; **(c)** the Groat Road outfall; **(d)** the Kennedale outfall.

2.3.3 M-K and Pettitt test

The statistical results of M-K analysis and Pettitt test for each nitrogen species from 1991 to 2018 are shown in Figure 2.6 and Figure 2.7, respectively. M-K results are significant at the 95% percentile level and the intervals are shown in yellow lines. Three significance level were selected (99%, 95% and 50%) for Pettitt test and were shown in three different dash lines.

The results at the 30th Avenue outfall are used herein as an example to interpret the meaning. For TN, the UF value was > 0 and a continuous upward trend from August 1995 to the end of 2012 (Figure 2.6a), indicating an increasing trend of TN loading, which agreed with the trend observed in Figure 2.2a. At the significance level of 0.01, the abrupt change of TN loading was

in 2013 (Figure 2.7a), the same as shown in Figure 2.2(a). For TON, the UF value had an increasing trend from 1999 to 2012 (Figure 2.6b), which meant an increase of TON loading. From 1991 to the end of 1998, the UF value was < 0 and fluctuated around the significance level during 1993 to 1999, meaning an unstable state of TON loading. The abrupt change of TON loading was detected in 1999 (Figure 2.7b), indicating that the TON loading had an increasing trend after 1999 and the trend was significant from 2003 to 2016.

The variation of UF line for NO_x-N was similar to that of TN, with the same abrupt change year of 2013 (Figure 2.7c). A significant increasing trend occurred during the time series between 1998 and 2014 (Figure 2.6c). The fluctuation of UF line for NH_4-N was much larger than others (Figure 2.6d). Between 1991 and 1995, the UF value was always < 0, and there is a significant decreasing trend from 1992 to 1993. The abrupt change of NH_4-N loading was in 1998 (Figure 2.7d). For the other three outfalls, similar analysis was conducted and the results are summarized in Table 2.2. P (probability) values were used to represent the significant trend provided by Pettitt test. For example, if the p value was lower than the significance (e.g., Kennedale TN loading (0.236 < 0.5)), this meant there was no significant trend in the series at 50% confidence level.

Table 2.2 Mann-Kendall test and Pettitt test for nitrogen species at the four catchment outfalls.

Catchment	Parameter	M-K Test		Pettitt Test			
		Significant period	Trend	Change point	K_T	P	Shift
30th Ave	TN	1999-2015	increasing	2013	13126	1	downward
	TON	2003-2015	increasing	1999	-11824	1	upward
	NO_x-N	1997-2013	increasing	2013	14983	1	downward
	NH_4-N	1999-2014	increasing	1998	-8864	1	upward
Quesnell	TN	2007-2017	increasing	2003	-9407	1	upward
	TON	2008-2018	increasing	2003	-11935	1	upward
	NO_x-N	1997-2009	increasing	1995	-6203	0.997	upward
	NH_4-N	2010-2015	increasing	2013	9958	1	downward
Groat road	TN	1992-1993	decreasing	2006	-6223	0.977	upward
	TON	1992-1993	decreasing	2004	-7681	1	upward
	NO_x-N	1998-2001	increasing	2012	-5209	0.986	upward
	NH_4-N	1991-1993/1999-2004	decreasing/increasing	1994	-3698	0.884	upward
Kennedale	TN	NA	NA	2006	-1306	0.236	upward
	TON	NA	NA	2010	-1298	0.233	upward
	NO_x-N	NA	NA	2006	-1269	0.224	upward
	NH_4-N	NA	NA	2010	-1788	0.396	upward

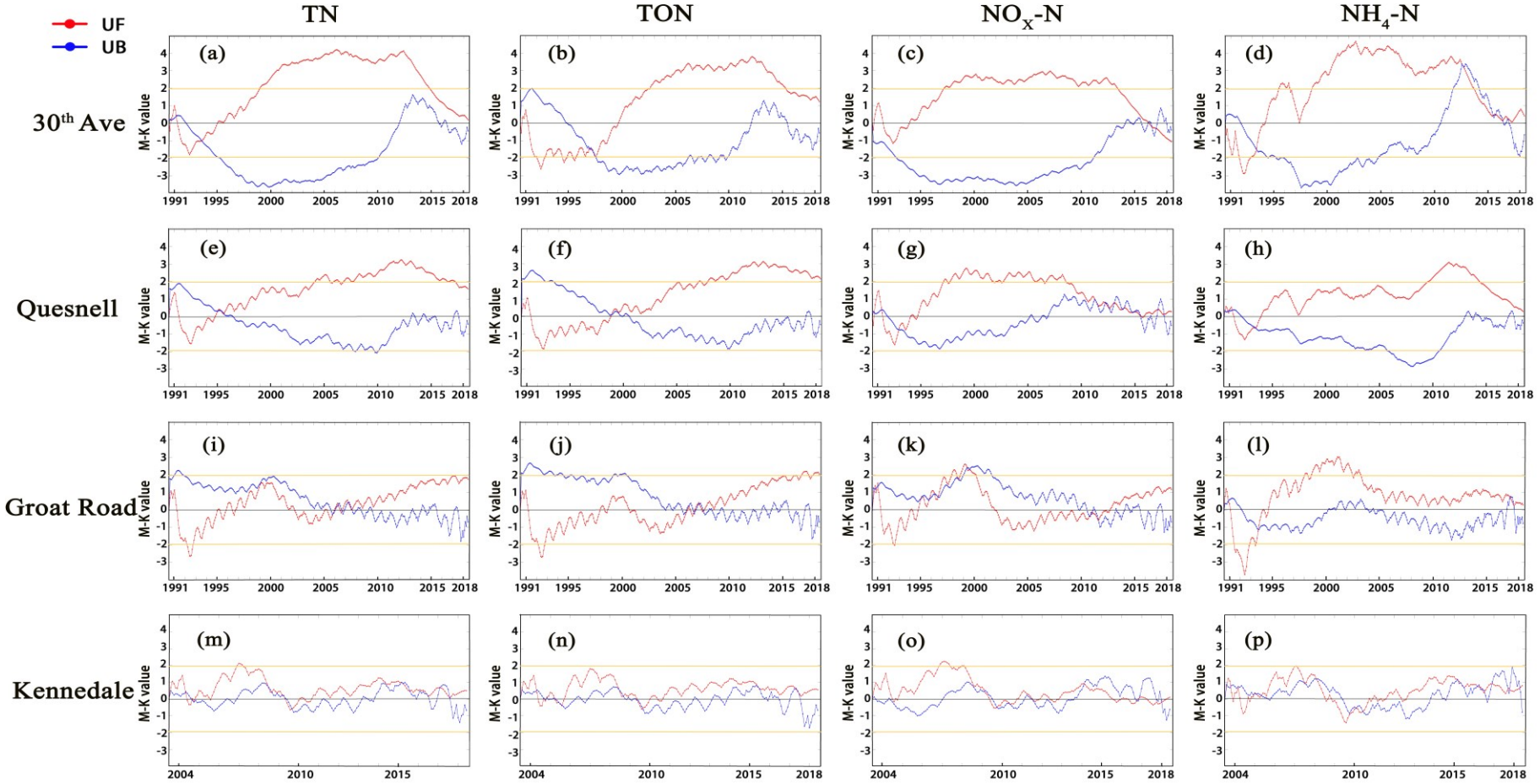

Figure 2.6 Mann-Kendall test for the loading time series of different nitrogen species at the four storm outfalls (Yellow lines represent 95% significance level)

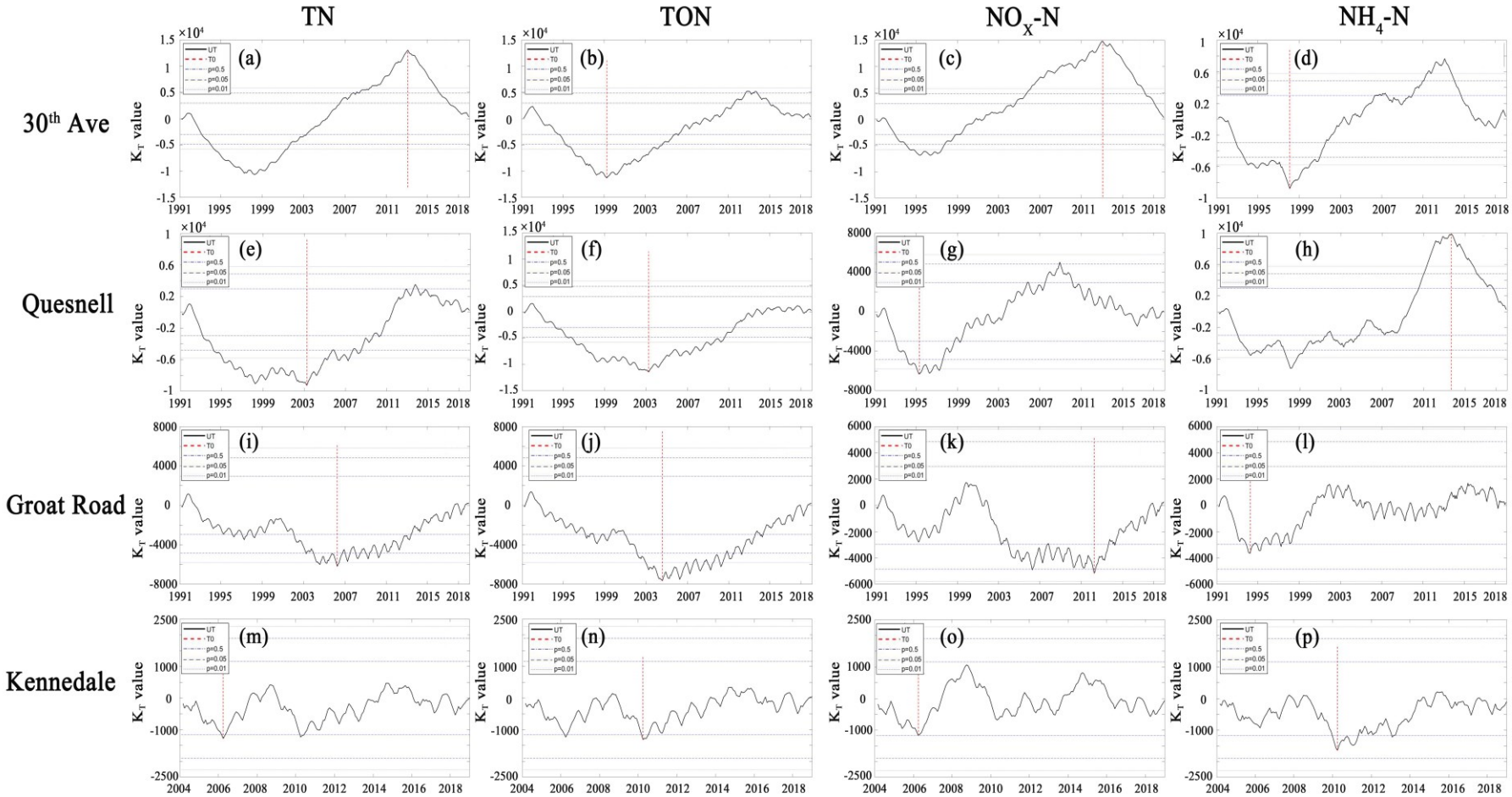

Figure 2.7 Pettitt test on the abrupt change time for the loading time series of each nitrogen species at the four storm outfalls.

2.3.4 Hurst exponent

The Hurst exponent (*H*) values for the loadings of different nitrogen species are summarized in Table 2.3. All the *H* values for the four outfalls were > 0.58, which indicated that the future trend of these nitrogen species would be consistent with the current situation (overall trend from 1991-2018). At two outfalls (the 30th Avenue and Quesnell), the *H* values were all > 0.85 and even approach to 1, suggesting that nitrogen loadings at these two outfalls have a strong persistence sequence. In other words, nitrogen loadings will continue the growth trend for a long period. While the persistence was not so strong at the other two outfalls (Groat Road and Kennedale), especially for NH_4-N loading sequences (*H* = 0.59 and 0.65, respectively). This means nitrogen loadings in these two catchments will be in an increasing trend, but the consistency was not so significant.

Table 2.3 Summary of Hurst exponent (*H*) values based on the rescaled range analysis.

Outfall	TON	NO_x-N	NH_4-N	TN
30th Ave	0.982	0.958	0.912	0.991
Quesnell	0.951	0.858	0.916	0.926
Groat Road	0.879	0.665	0.587	0.818
Kennedale	0.669	0.654	0.647	0.652

2.3.5 Wet and dry season analysis

The total loadings of each nitrogen species (TON, NH_4-N, NO_x-N and TN,) combined from all the four outfalls in dry season (November to March) and wet season (April to October) are shown in Figure 2.8, as well as the loading ratios of wet season to dry season. In Edmonton, surface runoff is dominated by snowmelt from November to March, and by storm flow from

April to October. The average loadings of TON, NO_x-N, NH_4-N and TN in wet season were, respectively, 39.27 tons/month, 31.93 tons/month, 16.24 tons/month and 87.36 tons/month, while in the dry season, they were 14.19 tons/month, 10.95 tons/month, 13.89 tons/month and 38.58 tons /month. The ratios monthly loadings of wet seasons to dry seasons for TN, TON and NO_x-N were 2.26, 2.77 and 2.93, respectively. However, NH_4-N loading in wet season and dry seasons was very close with the ratio of 1.17 (as shown in Figure 2.5).

Mangimbulude et al. (2009) reported that TN loading is higher during wet periods because of higher surface discharge, while TN concentrations are higher during dry period. According to historical record, urban runoff volume showed significant seasonality in the past 28 years, with wet season accounting for 75.9% of the entire year and dry seasons 24.1%. The correlations between the TN loading ratio of wet season to dry season and climatic/anthropogenic factors (ratio of average air temperature, precipitation and population from wet season to dry season) were evaluated (Figure A2.5). The ratio was found to have a weak correlation with air temperature and precipitation for the four catchments, with all the Pearson R^2 values < 0.2.

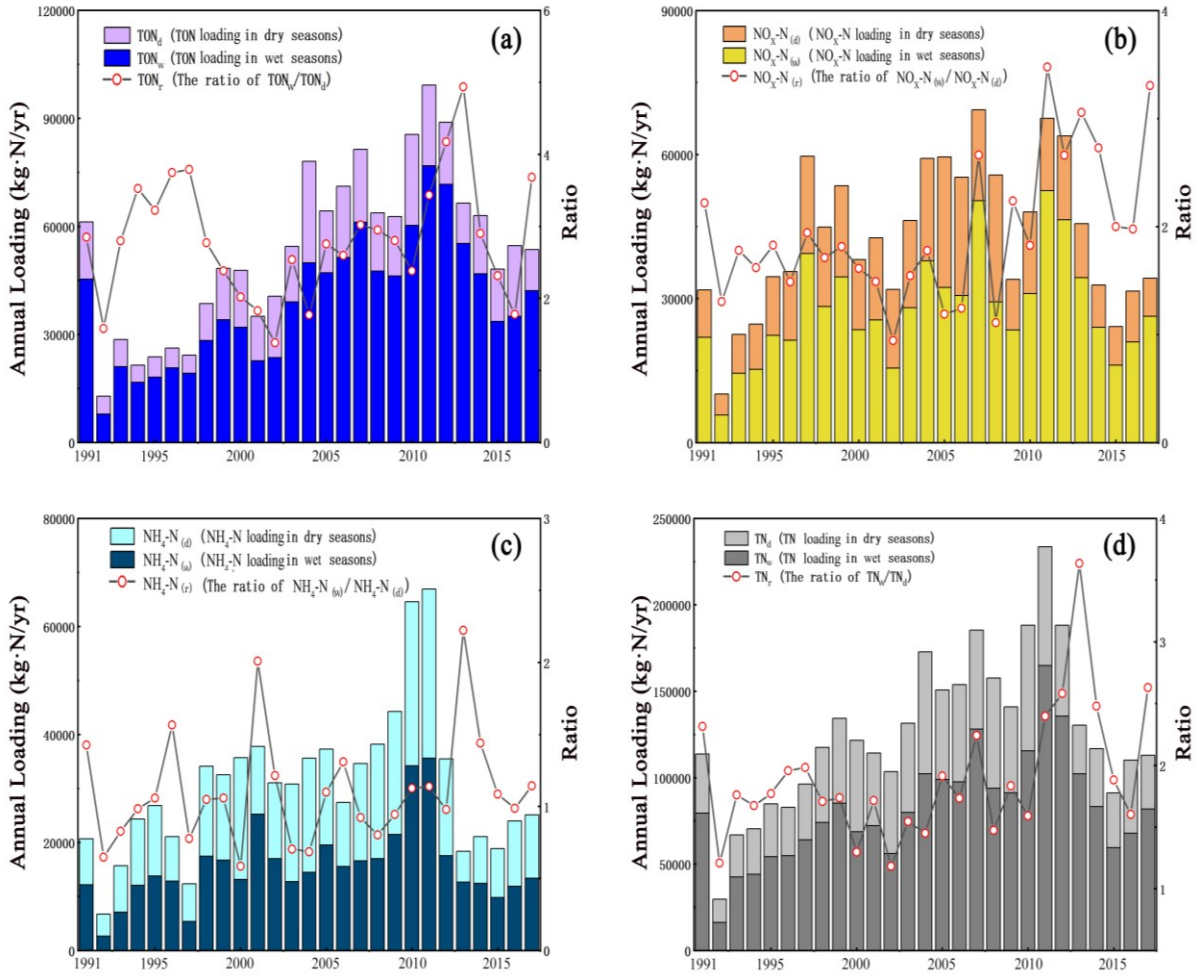

Figure 2.8 Total loadings of each nitrogen species combined from all the four storm outfalls in dry season (November to March) and wet season (April to October) from 1991 - 2018, as well as the loading ratio of wet season to dry season. (a) TON; **(b)** NO_x-N; **(c)** NH_4-N; and **(d)** TN.

2.4 Discussion

2.4.1 Comparison of nitrogen EMCs in snowmelt and storm runoff with other countries

Nitrogen concentration in surface runoff is an important factor for the loading level. The event mean concentrations (EMCs) of TKN, NH_4-N, NO_x-N and TN in snowmelt and storm runoffs from 2007 to 2018 are shown in Table 2.4 and Figure 2.9. Generally, snowmelt had larger EMCs of three nitrogen species (TKN, NH_4-N and TN) than stormflow, and the averaged EMCs of them at the four storm outfalls were 18.0% (3.54 vs. 3.00 mg/L), 94.0% (0.97 vs.

0.50 mg/L) and 10.8% (4.40 vs. 3.97 mg/L) larger in snowmelt than stormflow, respectively. However, this was opposite for NO_x-N, for which the average EMC at the four outfalls was 9.3% (0.86 vs. 0.97 mg/L) lower in snowmelt than stormflow. No obvious trend was found between the EMC ratio of TN in snowmelt to stormflow and years.

Table 2.4 Event mean concentrations (EMCs) of TKN, NH_4-N, NO_x-N and TN in snowmelt and stormflow from 2007 to 2018.

Outfall	Type	TKN (mg/L)	NH_4-N (mg/L)	NO_x-N (mg/L)	TN (mg/L)
30th Avenue	Snowmelt	3.89±1.96	1.35±1.19	1.01±0.47	4.91±2.15
	Stormflow	2.85±2.01	0.68±0.58	1.31±0.82	4.17±2.48
Quesnell	Snowmelt	3.36±1.53	0.86±0.45	0.76±0.29	4.12±1.69
	Stormflow	3.42±2.17	0.69±0.54	0.79±0.43	4.21±2.36
Groat Road	Snowmelt	3.75±1.85	0.87±0.57	0.84±0.38	4.59±1.89
	Stormflow	3.47±2.33	0.37±0.36	0.82±0.45	4.29±2.48
Kennedale	Snowmelt	3.17±2.07	0.79±0.37	0.82±0.40	3.99±2.23
	Stormflow	2.26±1.21	0.26±0.22	0.97±0.51	3.22±1.52
Average of the 4 outfalls	Snowmelt	3.54±0.82 (18.0% higher)*	0.97±0.49 (94.0% higher)*	0.86±0.21 (9.3% lower)*	4.40±0.84 (10.8% higher)*
	Stormflow	3.00±1.19	0.50±0.41	0.97±0.26	3.97±1.14

Note: * comparison of EMCs between snowmelt and stormflow.

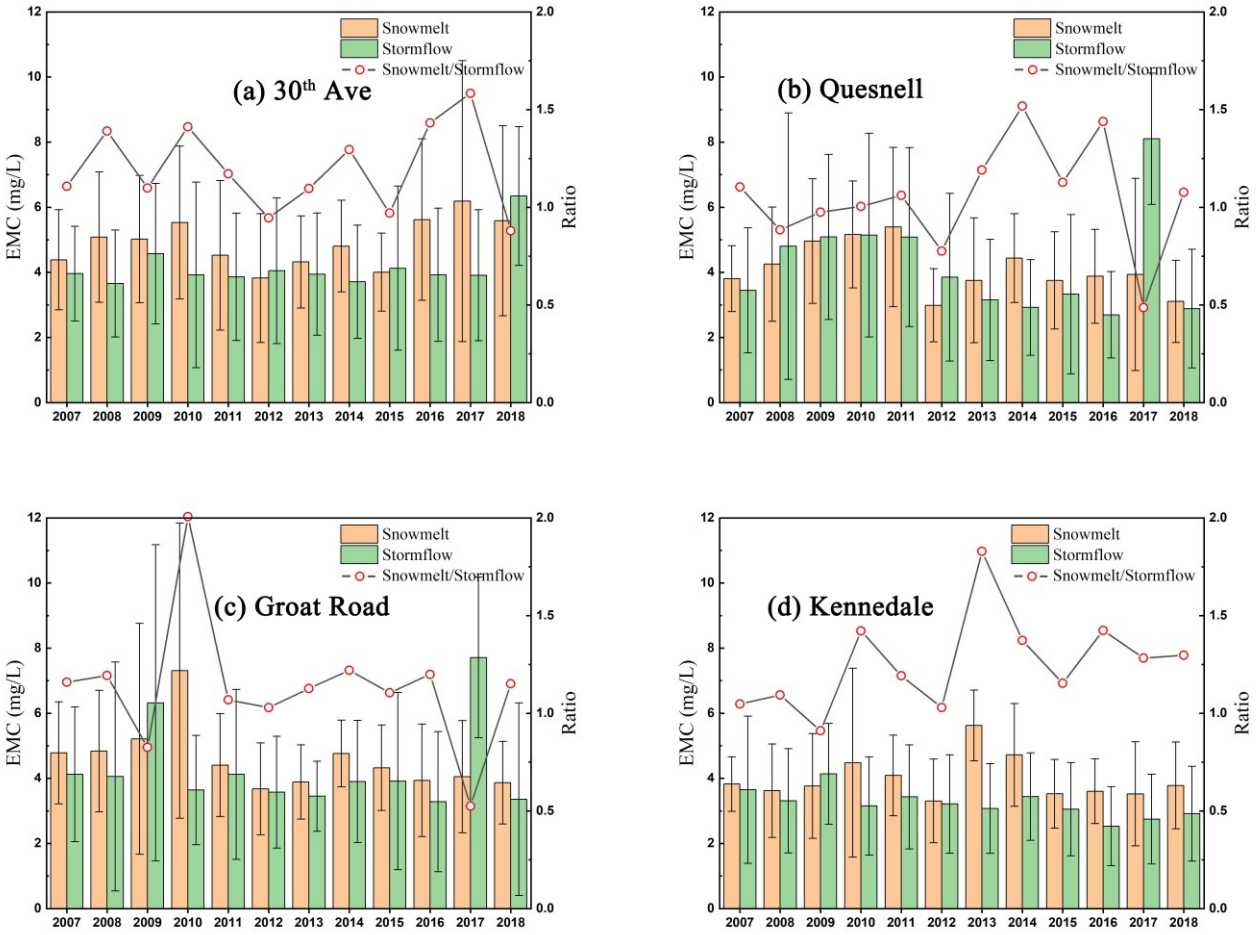

Figure 2.9 Event mean concentrations (EMCs) of TN in snowmelt and storm flow at the four storm outfalls: **(a)** 30th Ave outfall; **(b)** Quesnell outfall; **(c)** Groat Road outfall; **(d)** Kennedale outfall.

EMCs of TN in snowmelt and stormflow in different countries were collected from the literature and compared with the present results (Table A2.1). In cold regions, the existing, limited monitoring data all suggest that TN tends to be larger (10.8 - 518.1% larger) in snowmelt runoff than in stormwater, including data in Assiniboine River Basin and Edmonton (present study), Canada; Beijing, China; Lahti, Finland; Ostersund, Sweden; and Saint Paul, USA. (Figure 2.10). This is due to the accumulation of nitrogen in snowpack and being flushed in snowmelt runoff during freeze-thaw cycles. Xia et al. (2014) explained that higher nitrogen concentration in snowmelt is due to the adsorption of nitrogen from air to surface snow.

Additionally, snow is exposed to atmosphere for a long time before melting, which is one of the reasons causing higher nitrogen EMCs. Chen et al. (2018) found the pH value in snowmelt was higher than stormwater, which led a slightly (24.7 %) higher NH_4-N concentration in snowmelt (94.0 % higher in this study).

Among the limited data, the highest EMC of TN in snowmelt were found in the capital (Beijing) of the developing country of China, with TN EMC of more than 52 mg/L, which was 10.9 times, 16.9 times, 31.0 times and 11.1 times higher than those in Canada, Finland, Sweden and USA. Interestingly, the lowest EMC of TN in snowmelt is also in China (Xi'an), possibly due to the difference of sampling site (e.g., road traffic intensity). In the present study in Edmonton, Canada, the EMC (on average 4.40 mg/L) of TN in snowmelt is similar to those in Assiniboine River Basin (2.91 mg/L) and Broadview (4.39 mg/L), Canada. Compared with other cities in developed countries, our snowmelt value is also generally similar to (slightly higher than) those in Lahti (2.92 mg/L), Finland, Ostersund (1.63 mg/L), Sweden, and Saint Paul (4.3 mg/L), USA.

The large variations of EMCs of TN in snowmelt are caused by the differences in catchment characteristics, climatic conditions and anthropogenic activities (Siudek et al., 2015). Meanwhile, the selection of sampling sites can also result in differences on nitrogen EMCs, e.g., Ren et al. (2008) found the largest TN EMC was in roads with high volume traffic, and then in roof and lawn in Beijing.

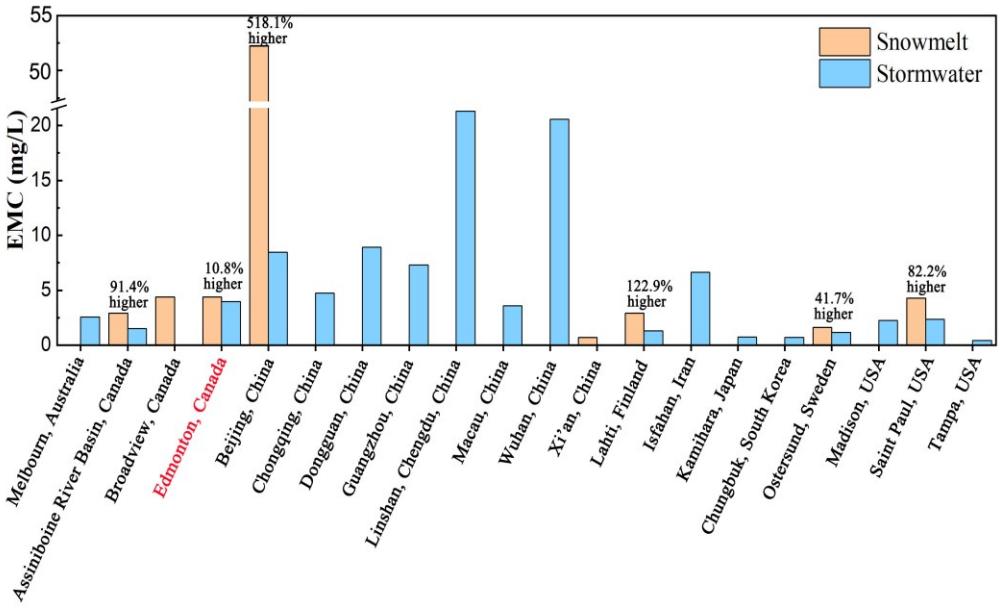

Figure 2.10 Event mean concentrations (EMCs) of TN in snowmelt and stormwater runoff in different countries.

For stormwater runoff, based on the limited data, cities in developing countries generally have high values of TN EMCs, e.g., Chongqing (4.73 mg/L), Wuhan (20.57 mg/L), Beijing (8.45 mg/L) and Guangzhou (7.32 mg/L) China, and Isfahan (6.65 mg/L), Iran. In the present study, the TN EMCs (on average 3.97 mg/L) in our catchments are higher than those in other cities of developed countries, including Melbourne (2.56 mg/L), Australia, Lahti (1.31 mg/L), Finland, Kamihara (0.76 mg/L), Japan, Chungbuk (0.71 mg/L), South Korea, Ostersund (1.15 mg/L), Sweden, and Madison (2.25 mg/L), Saint Paul (2.36 mg/L) and Tampa (0.42 mg/L), USA.

Previous studies have shown that nitrogen concentration in stormwater runoff not only depends on land use, but also on flow rate and humidity (Gobel et al., 2006; Clark and Pitt, 2012). Li et al. (2015) indicated that EMC of TN in stormwater runoff was greater in mixed commercial and residential catchments (16.7 mg/L; 87% imperviousness) than that in industrial area (9.0

mg/L; 74% imperviousness) and parking lots (1.1 mg/L; 27% imperviousness) in Dongguan, China. Pennino et al. (2016) reported that higher TN EMCs were detected during winter and spring due to greater flow rate. A few studies also showed that TN EMCs had higher values in semi-arid area than humid sub-tropical area in USA (Yang et al., 2016; Yang et al., 2017; Toor et al., 2017). Our study location is in semi-arid area, which might explain the high EMC of TN in this study compared to other cities in developing countries.

2.4.2 Comparison of nitrogen loadings with other countries

Based on the data from American U.S. Geological Survey (USQS), Australia Victoria State Government, European Baltic NEST as well as data from other countries (Smith et al., 2003; Alvarez-Cobelas et al., 2008), the present annual nitrogen loadings per unit area were compared with world-wide data reported since 1990 (Table A2.2). The TN loadings in world-wide catchments are shown in Figure 2.11(a). Based on the current limited data, the highest TN loadings were found in Europe (831 $kg{\cdot}N/km^2{\cdot}yr^{-1}$), and the lowest loadings were in Africa (< 100 $kg{\cdot}N/km^2{\cdot}yr^{-1}$).

TN loadings in the Southern Hemisphere (e.g., Australia, 361 $kg{\cdot}N/km^2{\cdot}yr^{-1}$; Colombia, 548 $kg{\cdot}N/km^2{\cdot}yr^{-1}$) appear to be lower than those in Northern Hemisphere (e.g., Spain, 1553 $kg{\cdot}N/km^2{\cdot}yr^{-1}$; USA, 803 $kg{\cdot}N/km^2{\cdot}yr^{-1}$). Note that the loading value for a country refer to the average value based on the limited data so far within the country (Figure 2.11a). Interestingly, TN loadings in developed countries (e.g., UK, 2224 $kg{\cdot}N/km^2{\cdot}yr^{-1}$; Germany, 864 $kg{\cdot}N/km^2{\cdot}yr^{-1}$) is generally higher than those in developing countries (e.g., India, 198 $kg{\cdot}N/km^2{\cdot}yr^{-1}$; Nigeria, 21 $kg{\cdot}N/km^2{\cdot}yr^{-1}$). In some developing countries (e.g., China, 1352 $kg{\cdot}N/km^2{\cdot}yr^{-1}$; Brazil, 1236 $kg{\cdot}N/km^2{\cdot}yr^{-1}$), TN loadings are slightly higher than some other developing countries (e.g.,

South Africa, 4 kg·N/km^2·yr^{-1}; Puerto Rico, 487 kg·N/km^2·yr^{-1}) due to a high population density (Wakida and Lerner, 2005; Kojima et al., 2011).

In Western Europe (e.g., UK; Spain; Italy), TN loading is much higher than other area, with an average more than 1500 kg·N/km^2·yr^{-1}. While in Northern Europe (e.g., Denmark, Finland, Sweden), the average TN loading is relatively low, less than 200 kg·N/km^2·yr^{-1}. The disparity might be attributed to catchment locations and land uses (e.g., coastal area with cropland in Northern Europe; while urban area and watershed in Western Europe). In USA, higher TN loadings were detected along the coastal lines with highly urbanized metropolitans (e.g., New York, Boston, Los Angeles and Seattle). Similarly, higher TN loadings were also found in Northeast coast of Australia. The highest loading in Australia was detected in the City of Brisbane (1350 kg·N/km^2·yr^{-1}).

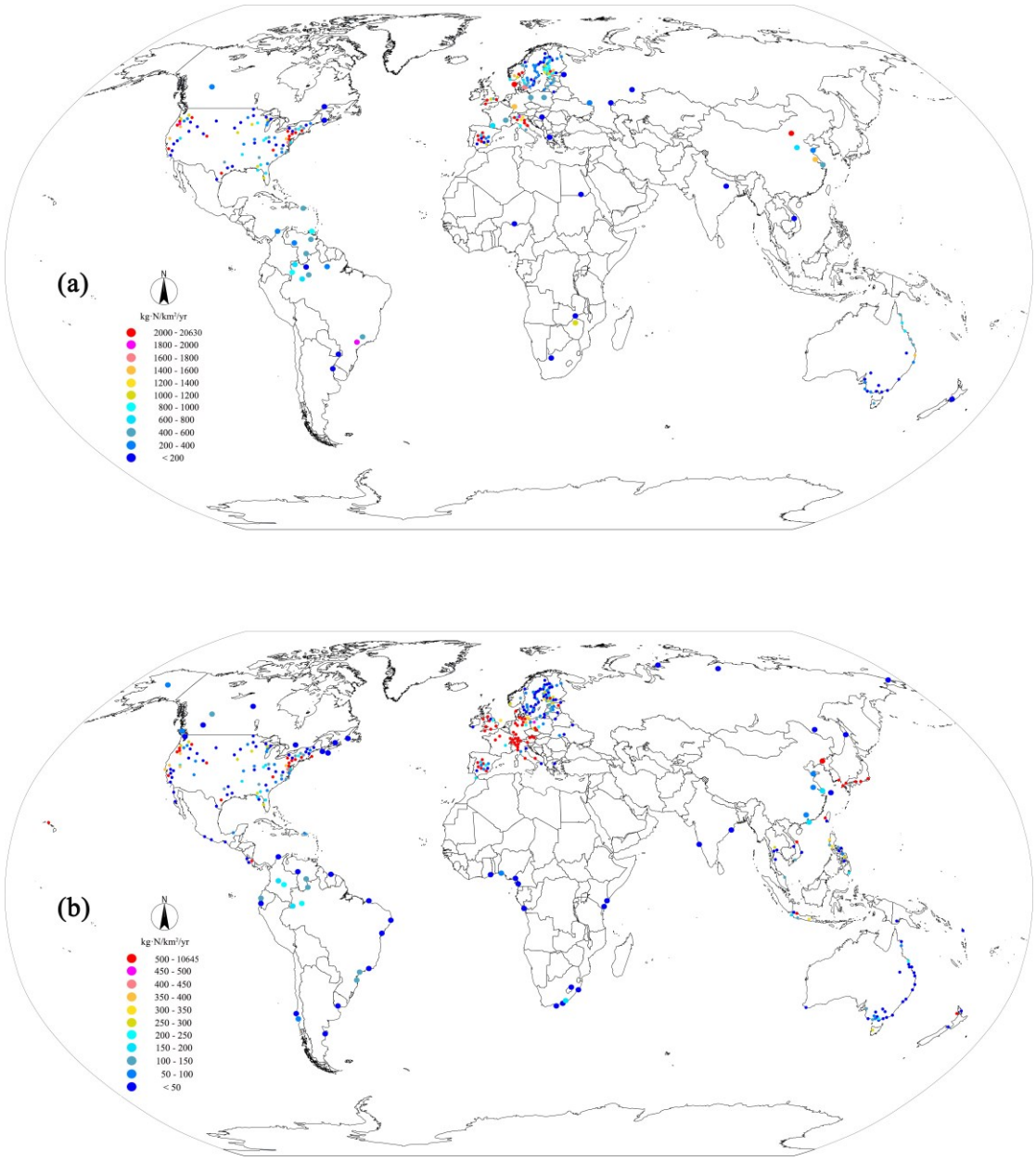

Figure 2.11 Comparison of annual nitrogen loading rates (kg·N/km^2/yr) in different cities worldwide: **(a)** TN; and **(b)** NO_3-N.

The majority of NO_x-N loading in our study catchments is NO_3-N loading (Bulat et al., 2018), and thus, we further used to compare our monitoring data with those worldwide (Table A2.2; Figure 2.11b). In general, NO_3-N loadings have a similar distribution on the globe as TN loadings. Western Europe, coastal areas of USA and Japan have largest values with the average values over 500 $kg{\cdot}N/km^2{\cdot}yr^{-1}$. Northern Europe, South America, Africa and Australia had the lowest loadings, with the average value less than 150 $kg{\cdot}N/km^2{\cdot}yr^{-1}$.

Based on the rather limited data, the present study the nitrogen loading levels (TN: 348 $kg{\cdot}N/km^2{\cdot}yr^{-1}$; NO_3-N: 118 $kg{\cdot}N/km^2{\cdot}yr^{-1}$) are quite larger than those (TN: on average 71 $kg{\cdot}N/km^2{\cdot}yr^{-1}$; NO_3-N: on average 35 $kg{\cdot}N/km^2{\cdot}yr^{-1}$) in other catchments in Canada. This is mainly because of the highly urbanized catchments in this study compared to others. Compared with catchments in other countries, nitrogen loadings in Canadian catchments were lower than those in Western European countries (e.g., Italy, France and Germany) probably due to low population density in Canada and cold climate. Compare with Northern Europe, nitrogen loadings in our catchments were similar to those countries (e.g., Finland and Sweden) also with a similar climate. Compare with USA catchments, our results were close to those catchments in Northern and central America, but less than those located along the coastal line. Compared with catchments in Africa and South America, NO_3-N loadings were close or slightly higher than catchments in those continents. TN loadings were much larger in some South American countries (e.g., Brazil and Colombia), with a relatively low value in Africa (e.g., Nigeria and South Africa).

Natural drives, anthropogenic drives and site characteristics must be taken into consideration to explain the disparities of nitrogen loadings in different areas/countries (Causse et al., 2015).

Natural drives include surface characteristics (e.g., slope, permeability and soil depth) and hydroclimatic variability (e.g., rainfall characteristics, temperature, humidity, dry and wet periods) (Kurunc et al., 2011; Truman et al., 2011). Anthropogenic drives include urbanization, infrastructure, atmospheric deposition, catchment characteristics (e.g., traffic volume, land use and land cover), stormwater management policies and road sweeping strategies (Causse et al., 2015). Zhou et al. (2006) point out that TN losses by surface runoff is sensitive to soil texture. Nitrogen deposition is an indirect anthropogenic drive mainly generated from urban traffic and agriculture practices (Liu et al., 2011b). Rainfall amounts showed positive linear correlation with nitrogen loading from both urban and agricultural plots (Liu et al., 2012). Anisfeld et al., (2007) showed that nitrogen deposition is very significant during storm events. Similarly, Liu et al., (2006) found that more than 80% of TN deposition occurs during rainy season in Beijing, China.

2.5 Conclusions

Stormwater pollutant loadings has important impacts to receiving water bodies but long-term monitoring data are missing to understand its spatiotemporal variabilities. This is particular true for cold regions, where loadings from both stormwater and snowmelt runoff are important but much less studied. In this study, we examined the annual, monthly and seasonal variations of different nitrogen (TN, TON, NO_x-N, NH_4-N) loadings in stormwater and snowmelt runoff from four urban catchments in a major North American city (Edmonton, Canada) located in cold region in the past almost 30 years (1991 to 2018).

Major conclusions are as followings:

- The annual trends of TN, TON, NO_x-N and NH_4-N loadings were similar for the four outfalls in the past 28 years, which was an increasing trend from 1992 to 2011, then a decreasing trend from 2011 to 2015, and finally a small rise from 2015 to 2018. The variations were associated with climatic condition, catchment infrastructure and stormwater management policies. These factors can affect nitrogen loadings simultaneously.

- The monthly trends of TN, TON and NO_x-N loadings also had similar trends: a steadily high value or a small increase from March to July, then decrease from August to October and continuous low values from November to February, finally a sharp increase to March. However, NH_4-N loading remained stable and less. March/April or July was detected to have the monthly loading peak and the maximum inter-annual fluctuation, which corresponded to the timing and frequency of snowmelt and storm events.

- M-K and Pettitt tests showed that nitrogen loadings had significant trend period and abrupt change time at 30th Ave, Groat Road and Quesnell outfalls. No obvious trend and change time found in Kennedale outfall, possibly due to the short monitoring time. As we got from R/S results, nitrogen loadings will continue increase in the future at the four outfalls, but the persistency are different.

- Generally, snowmelt had larger EMCs of three nitrogen species (TN, TKN and NH_4-N) than stormflow, but not for NO_x-N (larger EMCs in stormflow). Loadings of TN, TON and NO_x-N in wet season (storm season) were 2.26, 2.77 and 2.93 times larger than in

dry season (snowfall/snowmelt season). On the contrary, NH_4-N loading in wet season and dry season were very close.

- Both TN and NO_3-N loading in Edmonton are quite larger than other catchments in Canada and similar with those catchments in Northern Europe, but lower than Western European countries. Compared with catchments in USA, nitrogen loadings are close to those catchments in Northern and central USA, but less than those catchments located along the coastal line.

Chapter 3 Predicting Stormwater Nitrogen Loadings from an Urban Catchment in Cold Region in Year 2050

3.1 Introduction

With the rapid pace of urbanization and urban densification, more lands are being converted to impervious areas, which alters urban hydrological cycle and affects the quantity and quality of urban stormwater runoff (Goonetilleke et al., 2005; Poelmeans, 2010). Urban stormwater runoff has become a primary source of water pollution in rivers, lakes and oceans (Treilles et al., 2021; Yang et al., 2021; Lyu et al., 2018). For instance, nutrients in urban surface runoff causes water quality deterioration of receiving water, eutrophication, harmful algal blooms and hypoxia, as well as indirect impacts to wildlife and human (Ekka et al., 2021; Griffiths and Mitsch, 2020). Therefore, assessing nutrient loadings from urban stormwater runoff is crucial for protecting the downstream water bodies (Zhang et al., 2021). So far, modeling of stormwater nutrient loadings is limited from a catchment, especially for predicting nitrogen loading considered the impacts of both climate change and urban densification by build-up and wash-off models. Most of these limited studies are for large catchments of watersheds, fewer on urban catchments.

To explore these knowledge gaps, we built a MIKE Urban model that integrates hydrological module and water quality module (build-up and wash-off models) for a cold region urban catchment in Canada. The model was calibrated and validated against monitoring data at the storm outfall of the catchment from 2010-2016 for the event mean concentrations (EMCs) and loadings of three nitrogen species (total Kjeldahl nitrogen, TKN; ammonium, NH_4-N; nitrite and nitrate, NO_x-N). The validated model was used to examine the impacts of climatic

parameters (e.g., rainfall precipitation, duration, intensity) and urban densifications on the loadings. The model was then successfully applied to predict the nitrogen loadings in 2050, based on forecasted precipitation and population. This study improves the understanding of stormwater nitrogen loadings in urban catchments in cold regions.

3.2 Literature review

A large amount of nitrogen in urban surface runoff is generated from atmospheric deposition, anthropogenic activities (e.g., the use of fertilizers, human/pet wastes, leaking sanitary sewers) (Kaushal et al., 2011; Yang and Lusk, 2018) and organic materials (e.g., tree canopy, leaf litter, grass clipping) (Carey et al., 2012; Divers et al., 2014). Numerous studies have indicated that atmospheric deposition accounts for 19 - 50% of TN loading (Hobbie et al., 2017; Kaushal et al. 2011) and 10 - 90% of NO_3-N loading in urban watersheds during storm events (Anisfeld et al., 2007; Riha et al., 2014; Yang and Toor, 2016). Existing studies have also highlighted chemical fertilizers are the major contributor of NO_3-N loading in urban stormwater in Germany (Mueller et al., 2016), China (Yi et al., 2017) and USA (Groffman et al., 2004; Hale et al., 2014). Hobbie et al., (2017) reported that lawn fertilizers contributed 37 - 59% of TN loading and 33 - 44% of NO_3-N loading in stormwater runoff of Saint Paul, Minnesota, USA. In addition, pet waste deposition on urban surfaces can also have an impact on nitrogen loadings in stormwater runoff. For example, Baker et al. (2001) determined pet wastes accounted for 2.3×10^6 kg·N/year in stormwater runoff to an arid urban residential region in Phoenix, USA. Organic materials are considered as a significant contributor of nitrogen in surface runoff in urban areas with high tree canopies and vegetation covers (Janke et al., 2017). Bratt et al, (2017) estimated that approximately 50% of the TN loading during snowmelt events

was contributed by leaf litters in an urban residential area of Saint Paul, USA.

Population in a catchment has a strong, positive correlation with TN loading (Boyer et al., 2006; Galloway et al., 2004). Nitrogen loadings will increase as a result of more population, impervious area and human activities, e.g., energy production from fossil fuels, and use of fertilizers (Bernhardt et al., 2008). Moreover, climate change is also an essential factor affecting nitrogen cycle in urban environment (Feng and Shen, 2021). Climate change, as represented by change of temperature and precipitation, will directly influence the hydrologic cycle, stormwater and snowmelt flow and water quality. Precipitation and temperature changes not only modify the timing of runoff, but also nitrogen cycle (Jeppesen et al., 2009; van Liew et al., 2013). Butterbach-Bahl and Dannenmann. (2011) showed that nitrification and denitrification processes are directly related to air temperature and soil moisture. A rising of temperature will increase ammonia (NH_3) emissions (Rotz, 2004; Montes et al., 2009; Hristov et al., 2011) and thus affect the nitrogen loadings in urban surface runoff. More extreme storm events will flush fertilizers or manures, leading an increase of nitrogen loadings (Suddick et al., 2013).

Organic and inorganic forms of nitrogen, as well as dissolved and particulate forms, are found in surface runoff (Yang et al., 2018). The proportion of inorganic versus organic forms depends on land use, geology and hydrologic conditions (Jarvie et al., 2010). Both organic nitrogen and inorganic nitrogen (i.e., NO_x-N and NH_4-N) can adhere to suspended particles, and could be detached by rainfall, affecting stormwater quality (Taylor et al., 2005). For instance, Vaze and Chiew (2004) found that 20-50% of particulate total nitrogen in stormwater runoff was associated with sediments of 11 - 150 μm. Lusk et al. (2016) and Brat et al. (2017) observed

high fractions (50-80%) of organic nitrogen in urban stormwater runoff in Tampa, Florida, and in snowmelt runoff in Saint Paul, Minnesota.

In terms of modelling, software packages such as Soil and Water Assessment Tool (SWAT) (Kim et al., 2020; Nguyen et al., 2018; Shrestha et al., 2012; Zhang et al., 2012), Storm Water Management model (SWMM) (Alamdari et al., 2017; Nazari-Sharabian et al., 2019; Wang et al., 2017), Substance Flow Analysis (SFA) and Generalized Watershed Loading Functions (GWLF) (Wu and Malmstrom. 2015) have been used to study stormwater nitrogen loadings (Table 3.1). Shrestha et al. (2012) employed a SWAT model to predict TN loading in 2042 - 2062 in Upper Assiniboine watershed, Canada, and predicted that the variation of the TN loading will closely match the dynamics of future runoff volume. Zhang et al. (2012) estimated the climate change effect on NH_4-N loading by combining SWAT model with the circulation model (HadCM3) in Changchun, China. Alamdari et al. (2017) predicted that average TN loading in stormwater will increase 7.1% from 2041 to 2068 due to the climate change by a SMWW model in Fairfax County, Virginia, USA, and the largest increase will be 66.7% under the effect of both climate change and land use/land cover change (Alamdari et al., 2022). Yazdi et al. (2021) used the same model and estimated the annual stormwater TN loading as a function of rainfall depth (0.03 $kg \cdot ha^{-1} \cdot cm^{-1}$) in an urban coastal catchment of Chesapeake Bay, Virginia, USA. Wu and Malmstrom (2015) indicated that TN loading in stormwater runoff increased with increasing precipitation by coupling SFA with a GWLF model in five urban catchments in Stockholm, Sweden.

Table 3.1 Projection of Stormwater TN loading in different countries (sorted by year)

Country	Catchment	Model	Performance	Simulation Period	Baseline	TN loading (kg)	Future	TN loading (kg)	TN loading change (%)	Study
Canada	Upper Assiniboine	SWAT	R^2 = 0.86	Jan. ~ Dec.	1980~2000	0.8~9.8 ($\times 10^6$)	2042~2062	1.2~13.2 ($\times 10^6$)	+10.3 ~ +49.6 (Annual)	Shrestha et al., 2012
Sweden	Stockholm	SFA-GWLF	NSE = 0.77	May. ~ Sept.	2000~2009	27~158	2021~2030	135~310	+6.7 ~ +140.0 (Monthly)	Wu et al., 2015
Australia	Torrens	SWAT	R^2 = 0.60; NSE = 0.60	Dec. ~ Feb.	2007~2015	NA	2021~2050	NA	–16.8 ~ –26.2 (Monthly)	Nguyen et al., 2018
South Korea	Mankyung	APEX- paddy & SWAT	R^2 = 0.82; NSE = 0.58	Jun.	2008~2017	6800	2031~2050	9100	+33.8 (Monthly)	Kim et al., 2020
USA	Fairfax	SWMM	R^2 = 0.83; NSE = 0.79	Jan. ~ Dec.	1971~1998	NA	2041~2068	NA	+33.4 ~ +67.6 (Annual)	Alamdari et al., 2022
Canada	Edmonton	MIKE Urban	R^2 = 0.83; NSE = 0.79	May. ~ Sept.	2010~2016	1712~20994	2050	5415~9081	–56.7 ~ +403.1 (Monthly)	This study

Stormwater quality models like SWMM and MIKE Urban rely on pollutant build-up and wash-off models, which can both predict pollutant dynamics in urban surfaces and sewer pipes (Ma et al., 2021). Pollutant build-up process is the accumulation of pollutant mass during the interval of storm/snow events; and the wash-off is the process that stormwater or snowmelt runoff flows on urban surface and washes off pollutants attached on surface sediments on its pathway (Carey et al., 2013; Long et al., 2014). Understanding the characteristics of pollutant build-up and wash-off under influence of anthropogenic activities and climate change is important to develop pollutant management in urban areas (Hobbie et al., 2017; Janke et al., 2017).

The processes of build-up and wash-off are governed by numerous factors. The factors for the build-up are antecedent dry days, deicing salts/sands used in cold regions, climatic conditions and road site conditions (Ma et al., 2021). While, the factors for the wash-off are the rainfall characteristics (rainfall duration, intensity), catchment characteristics (road imperviousness, land use) and traffic characteristics (volume, average daily traffic, vehicles during a storm) (Chow et al., 2015). Kim et al. (2006) determined the build-up rates of TSS (0.544 $g/m^2/day$) and TKN (0.0039 $g/m^2/day$) from highway sites in Southern California, USA. Kaushal et al. (2008; 2014) found that the change of NO_3-N loading was mainly influenced by antecedent dry period during build-up period in Baltimore, Maryland, USA. Hale et al. (2015) reported that inorganic nitrogen loading in stormwater from arid urban watersheds in Arizona, USA, were associated with precipitation volume and impervious area during wash-off period. Meanwhile, Lewis et al. (2007) found a positive correlation of organic nitrogen loading with rainfall intensity during wash-off period in an urban catchment of Phoenix, Arizona. Similarly,

Crabtree et al, (2008) reported that TN loading had a positive relationship with rainfall intensity; however, some other studies showed negative relationships (Crabtree et al., 2006; Kim et al., 2005).

The first flush effect means that a large portion of pollutant is contained in the first portion of stormwater runoff, which will influence nitrogen concentration and loadings in stormwater runoff (Hathaway et al., 2012; Li et al., 2015; Taebi et al., 2004). Li et al, (2015) reported a strong correlation between rainfall intensity, antecedent dry days and first flush effect. Deng et al. (2011) developed a variable residence time (VART) model to evaluate NO_3-N loading in stormwater during first-flush stage. Existing studies on FF effect mainly focused on TSS (Hathaway and Hunt, 2011; McCarthy, 2009; Soller et al., 2005), and only a few on NO_x-N (Bathoney et al.,2010) as well as TKN (Flint and Davis, 2007).

3.3 Materials and methods

3.3.1 Study area

The study urban catchment was the 30th Ave stormwater basin in the south of the City of Edmonton, Alberta, Canada (Figure 3.1a). The catchment is located in cold region (Plant Hardiness Zone: 3b) and has a humid continental climate, with the annual mean temperature, rainfall precipitation and precipitation of 2.8°C, 324 mm and 461 mm. The catchment has a total area of 6,051 ha and a total population of 0.16 million. The catchment has a mixed land use: residential (72.7%), commercial (8.2%), industrial (9.9%) and park/greenland (9.1%), with imperviousness of 65% (Figure 3.1b). The catchment has an average elevation of 645 m, a steep slope (0.8 %) to the northwest and milder slope (0.5 %) to the south. The catchment

uses separate sewer systems, and the storm sewer system is shown in Figure 3.1c. Stormwater flows from Southeast to Northwest and eventually to the catchment outfall. There are 10 rain gauges available for use in and around the catchment (Figure 3.1d).

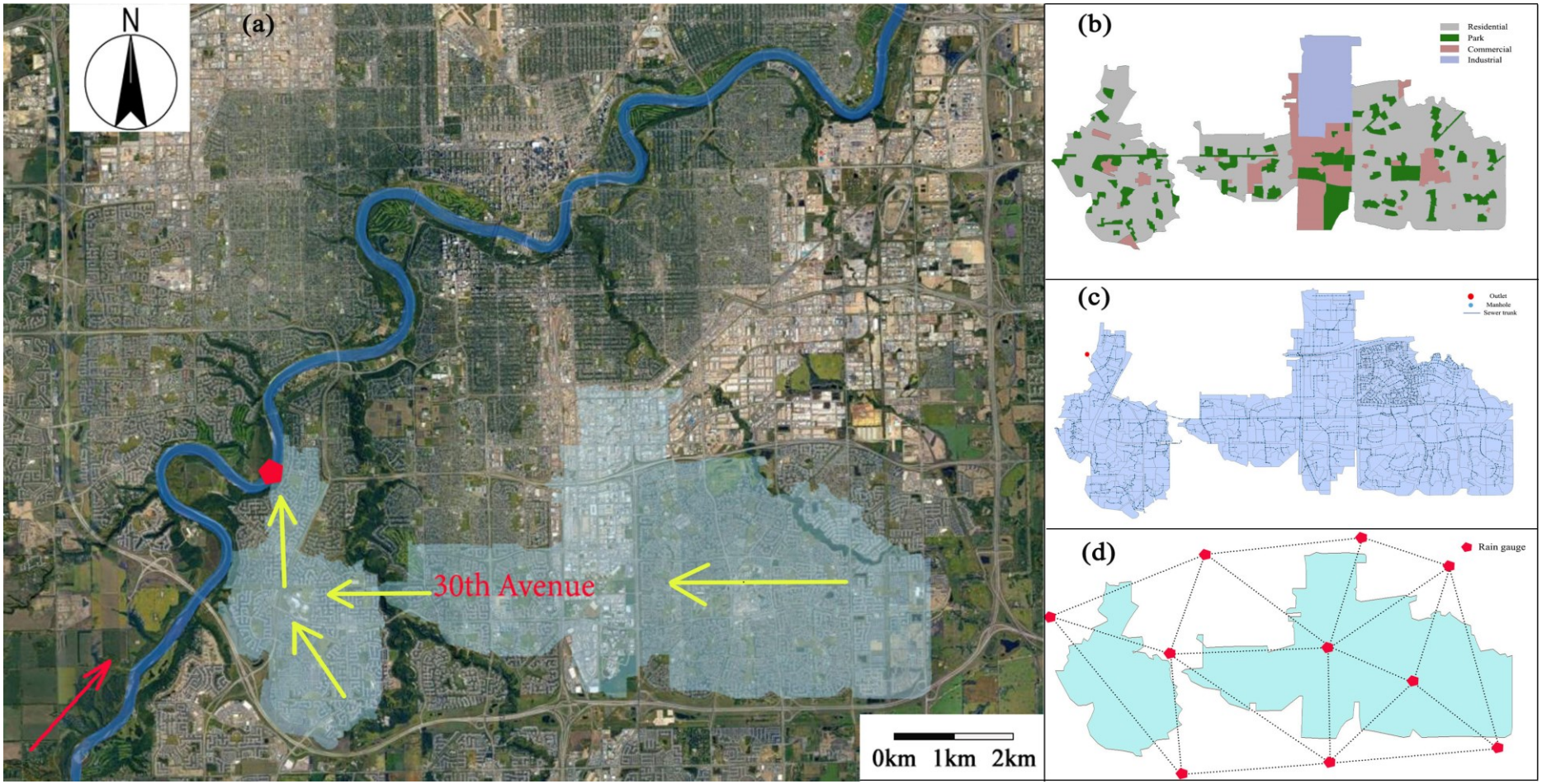

Figure 3.1 The study (30th Ave) catchment: **(a)** location, **(b)** land use map, **(c)** storm sewer system, and **(d)** rain gauges. Yellow arrows represent the general stormwater flow direction, and red arrow represents the river flow direction.

3.3.2 Model setup

3.3.2.1 Data collection

The digital elevation model (DEM) with spatial resolution of 1.5 m and spatial topography of 0.1 m was received from the City of Edmonton. Rainfall data (every 5 minutes) and sewer network information were received from EPCOR Drainage Services. Baseflow samples were collected as grab samples twice a month. Stormwater flow and water samples were collected every 30-minute in May - September, 2010 to 2016, by the City or EPCOR at the catchment storm outlet (Figure 3.1a) by using a flow meter and an auto-sampler (American Sigma Model 1600 and Campbell Scientific CR10, USA), respectively. Stormwater samples were measured for the EMCs of TKN, NO_x-N, NH_4-N and TSS during each storm event.

3.3.2.2 MIKE Urban model

MIKE Urban was used as the modeling software in this study, which is a GIS-based dynamic hydrologic-hydraulic model for simulating long term continuous surface runoff quality in urban areas (DHI, 2017). We also applied SWAT model, but it cannot work well due to the catchment is separated into two parts by a creek. The MIKE Urban model was setup with sub-catchments and storm sewer pipe system, and the flow and water quality were simulated simultaneously. Flow routing was modeled using kinematic wave routing method. The surface runoff quality was simulated based on the build-up (Eq. 3-1) and wash-off (Eq. 3-2) models:

$$B = C_L(1 - e^{-C_1 t}) \tag{3-1}$$

$$W = C_2 Q^{C_3} B \tag{3-2}$$

In Eq. 3-1, B is the pollutant build-up loading, t is the antecedent dry days, C_L is the maximum

build up limit and C_1 is the build-up rate. In Eq. 3-2, W is pollutant wash-off loading, C_2 is the wash-off coefficient or the detachment coefficient, C_3 is the wash-off exponent, Q is the runoff rate per unit area.

The MIKE Urban model was carefully calibrated and validated. The flow hydrograph at the catchment outfall was calibrated and validated in a previous study (Gaafar et al., 2020), with $R^2 = 0.95$ and NSE = 0.91. In this study, the build-up and wash-off models were calibrated and validated against the monitored data of nitrogen EMCs and monthly loadings at the catchment outfall. The calibration was selected for Year 2013, because it was the abrupt change year for nitrogen loading in the catchment (Zhang et al. 2021) and therefore suitable to test the model performance. The year 2014 was selected for model validation. To further validate the model, five additional years of 2010-2016 (except 2013 and 2014 selected for model calibration and validation; i.e., 2010-2012 and 2015-2016) were also used.

Parameters for the model calibration and validation include: build-up rate (C_1), maximum build up limit (C_L), antecedent dry days (t), wash-off coefficient (C_2) and wash-off exponent (C_3). In this study, C_1 was calculated on monthly basis based on the increasing TSS loading between stormwater loading and baseflow loading divided by t and catchment area. C_L was also on monthly basis and calculated through dividing monitored monthly TSS loading by catchment area. Size of TSS particle on urban road surface was directly from the City of Edmonton, which has a range from 1 μm – 150 μm. The affinity of nitrogen species to specific size range of TSS and its attachment ratio were from Miguntanna et al. (2010).

3.3.2.3 Modeling for Year 2050

To predict stormwater nitrogen loadings in 2050 under the impacts of climate change and urban densification, projections are required for precipitation and population in the study catchment. According to the population projection from the City of Edmonton, the increasing rate of population in Edmonton is around 1.58%, with population in Edmonton and the catchment will reach 1.5 million and 0.22 million, respectively (City of Edmonton, 2018; Hayhoe and Stoner, 2019). Simulations of future precipitation were modelled by the City of Edmonton with the climate change model used by the Intergovernmental Panel on Climate Change. Precipitation during the climate change projection was characterized by more frequent heavy rain, with annual average precipitation rise from the current 461 mm to 498 mm, and the annual average rainfall will from 324 mm to 350 mm by 2050. We assume the future scenario has a medium-high greenhouse gas emission (Nakicenovic and Swart, 2000).

For the prediction on nitrogen loading in the year of 2050, C_1, C_2, C_3 and t were setup the same as the calibration setup values. C_L was determined based on the projection of monthly TSS loading in Year 2050. It is calculated by linear regression equation between population in City of Edmonton and total TSS loading from May to September (Pearson $R^2 = 0.62$) (Figure 3.8). Averaged contribution of TSS loading in 30th Ave to the city was used to predict TSS loading in 30th Ave in Year 2050. Monthly TSS loading in 2050 was calculated based on the averaged contribution (past 20 years) of TSS loading each month to total loading. We cannot predict future storm events distribution, so the input of precipitation was based on the year of 2013 due to the year of 2013 had a well distributed storm events and rainfall precipitation (i.e., antecedent dry days are close to our calibrated input value and rainfall precipitation is close to

the average value). We assumed no weather extremes (i.e., drought or flooding) and a well distributed storm events in Year 2050.

3.3.3 Model assessment

Three methods were used to assess the model efficiency: Nash-Sutcliffe efficiency (NSE), the Pearson coefficient of determination (R^2) and absolute relative error (|RE|). NSE is defined as:

$$NSE = 1 - \frac{\sum_{i=1}^{N}(O_i - P_i)^2}{\sum_{i=1}^{N}(O_i - \bar{O})^2} \quad (3\text{-}3)$$

where N is the total number of monitoring samples, O_i is the i^{th} observed value, P_i is the i^{th} predicted or modeled value, and $\bar{O}$ is the mean of the observed values. NSE value ranges from $-\infty$ to 1, where 1 indicates a perfect fit. An NSE value > 0.5 (Nash and Sutcliffe, 1970), $R^2 \geq 0.7$ (Santhi et al., 2011;) and absolute $|RE| \leq 20\%$ (Liew et al., 2003) generally indicate an acceptable model performance.

3.3.4 Sensitivity analysis

In this study, sensitivity analysis was conducted after the model was validated to determine the impacts of important parameters for the build-up and wash-off models (i.e., the build-up rate, maximum build up limit, wash-off coefficient and wash-off exponent). In each case, the investigated parameter was altered by 10%, and the corresponding changes in model output were represented by NSE values.

3.4 Results and discussion

3.4.1 Model calibration and validation

The model calibration results against the 2013 monitoring data are shown in Figure 3.2 and

Table 3.3 for EMCs and monthly loadings of TKN, NO_x-N and NH_4-N. The model performed well for EMCs of storm events (R^2 = 0.89, 0.96 and 0.97, NSE = 0.88, 0.95 and 0.96, |RE| = 18.4%, 8.2% and 13.8% respectively, for the three nitrogen species) and monthly loadings (R^2 = 0.87, 0.86 and 0.82, NSE = 0.82, 0.68 and 0.47, |RE| = 12.7%, 14.5% and 7.0 %, respectively).

The model validation results against the 2014 monitoring data are shown in Figure 3.3 and Table 3.3. The assessment measures were all within the acceptable criteria for EMCs (R^2 = 0.80, 0.88 and 0.94, NSE = 0.71, 0.85 and 0.93, |RE| = 20.0%, 14.1% and 14.4% for TKN, NO_x-N and NH_4-N, respectively) and monthly loadings (R^2 = 0.88, 0.78 and 0.65, NSE = 0.75, 0.59 and 0.41, |RE| =12.8%, 14.5% and 24.4%, respectively). As shown in Figure 3.3, there were some discrepancies between the modeling and measured EMCs for a few storm events (e.g., TKN EMCs of June 28 and July 1 storm events). This is because (a) we assumed the same antecedent dry days within a specific month; and (b) the calibration results in 2013 may not apply well to a specific storm event, due to the randomness of storms.

Table 3.2 Input parameters for model calibration.

Input Parameters	This study	Liu et al. (2010)	Nguyen et al. (2020)
Build-up Rate (kg/ha/day)	0.25; 0.45; 0.42; 0.14; 0.18	0.50-18.20	0.21
Max. Build-up (kg/ha)	11.18; 32.80; 26.50; 7.48; 1.49	7.90-23.10	21.00
Wash-off coefficient (m/h)	0.001	0.001	0.001
Wash-off exponent	2	2	2
Antecedent dry days (d)	7; 5; 3; 7; 12	1.5-15.8	15

Note: Values of build-up rate, max build-up limit and antecedent dry days corresponded from May to September.

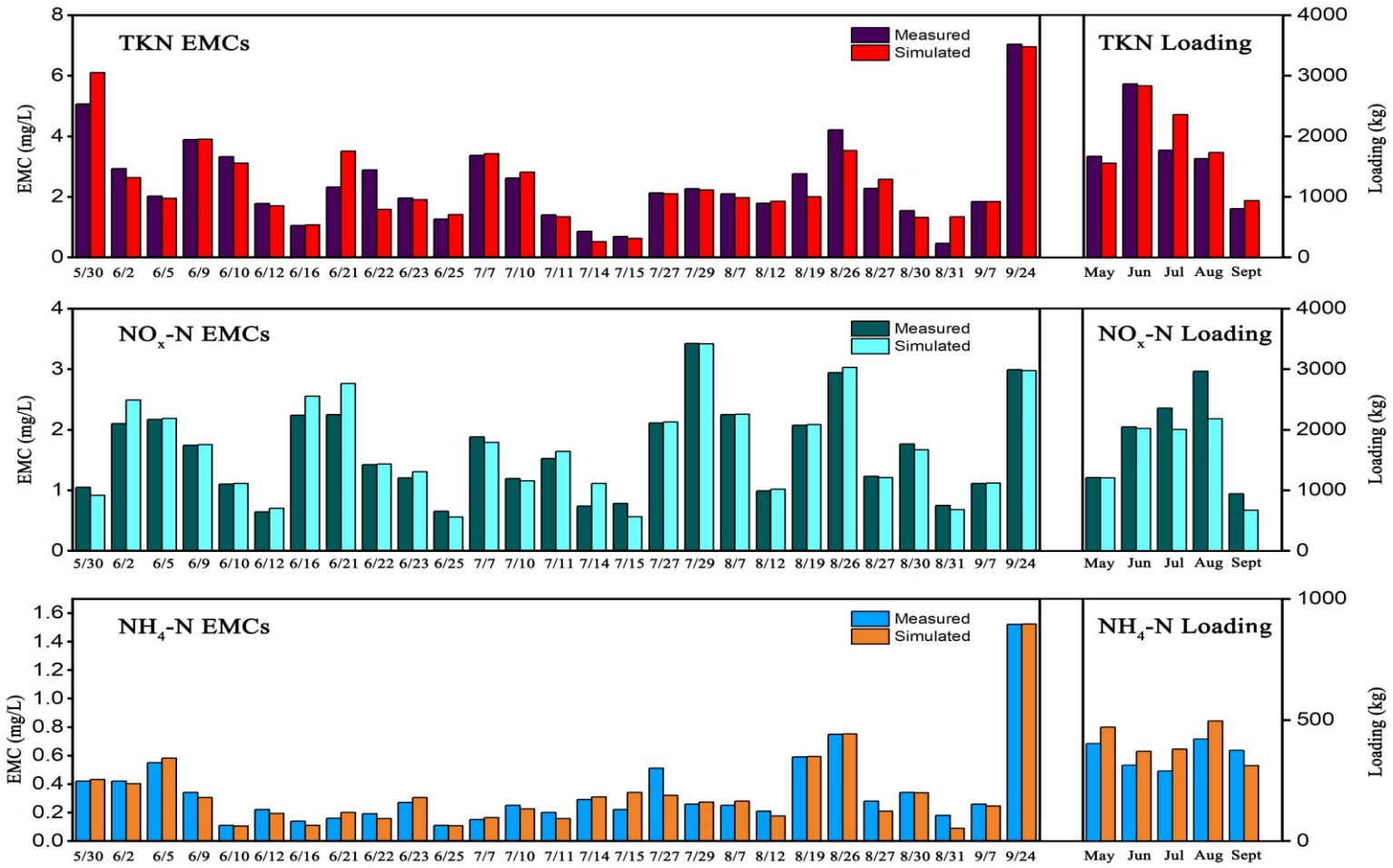

Figure 3.2 Calibration (Year 2013) of the model for the EMCs and monthly loading of the three nitrogen species.

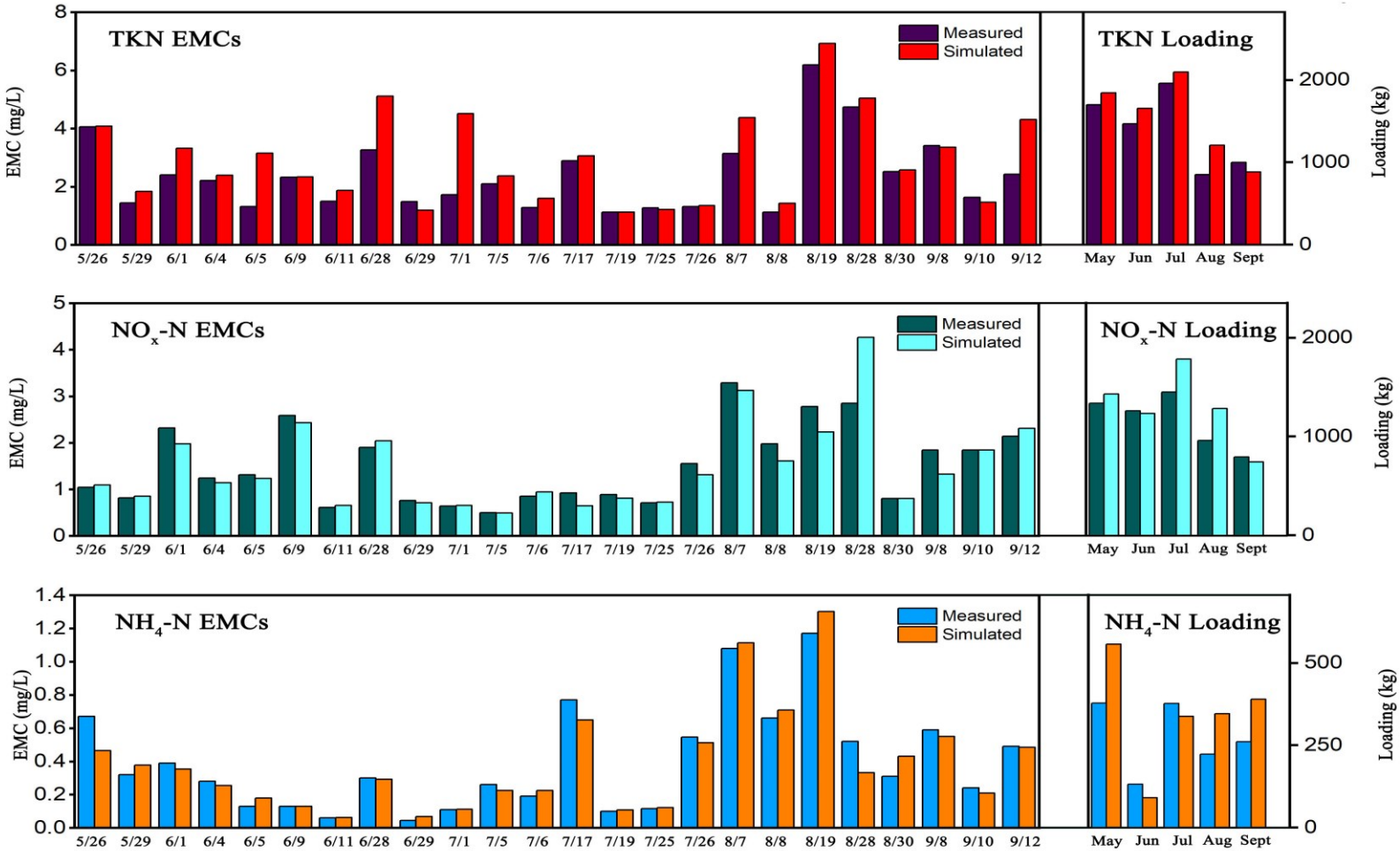

Figure 3.3 Validation (Year 2014) of the model for the EMCs and monthly loading of the three nitrogen species.

To further evaluate the model, we extended the validation years to 2010-2012 and 2015-2016 and examined both EMCs and monthly loadings of the three nitrogen species (Figure 3.4 and Table 3.3). Overall, the model performance is still acceptable for EMCs (R^2 = 0.77, 0.71 and 0.74, NSE = 0.69, 0.64 and 0.59, |RE| = 25.5%, 19.5% and 20.7% for TKN, NO_x-N and NH_4-N, respectively) and monthly loadings (R^2 = 0.84, 0.65 and 0.67, NSE = 0.71, 0.64 and 0.51, |RE| = 29.4%, 36.8% and 20.6%, respectively). Of course, the further validation results were not good as the validation results (against 2014 data). The is attributed to the difference of build-up rate and maximum build-up limit between actual values and the calibration setup values, again due to the randomness and complexity of storm events.

Compare with the calibration and validation statistics (R^2 = 0.83 and NSE = 0.79 for study in Fairfax, USA; R^2 = 0.82 and NSE = 0.58 for study in Mankyung, South Korea) of those similar studies (build-up and wash-off models; and maybe other models such as SWAT on loadings, especially nitrogen loadings) in the literature. Thus, the present model is still considered satisfactory.

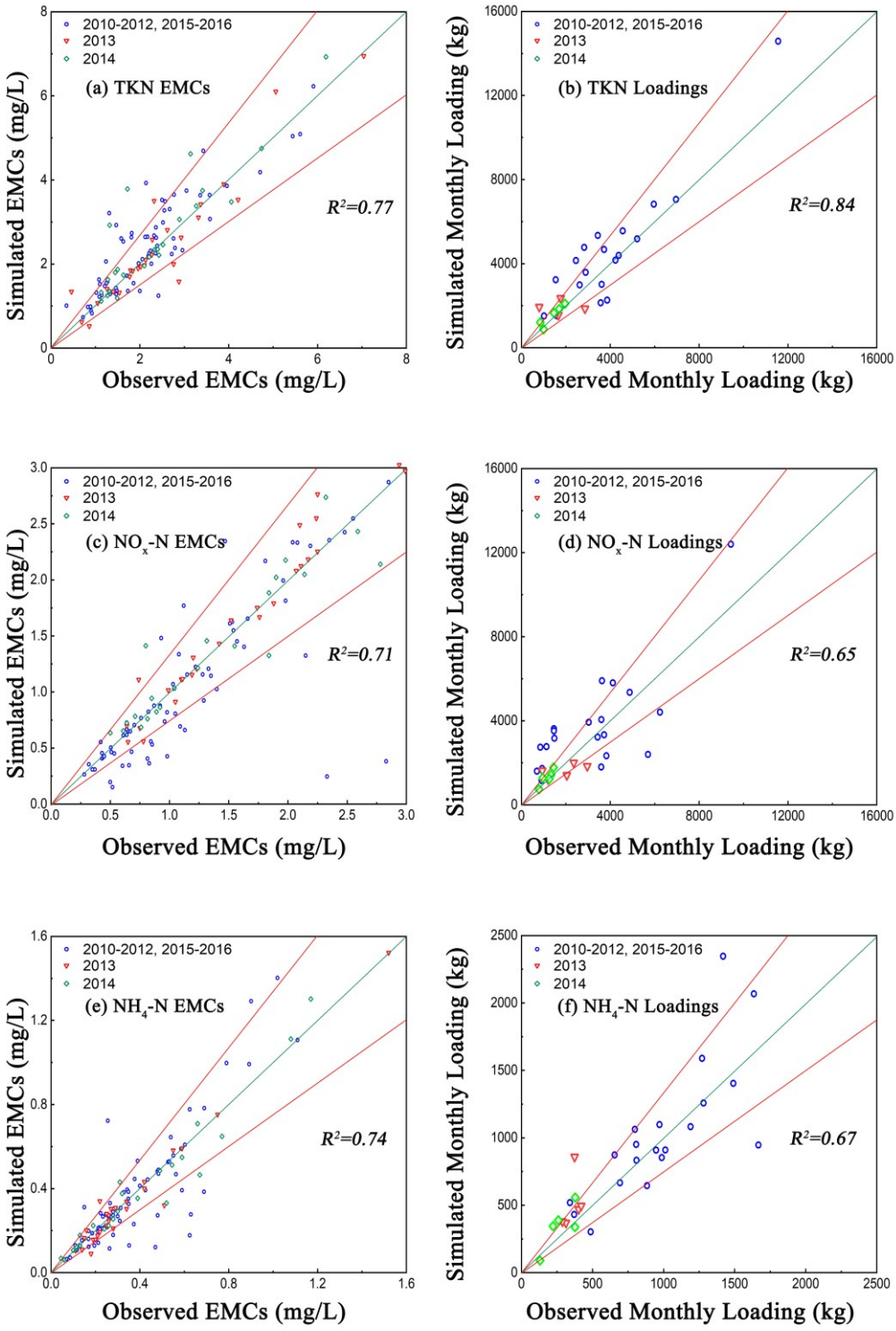

Figure 3.4 Further validation (Year 2010 - 2012 and 2015 - 2016) of the model for EMCs and stormwater monthly loadings of the three nitrogen species with ± 25% error line. Comparison for Year 2013 and 2014 are also shown. R^2 value is for blue dots in each subplot.

Table 3.3 Statistics of model calibration and validation for the EMCs and monthly loadings of three nitrogen species during storm events.

Model	Statistics	Nitrogen EMCs			Nitrogen Loadings		
		TKN	**NO_X-N**	**NH_4-N**	**TKN**	**NO_X-N**	**NH_4-N**
Calibration (2013)	R^2	0.89	0.96	0.97	0.87	0.86	0.82
	NSE	0.88	0.95	0.96	0.82	0.68	0.47
	|RE|	18.4%	8.2%	13.8%	12.7%	14.5%	7.0%
Validation (2014)	R^2	0.80	0.88	0.94	0.88	0.78	0.65
	NSE	0.71	0.85	0.93	0.75	0.59	0.41
	|RE|	20.0%	14.1%	14.4%	12.8%	14.5%	24.4%
Further validation (2010 - 2012, 2015 - 2016)	R^2	0.77	0.71	0.74	0.84	0.65	0.67
	NSE	0.69	0.64	0.59	0.71	0.64	0.51
	|RE|	25.5%	19.5%	20.7%	29.4%	36.8%	20.6%

Based on the model calibration and validation, the build-up rate and maximum build-up limit varied with months, with a range of 0.20 - 0.45 kg/ha/day and 1.49 - 32.80 kg/ha, respectively (Table 3.2), and these values were both close to those reported in the literature (Li et al., 2007; Liu et al., 2010; Nguyen et al., 2020). The wash-off exponent and coefficient were 2 and 1.0×10^{-4}, respectively, which were the same as to the previous researches (Table 3.2). Antecedent dry days were set up with 7, 5, 3, 7, 12 days for May, June, July, August, September, respectively. with the affinity of TKN, NO_x-N and NH_4-N of 4.8, 3.6 and 1.2 mg/g, respectively (Miguntanna et al., 2010). The input of rainfall intensity was based on the rainfall event in the year of 2013, with rainfall intensity values increased by 1.12 times to meet the projected rainfall precipitation in 2050.

The results of sensitivity analysis show EMCs and loadings were sensitive to build-up rate and maximum build-up limit. Wash-off exponent and wash-off coefficient were not sensitive. The rank of the sensitivity for the four parameters are build-up rate, maximum build-up limit and then wash-off exponent and wash-off coefficient, which agrees with the previous research (Liu et al., 2010).

3.4.2 Impacts of climate and urban densification on nitrogen loadings

3.4.2.1 Impact of antecedent dry days

Antecedent dry days has a direct impact on pollutant build-up. As the carrier of nitrogen, the accumulation of TSS loading on road surface during antecedent dry days needs to be investigated, which is the preparation for predicting future nitrogen loading. Based on the monitoring data of TSS loadings and during each storm events from 2010 to 2016, we evaluated

the relationship between antecedent dry days with the TSS loading during each storm event, and a relatively moderate correlation was found with Pearson R^2 = 0.57 (Figure 3.5). The variation between TSS loading with the same dry days is because the TSS loading is also influenced by other factors such as anthropogenic activities, daily traffic volume and road surface condition (Chow et al., 2015). Higher build-up masses are usually found in residential area, followed by commercial area (Liu et al., 2012).

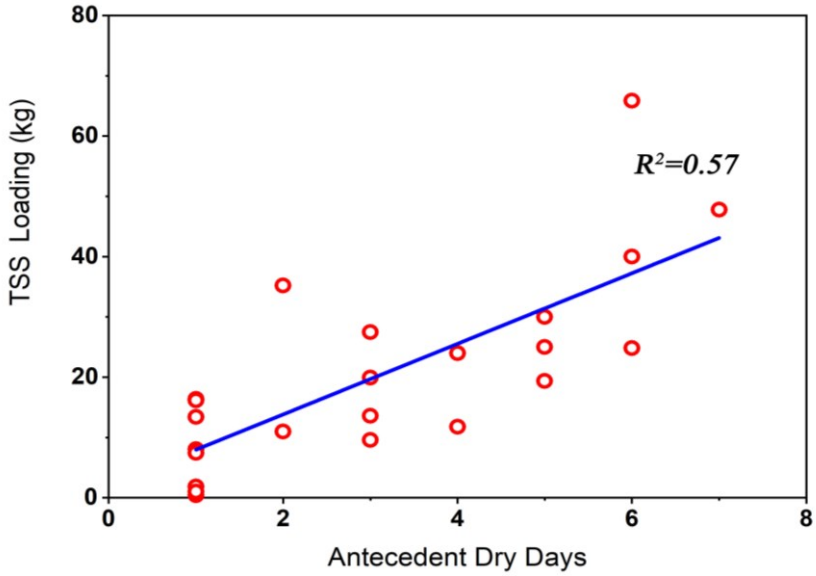

Figure 3.5 Relationship between build-up TSS loading with antecedent dry days based on observed data from 2010 to 2016.

In general, longer antecedent dry days should result in a larger accumulation of nitrogen on impervious surface (Kim et al., 2006; Cheema et al., 2017). However, some previous studies suggested antecedent dry days is disconnected with nitrogen loadings (Davidson et al., 2020; Wang et al., 2022). Our correlations agreed with them and the relationship between antecedent dry days to TKN, NO_x-N and NH_4-N loadings were very weak (Figure 3.6j-l) (Pearson $R^2 \leq$ 0.1), which may relate to the only sampling site at the catchment outlet and there might be some nitrogen loss on the pathway (e.g., road surface and sewer pipe).

3.4.2.2 Impact of rainfall characteristics on nitrogen loadings

Nitrogen wash-off from sediments has a significant relationship with rainfall characteristics. The correlations between the average rainfall intensity, peak rainfall intensity and total rainfall depth of each storm event with the loadings of the three nitrogen species from 2010 to 2016 are shown in Figure 3.6. The average and peak rainfall intensity had weak relationship with the loadings of TKN and NO_x-N, with $R^2 \approx 0.3$. While, the correlations with NH_4-N were moderate, with $R^2 = 0.53$ and 0.58, respectively. However, total rainfall depth had a clear relation with the loadings of three-nitrogen species, with $R^2 = 0.59$, 0.58, 0.62, respectively. This indicates that rainfall precipitation has a positive relationship with loadings but not significant.

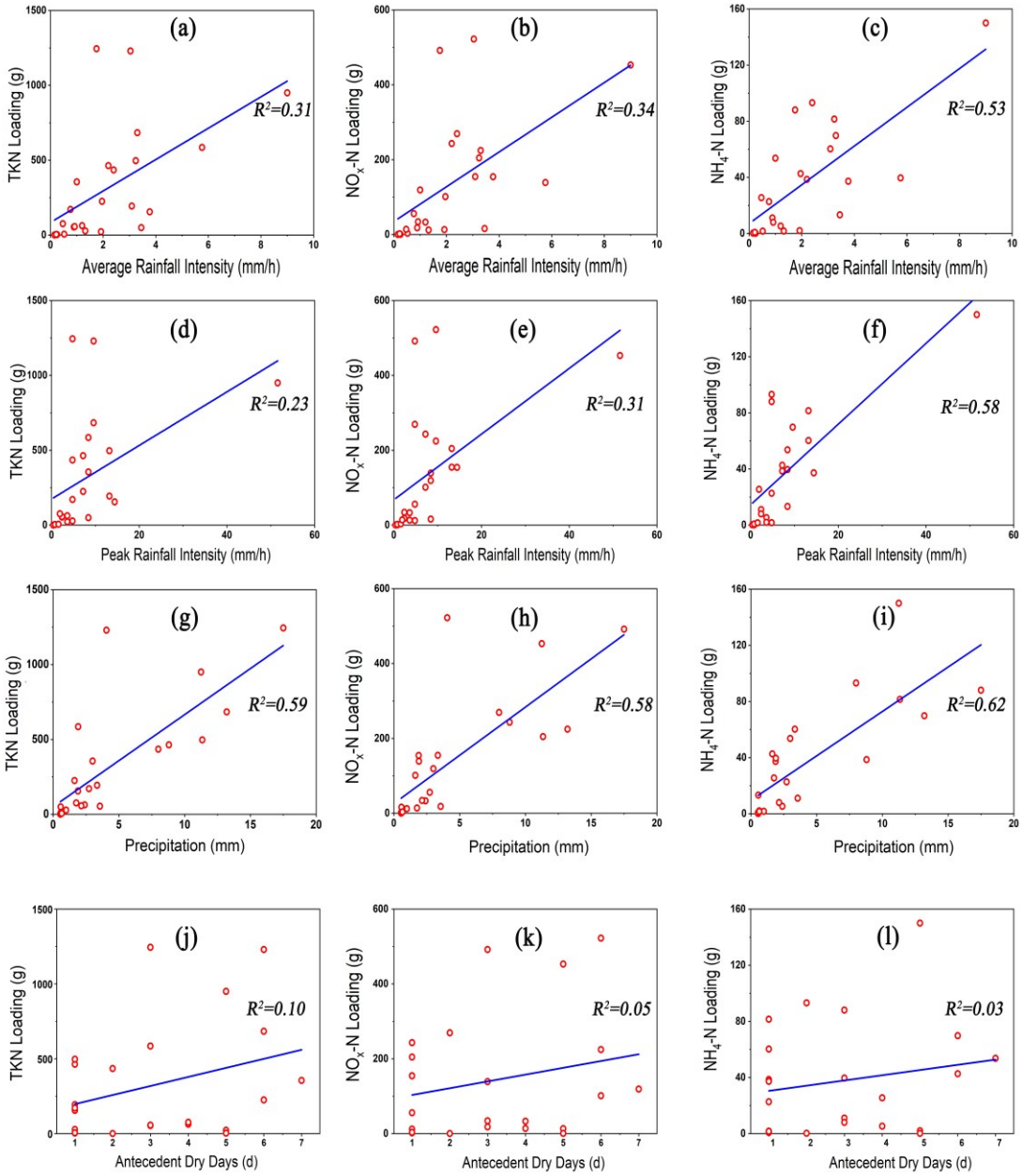

Figure 3.6 Correlations of the nitrogen loadings in each storm event with **(a-c)** the average rainfall intensity, **(d-f)** peak rainfall intensity, **(g-i)** total rainfall depth, **(j-l)** antecedent dry days based on observed data (monitored EMCs with simulated daily discharge volume) in 2010 - 2016.

Egodawatta et al. (2007) pointed out that the relationship between TSS wash-off and rainfall intensity is a step-wise function which means the influence of rainfall intensity at different thresholds could be different and thus affect nitrogen attached on TSS. Therefore, we further clustered the 7-year monitoring data into four groups in order to better understand the influence

of each rainfall factor on nitrogen EMCs (Table 3.4). Group 1 and Group 2 had the average rainfall intensity < 2 mm/h, while Group 3 and Group 4 had > 2 mm/h; and Group 1 and Group 3 had rainfall duration < 2 hours, while Group 2 and Group 4 had > 2 hours. In terms of the average nitrogen concentration, Group 1 rainfall events display a slightly higher average NH_4-N EMC value compared with other groups with 0.46 mg/L, while Group 3 and Group 4 show the highest average TKN and NO_x-N EMC values with 2.72 mg/L and 1.51 mg/L, respectively. The disparity between Group 3 and 4 can be attributed to the nitrification and denitrification process in the stormwater runoff. Moreover, NO_x-N and NH_4-N have the largest range in Group 4 which is related to the relatively higher kinetic energy of high-intensity rainfall events resulting in more pollutants being transported (Kleibman et al., 2006). TKN EMCs in Group 4 is lower than in Group 3 probably due to the nitrification process. With the increase of rainfall intensity and duration, the more ammonia will transform to nitrate and led a high average EMC value of NO_x-N in Group 4 (Li et al., 2022). Meanwhile, as the increase of rainfall intensity and rainfall depth, interaction between dilution and washout may also affect nitrogen EMC in urban stormwater runoff (Egodawatta et al., 2007)

Table 3.4 Rainfall characteristics and stormwater nitrogen EMCs in 2010 - 2016. Both average values and data ranges (in the brackets) are provided.

Rainfall events	Rainfall Characteristics			Stormwater EMCs		
	Intensity (mm/h)	**Duration (h)**	**Antecedent dry days (d)**	**TKN (mg/L)**	**NO_x-N (mg/L)**	**NH_4-N (mg/L)**
Group 1	0.34 (0.07-0.77)	1.08 (0.33-2)	4.3 (1-14)	2.07 (0.72-5.89)	1.08 (0.28-2.83)	0.46 (0.11-1.08)
Group 2	1.27 (0.07-1.96)	4.75 (2.08-16)	3.8 (1-17)	2.32 (0.46-6.19)	1.39 (0.34-2.78)	0.34 (0.05-1.17)
Group 3	2.89 (2.02-3.83)	0.97 (0.25-2)	5.8 (1-18)	2.72 (1.08-7.31)	1.25 (0.52-2.99)	0.42 (0.06-1.52)
Group 4	8.04 (3.9-35.1)	5.29 (2.08-14.83)	4.1 (1-12)	2.42 (0.69-7.56)	1.51 (0.5-3.91)	0.44 (0.11-1.81)

To further quantify the influence of rainfall intensity, rainfall duration and antecedent dry days on the TKN concentration and on first flush during a storm event, we used the model to examine 12 scenarios and a control group by changing one parameter each time (Table 3.5). The control group was set with the rainfall intensity 2.4 mm/h, rainfall duration 2 hours and dry days was 6. The simulated results showed that both rainfall intensity and antecedent dry days affected the maximum TKN concentration in stormwater during a rainfall event (Figure 3.7). In MIKE Urban, the change of rainfall intensity not only affected the peak concentration but also the time to reach the peak, while the variation of antecedent dry days only changed the peak concentration with other parameters remained constant. On the contrary, rainfall duration only changed the time of concentration back to baseflow condition which will not affect the maximum concentration value during a storm event. Same responses were also shown in catchments at Wuhan, China (Li et al., 2007) and Danang City, Vietnam (Nguyen et al., 2020).

Table 3.5 Scenarios for testing the impacts of rainfall characteristics on nitrogen concentrations during storm events.

Scenario	Rainfall intensity (mm/h)	Rainfall duration (h)	Antecedent dry days
0 (Control)	2.4	2	6
1	1.2	2	6
2	1.8	2	6
3	4.8	2	6
4	7.2	2	6
5	2.4	0.5	6
6	2.4	1	6
7	2.4	4	6
8	2.4	8	6
9	2.4	2	2
10	2.4	2	4
11	2.4	2	10
12	2.4	2	15

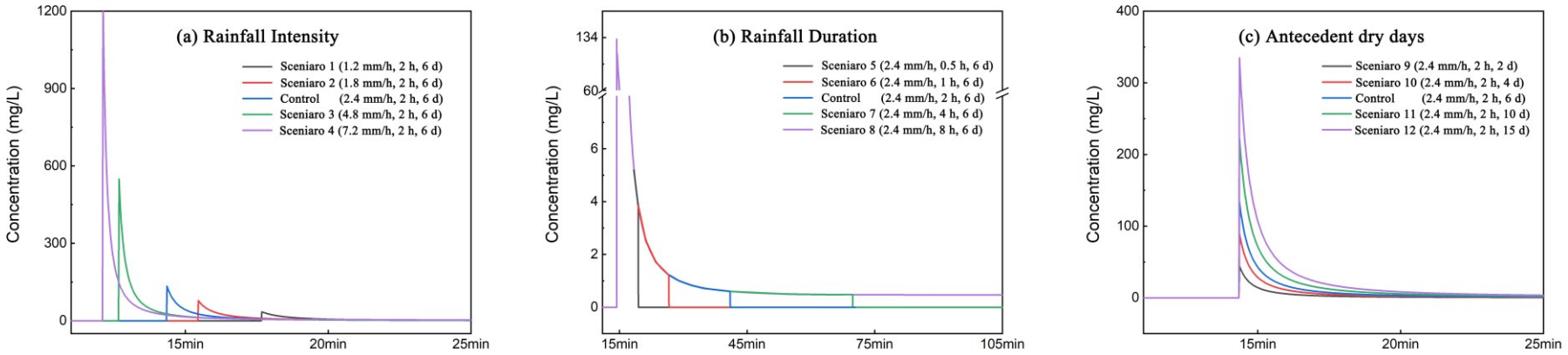

Figure 3.7 Impacts of different rainfall characteristics on TKN concentration at the storm outfall during a storm event: (a) rainfall intensity; (b) rainfall duration; and (c) antecedent dry days.

3.4.2.3 Impact of urban densification

Urban population growth is a typical phenomenon of urban densification. As the population increases, anthropogenic activities, traffic characteristics and road conditions will change and thus affect TSS loading accumulated on urban surface. Understanding the relationship between TSS loading with population is necessary which can help us predict TSS loading in the future. Population in 30th Ave catchment only collect at the year of 2008, 2009, 2012, 2014, 2016 and 2019 from municipal census, which had a small growth rate of 0.89% and has weak correlation with TSS loading. Therefore, we evaluated the relationship between Edmonton population and total TSS loading in storm seasons (May to September) in the city from 2000 to 2019, also the average contribution of TSS loading in 30th Ave (20.2%) to the total TSS loading from stormwater. With the increasing of catchment population, TSS loading also increases with a R^2 of 0.62 (Figure 3.7). Based on the population projection in 2050, population in Edmonton and the 30th Ave catchment will reach to 1.5 million and 0.22 million people, with the TSS loading will up to 1.23 million kg in 30th Ave.

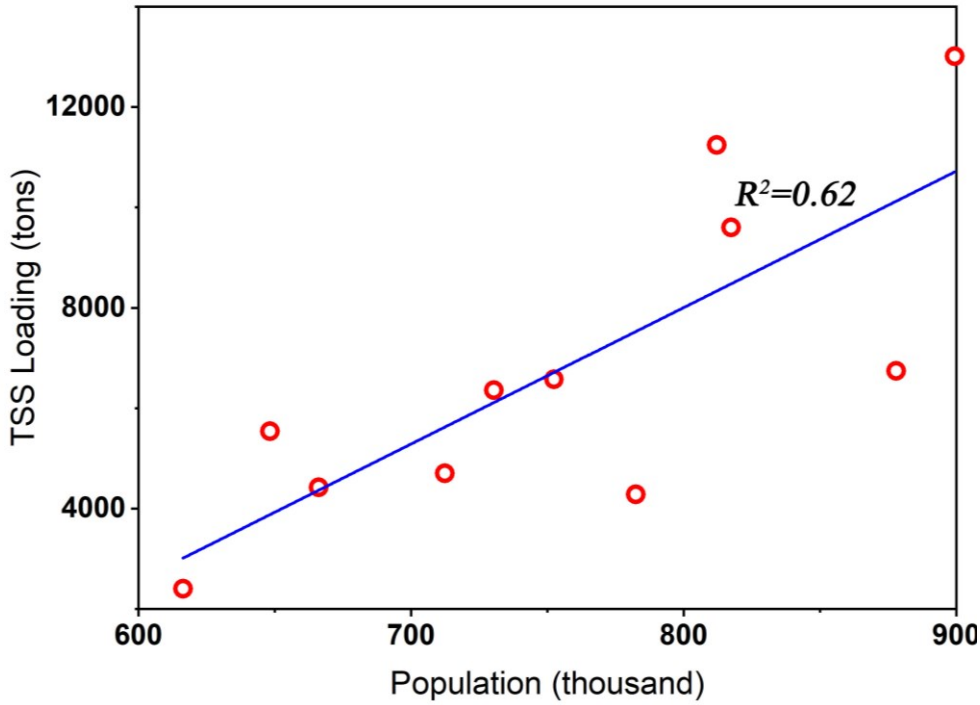

Figure 3.8 Relationship between TSS loading in storm seasons (May - September) with population in Edmonton from 2000 to 2019 (only 11 years had municipal census).

3.4.2.4 First flush effect

The first flush effect is also a phenomenon occurring in stormwater runoff which is depends on rainfall intensity, rainfall duration, antecedent dry days, watershed area and imperviousness area (Lee et al., 2002). Under the first flush effect, the concentration of pollutants is usually substantially higher in the beginning of the storm events. FF_{30} was used to assess the magnitude of the first flush effect which means the percentage of pollutant mass transported by the early 30% of the total discharge volume. The value of FF_{30} is classified into three levels as high, medium and non-first flush effect with $FF_{30} \geq 50\%$, $30\% \leq FF_{30} \leq 50\%$ and $FF_{30} \leq 30\%$ (Zhang et al., 2013). The modelling results show that the fractions of nitrogen loading transported by the first 30% of runoff volume ranged from 32.1% to 59.8% during the storm events in year of 2010 to 2016. The similar results also found in Chongqing, China, with the

mean FF_{30} values for TN, NH_4-N and NO_3-N were 58.1%, 52.8% and 62.0%, respectively (Zhang et al., 2013). Hathaway et al. (2012) also indicated that nitrogen species displayed a strong FF effect with NH_4-N > TKN > NO_x-N in Raleigh, USA.

3.4.3 Predicting nitrogen loadings in 2050

The monthly values for the year of 2050 were compared with the monthly mean values in historical period (Table 3.6). The monthly loading variation of each nitrogen species during storm events from May to September between future time and the historical time period was shown in Table 3.7. The simulation results indicated that the total loading of TN, TKN, NO_x-N and NH_4-N during May to September in 2050 were predicted to increase by 33.7%, 39.4%, 27.1%, and 31.1% compared to average loading during May to September from 2010 to 2016. TN loadings are calculated by adding loadings of TKN and NO_x-N. July was detected has the largest nitrogen loading in 2050 (TN, 1.79 kg·N/ha/month; NO_x-N, 0.64 kg·N/ha/month; NH_4-N, 0.21 kg·N/ha/month) which is closely related to the increasing precipitation and population. Increased precipitation would result in increased surface runoff value and thus increased the loading in July. The increasing of population would cause more anthropogenic activities and thus more sediment will generate on urban road surface which will lead more nitrogen wash off during storm events. May and September were detected as two months have the largest increasing (over 25%) of the nitrogen loadings in 2050 possibly due to these two months had relatively low values in the historical period.

Table 3.6 Observed nitrogen loadings for the historical period, and modeled nitrogen loadings for 2050. Data were averaged over each month and per hectare (May - September).

Period	Month	Nitrogen Loadings (kg·N/ha/month)			
		TN	TKN	NO_x-N	NH_4-N
Historical (2010 - 2016)	May	0.82	0.46	0.36	0.16
	June	0.98	0.56	0.42	0.11
	July	1.33	0.72	0.61	0.12
	August	0.91	0.41	0.51	0.11
	September	0.74	0.41	0.33	0.18
Future (2050)	May	1.23	0.70	0.53	0.18
	June	1.15	0.65	0.49	0.16
	July	1.50	0.85	0.64	0.21
	August	1.06	0.51	0.54	0.13
	September	1.45	0.83	0.62	0.21

Note: TN loading was calculated by adding TKN loading and NO_x-N loading

Projection of TN loading under climate change by modelling works in urban stormwater in different catchments worldwide were collected from the literature and compared with the present results (Table 3.1). All the studies represented an increasing TN loading in the future except for the catchment in Australia. This is due to future land use and climate change were considered together. There will be an increased impermeable area on grassland and will lead a decrease on TN loading. In cold regions, the existing, limited simulation results all suggest than TN tend to have a large increasing in the future, including projections in Stockholm, Sweden (6.7% - 140%), Upper Assiniboine River Basin, Canada (10.3% - 49.6%) and Edmonton (present study). Overall, the simulated nitrogen loading closely matched the dynamic of future rainfall patterns (e.g., rainfall intensity and maximum daily rainfall) and surface runoff. Some studies (i.e., studies in Mankyung, South Korea; Mahabad, Iran; Singapore) applied different Global Climate Models (GCMs) scenarios and considered

frequent occurrence of heavy precipitation which may result in a disparity of future TN loading with the baseline.

Table 3.7 Monthly changes of nitrogen loadings in the future (2050), compared to the historical data (2010-2016). Mean value and data range (in the bracket) are both listed.

Month	Changes (%) in Nitrogen Loadings			
	TN	**TKN**	**NO_x-N**	**NH_4-N**
May	49.7 (-5.8~321.5)	52.8 (-0.1~237.2)	45.9 (-16.9~532.1)	7.8 (-48.8~108.2)
June	17.7 (-41.2~178.0)	18.3 (-42.9~171.4)	16.8 (-38.9~228.1)	25.4 (-33.3~658.8)
July	12.8 (-56.7~279.5)	19.3 (-55.1~236.1)	5.2 (-58.7~358.4)	34.4 (-8.6~350.5)
August	15.9 (-43.4~216.3)	25.6 (-32.2~264.0)	8.1 (-61.8~233.9)	14.0 (-39.1~248.5)
September	97.0 (11.7~403.1)	102.6 (21.0~525.2)	90.1 (1.3~374.8)	17.0 (-26.9-381.5)

3.4.4 Limitations of the present model

Compared with other stormwater pollutant loading models, the first limitation of the current model is that it only considers catchment characteristics (e.g., impervious area, land use) as a lumped characteristic for the entire catchment. This is limited by MIKE Urban itself and may cause some error on the modeling result (Liu et al., 2012). For example, the model is unable to consider different build-up rates (Liu et al., 2013) and wash-off coefficients from different land use types (Lee et al., 2009; van der Sterren et al., 2012). Therefore, unable to quantify accurately the loading distribution from each land type. The second limitation is that MIKE Urban and thus the present model do not consider soil properties, climatic conditions including wind speed, solar radiation and humidity. More modeling studies are needed on considering

these factors (e.g., SWAT) in our future research and make comparisons between model results. The third limitation is that this model cannot simulate water quality in snowmelt runoff. Thus, some other software packages or modeling studies are needed to examine the nitrogen wash-off process during snowmelt runoff in the context of climate change.

3.5 Conclusions

Modeling of stormwater nitrogen loading from an urban catchment in cold region under the impacts of both climate change and urban densification by build-up and wash-off models is limited. This study presents a build-up and wash-off model (MIKE Urban) to simulate the loading of nitrogen species (TN, TKN, NO_x-N and NH_4-N) in an urban catchment by the projections of rainfall precipitation and population. The current model results are un-biased due to we only considered one scenario. We also investigate the impact of rainfall intensity, rainfall duration, antecedent dry days and urban densification on the variation of loadings based on both observed data and numerical simulation.

- According to our observed data, antecedent dry days had a moderate correlation with TSS loading but weak correlation with nitrogen loadings. Rainfall precipitation had a stronger correlation with loadings than rainfall intensity, which indicated that loading was not affected by a single rainfall factor.

- Based on calibrated and validated nitrogen EMCs and monthly loadings, MIKE Urban shows an acceptable performance on simulating stormwater quality on urban surface runoff. The responses of the input parameters are agreed with previous studies (i.e., build-up rate and maximum build up limit are the most sensitive parameters).

- Based on the model, rainfall intensity and duration and antecedent dry days are important factors for nitrogen loadings. The model also showed first flush effect well for storm events, with 32.1 - 59.8% of the nitrogen loadings transported by the first 30% of runoff volume.

- By the projection of rainfall precipitation, population and TSS loading supported by statistic results in the past 20 years, we predicted nitrogen loadings in 2050 at 30th Ave catchment in Edmonton. The results indicated that the total loading of TN, TKN, NO_x-N and NH_4-N during May to September in 2050 were predicted to increase by 33.7%, 39.4%, 27.1%, and 31.1% compared to average loading during May to September from 2010 to 2016. July was detected as the largest monthly nitrogen loadings in 2050 due to a largest rainfall precipitation and more anthropogenic activities.

Chapter 4 General Conclusions and Future Research Directions

4.1 General Conclusions

This thesis first examined nitrogen loadings (TN, TON, NO_x-N and NH_4-N) and their temporospatial variabilities of stormwater/snowmelt runoff at the outfalls of four urban catchments in a major, cold-region city (Edmonton), Canada, for the past almost 30 years (1991 to 2018). Then, the thesis developed build-up and wash-off models using MIKE Urban for stormwater in one catchment, calibrated and validated the model against nitrogen EMCs and loadings measured in 2010-2016, and predicted the loadings in 2050 in the context of climate change and urban densification.

The innovation of this research is summarized below: **(1)** it examined long-term (28-year) nitrogen loadings in urban stormwater/snowmelt, which has not been reported and enable us to assess the temporal variabilities (trend and abrupt change) of the loadings for the first time in the literature. **(2)** it evaluated nitrogen loading in both snowmelt and stormflow in an urban catchment which has scarce relevant studies. **(3)** it compared nitrogen loading in urban surface runoff across different catchments worldwide, which has not been summarized before. **(4)** it predicted stormwater nitrogen loading in the future based on build-up and wash-off models with the projections of precipitation and population, which is limited for an urban catchment in cold region. This research advances the knowledge of nitrogen loadings in urban stormwater and snowmelt in cold regions, which will be useful for guiding the development and updating policies on urban stormwater/snowmelt management. The detailed conclusions have been provided in Chapters 2 and 3. General conclusions from this research are summarized below:

- Annual variabilities of TN, TON, NO_x-N and NH_4-N loadings at four catchment outfalls were similar, which had an increasing trend first from 1992 to 2011 due to the increase of precipitation, then decrease to 2015 due to the city began to discharge stormwater into creeks and finally a small rise to 2018 because of cross-connections between sanitary and storm sewer lines.
- Monthly variabilities of TON and NO_x-N are similar to TN with higher values during wet season. March and July are usually detected as two peaks and largest inter-fluctuation due to the timing and frequency of snowmelt and storms. On the contrary, NH_4-N loading usually remain low and stable due to NH_4-N mainly from baseflow.
- Loadings of TN, TON and NO_x-N in wet season (storm season) are substantially larger than in dry season (snowfall/snowmelt season) with ratios of 2.26, 2.77 and 2.93, respectively. However, NH_4-N loadings in dry season and wet season are very close.
- Loading is simultaneously affected by multiple and complex factors (climate such as temperature, rainfall/snow characteristics, antecedent dry days, population, sewer systems, stormwater management, land covers and land uses, etc.).
- TN loading in Edmonton is quite larger than other catchments in Canada and similar with those catchments in Northern Europe, but lower than Western European countries. Compared with catchments in USA, TN loading is close to those catchments in Northern and central USA, but less than those catchments located along the coastal line.
- Based on calibrated and validated EMCs and loading of TKN, NO_x-N and NH_4-N, build-up and wash-off model shows a great performance on simulating stormwater quality on

urban runoff.

- Based on our observed nitrogen EMCs and monthly loading, antecedent dry days had a moderate correlation with TSS loading but weak correlation with nitrogen loadings. Rainfall precipitation had a stronger correlation with loadings than rainfall intensity.
- The simulation results showed that total nitrogen loadings (TN, TKN, NO_x-N and NH_4-N) from May to September will increase 33.7%, 39.4%, 27.1% and 31.1% in 2050, compared to the average loadings from 2010 to 2016. July had the largest monthly nitrogen loadings in 2050 due to a largest rainfall precipitation and more anthropogenic activities.

4.2 Future Research Directions

Based on the current research, suggestions on future research directions are listed below.

- It is suggested to carry out an extensive stormwater quality and flow monitoring program at specific locations of storm sewer system that corresponds to different land use (e.g., park area, commercial area, unregulated industrial sites). These monitoring will help identify actual nitrogen loadings in different land uses.
- Given that multiple factors can affect the nitrogen loadings simultaneously, further correlation analysis (e.g., principal component analysis) should be conducted to rank each influencing factor, and correlate the loadings to multiple factors simultaneously.
- More trend analysis test methods should be tested to discern the characteristics of water quality data sequence. The Mann-Kendall and Pettitt test methods used in this study have been used mostly for meteorological or climate data (e.g., temperature, precipitation).
- More studies are needed on the loadings of other water quality parameters in stormwater

and snowmelt, such as phosphorous, chloride and TSS (due to road de-icing), as well as E. coli. Currently, seldom researches have studied the long-term variation of these pollutants under cold climates.

- System managers should pay attention to the pollutant loadings in receiving water bodies contributed from stormwater/snowmelt, particularly for the shock effect due to the first flush of pollutants in spring. Therefore, new regulations should set standards on pollutant loading together with concentration in receiving water bodies to mitigate stormwater environmental risks.
- MIKE Urban model considered catchment characteristics (e.g., impervious area, land use) as a lumped characteristic which may cause errors on the model result (Liu et al., 2012). To overcome this deficiency, we can divide the catchment into different land use and simulate each part separately or we can apply modeling tools, which consider the effect of land use (e.g., PLOAD).
- The build-up rate and maximum build-up limit of TSS was calculated based on monitored TSS loading and discharge volume. The improvement can be achieved by conducting more field monitoring on sediment accumulation at different land uses to get accurate build-up rate for each land type. This can enable the estimation of loading from each land use separately within the catchment.
- Soil properties, climatic conditions including wind speed, solar radiation and humidity are also important factors affecting the results. MIKE Urban does not take into consideration on these factors. These factors need to be considered by using other

modeling tools/software (e.g., SWAT) in the future research, and the results can be compared with the current modeling results.

- In addition to urban densification (population) and climate change, the development of industry, commerce and institutions may different from the current condition in Edmonton. These are also important factors affecting pollutant build-up process that should be considered in the future research.
- MIKE Urban model cannot simulate water quality in snowmelt runoff. Thus, other software packages or modeling tools (e.g., GWLF) are needed to stimulate the nitrogen loadings in snowmelt runoff.

References

Alamdari, N., Claggett, P., Sample, D.J., Easton, Z.M., & Yazdi, M.N. (2022). Evaluating the joint effects of climate and land use change on runoff and pollutant loading in a rapidly developing watershed. *Journal of Cleaner Production*, 330, 129953.

Alamdari, N., Sample, D.J., Steinberg, P., Ross, A C., & Easton, Z M. (2017). Assessing the effects of climate change on water quantity and quality in an urban watershed using a calibrated stormwater model. *Water*, 9(7).

Alvarez-Cobelas, M., Angeler, D.G., & Sanchez-Carrillo. (2008). Export of nitrogen from catchments: A world-wide analysis. *Environmental Pollution*, 156: 261-269.

Andersen, H.E., Pedersen, M.L., Jørgensen, O., & Kronvang, B., (2001) Analysis of the hydrology and flow of nitrogen in 17 Danish catchments. *Water Science and Technology*, 47, 63-68.

Anisfeld, S.C., Barnes, R.T., Altabet, M.A., & Wu,T. (2007). Isotopic apportionment of atmospheric and sewage nitrogen sources in two Connecticut rivers. *Environmental Science and Technology*, 41: 6363-6369.

Arheimer, B., Andersson, L., & Lepisto¨, A., (1996) Variation of nitrogen concentration in forest streams e influences of flow, seasonality and catchment characteristic*s*. *Journal of Hydrology*, 179, 281-304.

Baker, L.A., Hope, D., Xu, Y., Edmonds, J., & Lauver, L. (2001). Nitrogen balance for the Central Arizona-Phoenix (CAP) ecosystem. *Ecosystems*, 4: 582-602.

Ballo, S., Liu, M., Hou, L.J., & Chang, J., (2009). Pollutants in stormwater runoff in Shanghai

(China): Implications for management of urban runoff pollution. *Natural Science*, 19, 873–880.

Balter, M. (2013). Archaeologists say the Anthropocene is here— but it began long ago. *Science*, 340(6130), 261–262.

Baltic NEST data: data.ecology.su.se/models/bed.htm

Batroney, T., Wadzuk, B.M., & Traver, R.G. (2010). Parking deck's first flush. *Journal of Hydrologic Engineering*, 15 (2), 123–128.

Behrendt, H., & Opitz, D., (2000) Retention of nutrients in river systems: dependence on specific runoff and hydraulic load. *Hydrobiologia*, 410, 111-122.

Bernhardt, E.S., Band, L.E., Walsh, C.J., & Berke, P.E. (2008). Understanding, managing, and minimizing urban impacts on surface water nitrogen loading. *Annals of the New York Academy of Sciences*, 1134: 61-96.

Bhaduri, B., Harbor, J., Engel, J., & Grove, M., (2000) Assessing watershed-scale, long-term hydrologic impacts of land use change using a GIS-NPS model. *Environmental Management*, Vol. 26, No. 6, pp. 643-658.

Borah, D.K., Yagow, G., Saleh, A., Barnes, P.L., Rosenthal, W., Krug, E.C., & Hauck, L.M., (2006). Sediment and Nutrient Modeling for TMDL Development and Implementation. Soil and Water Division of ASABE, 49, 967-986.

Borah, D.K., Weist, J.H., Wall, J.D., & Powell, D.N., (2009). Watershed models for storm water management: comparing hydrologic and hydraulic procedures. *World Environmental and Water Resources Congress*, 6517–6526.

Boyer, E.W., Howarth, R.W., & Galloway, J.N. (2006). Riverine nitrogen export from the continents to the coasts. *Global Biogeochemical Cycles*, 20, GB1S91.

Bratt, A.R., Finlay, J.C., Hobbie, S.E., Janke, B.D., Worm, A.C., & Kemmitt, K.L. (2017). Contribution of leaf litter to nutrient export during winter months in an urban residential watershed. *Environmental Science and Technology*, 51:3138-47.

Butler, D., & Clark, P., (1995). Sediment management in urban drainage catchments. *Report* 134. London: Construction Industry Research Information Association.

Butterbach-Bahl, K., & Dannenmann, M. (2011). Denitrification and associated soil N_2O emissions due to agricultural activities in a changing climate. *Current Opinion in Environmental Sustainability*, 3: 389-395.

Cade-Menun, B.J, Bell, G., Baker-Ismail, S., Fouli, Y., Hodder, K., McMartin, D.W., Perez-Valdivia, C., & Wu, K.S., (2013). Nutrient loss from Saskatchewan cropland and pasture in spring snowmelt runoff. *Canadian Journal of Soil Science*, 22 April, 2013.

Camargo, J.A., Alonso, A. (2006). Ecological and toxicological effects of inorganic nitrogen pollution in aquatic ecosystems: A global assessment. *Environmental International*, 32: 831-849.

Cao, W., Hong, H., Zhang, Y., Chen, N., Zeng, Y., & Wang, W., (2006) Anthropogenic nitrogen sources and exports in a village-scale catchment in southeast China. *Environmental Geochemistry and Health*, 28, 45-51.

Caraco, N.F., & Cole, J.J., (1999). Human impact of nitrate export: an analysis using major world rivers. *Ambio*, 28, 167-170.

Carey, R.O., Hochmuth, G.J., Martinez, C.J., Boyer, T.H., Nair, V.D., & Dukes, M.D. (2012). Regulatory and resource management practices for urban watersheds: The Florida experience. *HortTechnology*, 22:418– 429.

Causse, J., Baures, E., Mery, Y., Jung, A., & Thomas, O. (2015). Variability of N export in water: A Review. *Critical Reviews in Environmental Science and Technology*, 45:20, 2245-2281.

Cha, Y., Stow, C.A., Reckhow, K.H., DeMarchi, C., & Johengen, T.H. (2010). Phosphorus load estimation in the Saginaw River, MI using a Bayesian hierarchical/multilevel model. *Water Research*, 44(10), 3270-3282.

Chen, L., Zhi, X.S., Shen, Z.Y., Dai, Y., & Aini, G. (2018). Comparison between snowmelt-runoff and rainfall-runoff nonpoint source pollution in a typical urban catchment in Beijing, China. *Environmental Science and Pollution Research*, 25:2377-2388.

Chow, M.F., Zulkifli, Y., & Mohamed, M., (2011). Quality and first flush analysis of stormwater runoff from a tropical commercial catchment. *Water Science and Technology*, 63 (6), 1211-1216.

Chow, M. F., Yusop, Z., & Abustan, I. (2015). Relationship between sediment build-up characteristics and antecedent dry days on different urban road surfaces in Malaysia. *Urban Water Journal*. Vol. 12, No. 3, 240-247.

City of Edmonton. (2018). Climate Resilient Edmonton, Adaptation strategy and action plan.

Clair, T.A., Pollock, T.L., & Ehrman, J.M., (1994). Exports of carbon and nitrogen from river basins in Canada's Atlantic provinces. *Global Biogeochemical Cycle*s, 8, 441-450.

Clark, S.E., & Pitt, R. (2012). Targeting treatment technologies to address specific stormwater pollutants and numeric discharge limits. *Water Research*, 46, 6715-6730.

Collins, K.A., Lawrence, T.J, Stander, E.K., Jontos, R.J., Kaushal, S.S., Newcomer, T.A., Grimm, N.B., & Ekberg. M, C., (2010). Opportunities and challenges for managing nitrogen in urban stormwater: A review and synthesis. *Ecological Engineering*, 36, 1507-1519.

Cooke, S.E., & Prepas, E.E., (1998). Stream phosphorus and nitrogen export from an agricultural and forested watershed on the Boreal Plain. *Canadian Journal of Fisheries and Aquatic Sciences*, 55, 2292-2299.

Crabtree, B., Moy, F., Whitehead, M., & Roe, A. (2006). Monitoring pollutants in highway runoff. *Water and Environment Journal*, 20(4), 287-294.

David, L.R., Charles, J.P., David, K.M., & Charles, G.C. (2012). Assessing total nitrogen in surface-water samples-precision and bias of analytical and computational methods. *Scientific Investigations Report*, 2012-5281.

Deng, Z. Q., Sun, S. W., & Gang, D. D. (2012). Modeling nitrate-nitrogen removal process in first-flush reactor for stormwater treatment. *Bioprocess and Biosystem Engineering*, 35:865-874.

DHI, Mike Urban Collection System-User guide. 2017.

Dierberg, F.E., & DeBusk, T.A., (2008). Particulate phosphorus transformations in south Florida stormwater treatment areas used for Everglade's protection. *Ecological* Engineering, 34, (2), 100-115.

Dimmell, M. (2021). Our Weight in Canada: Western Canadian population growth tips the scales. Canada West Foundation. https://cwf.ca/research/publications/our-weight-in-canada-western-canadian-population-growth-tips-the-scales/

Divers, M.T., Elliott, E.M., & Bain, D.J. (2014). Quantification of nitrate sources to an urban stream using dual nitrate isotopes. *Environmental Science and Technology*, 48:10580-10587.

Egodawatta, P., Thomas, E., & Goonetilleke, A. (2007). Mathematical interpretation of pollutant wash-off from urban road surfaces using simulated rainfall. *Water Resource*. 41: 25-31.

Ekka, S.A., Rujner, H., Leonhardt, G., Blecken, G.T., Viklander, M., Hunt, & W.F. (2021). Next generation swale design for stormwater runoff treatment: a comprehensive approach. *Journal of Environmental Management*, 279, 16.

El-Khoury, A., Seidou. O., Lapen,D.R., Que, Z., Mohammadian, M., Sunohara, M., & Bahram, D., (2015). Combined impacts of future climate and land use changes on discharge, nitrogen and phosphorus loads for a Canadian river basin. *Journal of Environmental Management*, 15, 76-86.

Emma, C.S., Penelope, W., Alan, R.T., & Eric, A.D. (2013). The role of nitrogen in climate change and the impacts of nitrogen–climate interactions in the United States: foreword to thematic issue. *Biogeochemistry*, 114:1-10.

Environmental Monitoring Program report. (2000-2018). EPCOR drainage system, Golder Associates Ltd.

Erik, J., Brian, K., Mariana, M., Martin, S., Kristina, M.H., Hans, E.A., Torben, L.L., Meryem, B., Arda, Ö., & Jørgen, E.O. (2009). Climate change effects on runoff, catchment phosphorus loading and lake ecological state, and potential adaptations. *Journal of Environmental Quality*, 38:1930-1941.

Fant, C., Srinivasan, R., Boehlert, B., Rennels. L., Chapra, S.C., Strzepek, K.M., Corona, J., Allen, A., & Martinich, J. (2017). Climate change impacts on US water quality using two models: HAWQS and US basins. *Water*, 9, 118.

FAO, F. (2018). Yearbook 2018. Food and Agriculture Organization of the United Nations.

Feng. M., & Shen, Z. Y. (2021). Assessment of the impacts of land use change on non-point source loading under future climate scenarios using the SWAT model. *Water*, 13, 874.

Filoso, S., Martinelli, L.A., Williams, M.R., Lara, L.B., Krusche, A., Ballester, M.V., Victoria, R., & De Camargo, P.B., (2003). Land use and nitrogen export in the Piracicaba River basin, Southeast Brazil. *Biogeochemistry*, 65, 275-294.

Gaafar, M., Zhang, Q. Y., & Davis, E. G. R. (2020). Impact of variability in decay coefficients on simulating monochloramine dissipation in storm sewers. *Journal of Hydrology*, 590 125238

Galfi, H., Österlund, H., Marsalek, J., & Viklander, M. (2016). Indicator bacteria and associated water quality constituents in stormwater and snowmelt from four urban catchments, *Journal of Hydrology*, Vol 539; 125-140.

Galloway, J.N., Dentener, F.J., & Capone, D.G. (2004). Nitrogen cycles: past, present, and future. *Biogeochemistry*, 70: 153-226.

Gao, C., Zhu, J.G., Zhu, J.Y., Gao, X., Dou, Y.J., & Hosen, Y., (2004) Nitrogen export from an agriculture watershed in the Taihu Lake area, China. *Environmental Geochemistry and Health*, 26, 199-207.

Gan, H.Y., Zhuo, M.N., Li, D.P., & Zhou, Y.Z., (2008). Quality characterization and impact assessment of highway runoff in urban and rural area of Guangzhou, China. *Environmental Monitoring and Assessment*, Vol 140: 147-159.

Göbel, P., Diekers, C., & Coldewey, W. G. (2006). Storm water runoff concentration matrix for urban areas. *Journal of Contaminant Hydrology*, 91, 26-42.

Goonetilleke, A., Evan, T., Simon, G., & Dale, G. (2005). Understanding the role of land use in urban stormwater quality management. *Journal of Environmental Management*, 74 (1), 31-42.

Griffiths, L.N., & Mitsch, W.J. (2020). Nutrient retention via sedimentation in a created urban stormwater treatment wetland. *Science of the Total Environment*, 727, 138337.

Groffman, P.M., Law, N.L., Belt, K.T., Band, L.E., & Fisher, G.T. (2004). Nitrogen fluxes and retention in urban watershed ecosystems. *Ecosystems*, 7:393-403.

Gurung, D.P., Githinji, L.J.M., Ankumah, R.O. (2013). Assessing the Nitrogen and Phosphorus Loading in the Alabama (USA) River Basin Using PLOAD Model. *Air, Soil and Water Research*. January.

Hale, R.L., Turnbull, L., Earl, S., Grimm, N., Riha, K., & Michalski, G. (2014). Sources and transport of nitrogen in arid urban watersheds. *Environmental Science and Technology*, 48:6211-6219.

Hale, R.L., Turnbull, L., Earl, S.R., Childers, D.L., & Grimm, N.B. (2015). Stormwater infrastructure controls runoff and dissolved material export from arid urban watersheds. *Ecosystems*, 18:62-75.

Hathaway, J. M., Hunt, W.F., & Simmons O.D. III. (2010). Statistical evaluation of factors affecting indicator bacteria in urban stormwater runoff. *Journal of Environmental Engineering*, Vol 136, 12.

Hathaway, J. M., Tucker, R. S., Spooner, M., & Hunt, W. F. (2012). A traditional analysis of the first flush effect for nutrients in stormwater runoff from two small urban catchments. *Water Air Soil Pollution*, 223:5903-5915

Hayhoe, K., & Stoner, A., (2019) Alberta's climate future, final report. *ATMOS Research & Consulting.*

Henry, F. W., Nora, J. C., Aaron, J. G., Pascal, B., & Lyle, B., (2020). Landscape Controls on Nutrient Export during Snowmelt and an Extreme Rainfall Runoff Event in Northern Agricultural Watersheds. *Journal of Environmental Quality*, Vol 48, Issue 4: 787-1126.

Hobbie, S., Baker, L., Buyarski, C., Nidzgorski, D., & Finlay, J. (2014). Decomposition of tree leaf litter on pavement: implications for urban water quality. *Urban Ecosystem*, 17:369-85.

Hobbie, S.E., Finlay, J.C., Janke, B.D., Nidzgorski, D.A., Millet, D.B, & Baker, L.A. (2017). Contrasting nitrogen and phosphorus budgets in urban watersheds and implications for managing urban water pollution. *Proceedings of National Academy of Science USA*, 114:4177-4182.

House, W.A., Leach, D., Warwick, M.S., Whitton, B.A., Pattinson, S.N., Ryland, G., Pinder, A., Ingram, J., Lishman, J.P., Smith, S.M., Rigg, E., & Denison, F.H., (1997). Nutrient transport in the Humber Rivers. *Science of the Total Environment*, 194-195, 303-320.

Howarth, R.W., & Marino, R. (2006). Nitrogen as the limiting nutrient for eutrophication in coastal marine ecosystems: evolving views over three decades. *Limnology and Oceanography*. 51(1):364–376.

Høyas, T.R., Vagstad, N., Bechmann, M., & Eggestad, H.O., (1997). Nitrogen budget in the river Auli catchment: a catchment dominated by agriculture, in Southeastern Norway. *Ambio*, 26, 289-295.

Hristov, A.N., Hanigan, M., Cole, A., Todd, R., McAllister, T.A., Ndegwa, P.M., & Rotz, A. (2011). Review: ammonia emissions from dairy farms and beef feedlots. *Journal of Animal Science*. 91:1-35.

Hu, H., & Huang, G. (2014). Monitoring of non-point source pollutions from an agriculture watershed in South China. *Water*. 6(12): 3828-3840.

Huang, J.L., Du, P.F., Ao, C. T., Zhao, D.Q., Ho, M.H., & Wang, Z.S., (2007). Characterization of surface runoff from a subtropical urban catchment. *Journal of Environmental Science*, Vol 19, Issue 2: 148-152.

Huber, W.C., & Dickenson R.E., (1988). Storm water management model, SWMM, Version 4, *User's Manual*, US EPA, Athens, Georgia 30613, USA.

Hurst, H.E. (1951). Long term storage capacity of reservoirs. *Transactions of the American Society of Civil Engineers*, 116 (12), 776-808.

Jani, J., Lusk, M.G., Yang, Y.Y., & Toor, G.S. (2020). Wet season nitrogen export from a residential stormwater pond. *PLoS ONE*, 15(4): e0230908.

Janke, B.D., Finlay, J.C., Hobbie, S.E., Baker, L.A., Sterner, R.W., Nidzgorski, D., & Wilson, B.N. (2014). Contrasting influences of stormflow and baseflow pathways on nitrogen and phosphorus export from an urban watershed. *Biogeochemistry*, 121: 209-228.

Janke, B.D., Finlay, J.C., & Hobbie, S.E. (2017). Trees and streets as drivers of urban stormwater nutrient pollution. *Environmental Science and Technology*, 51: 9569-9579.

Jarvie, H.P., Withers, P.J.A., Bowes, M.J., Palmer-Felgate, E.J., Harper, D.M., & Wasiak, K. (2010). Stream water phosphorus and nitrogen across a gradient in rural - agricultural land use intensity. *Agricultural Ecosystem Environment*, 135:238-252.

Jones Jr., J.B., Petrone, K.C., Finlay, J.C., Hinzman, L.D., & Bolton, W.R., (2005). Nitrogen loss from watersheds of interior Alaska underlain with discontinuous permafrost. *Geophysical Research Letters*, 32.

Kaushal, S.S., Groffman, P.M., Band, L.E., Shields, C.A., Morgan, R.P., & Palmer, M.A. (2008). Interaction between urbanization and climate variability amplifies watershed nitrate export in Maryland. *Environmental Science and Technology*, 42: 5872-5878.

Kaushal, S.S., Mayer, P.M., Vidon, P.G., Smith, R.M., Pennino, M.J., & Newcomer, T.A. (2014). Land use and climate variability amplify carbon, nutrient, and contaminant pulses: a review with management implications. *Journal of the American Water Resources Association*, 50:585-614.

Kim, J. S., Oh, S. Y., & Oh, W. Y., (2006). Nutrient runoff from a Korean rice paddy watershed

during multiple storm events in the growing season. *Journal of Hydrology*, 327, 128-139.

Kim, L.H., Kayhanian, M., Zoh, K.D., & Stenstrom, M.K. (2005). Modeling of highway stormwater runoff. *Science of the Total Environment*, 293(1–3), 163-175.

Kim, L.H., Zoh, K.D., Jeong, S.M., Kayhanian, M., & Stenstorm, M.K. (2006). Estimating pollutant mass accumulation on highways during dry periods. *Journal of Environment Engineering*, 132: 985-993.

Kim, D.H., Jang, T., & Hwang, S. (2020). Evaluating impacts of climate change on hydrology and total nitrogen loads using coupled APEX-paddy and SWAT models. *Paddy and Water Environment*, 18: 515-529.

Kleinman, P.J.A., Srinivasan, M.S., Dell, C.J., Schmidt, J.P., Sharpley, A.N., & Bryant, R.B. (2006). Role of rainfall intensity and hydrology in nutrient transport via surface runoff. *Journal of Environmental Quality*. 35:1248-1259.

Kojima, K., Murakami, M., Yoshimizu, C., Tayasu, I., Nagata, T., & Furumai, H. (2011). Evaluation of surface runoff and road dust as sources of nitrogen using nitrate isotopic composition. *Chemosphere*, 84, 1716-1722.

Kronvang, B., Svendsen, L.M., Jensen, J.P., Dorge, J., (1999). Scenario analysis of nutrient management at the river basin scale. *Hydrobiologia*, 410, 207-212.

Krug, A., (1993). Drainage history and land use pattern of a Swedish river system e their importance for understanding nitrogen and phosphorus load. *Hydrobiologia*, 251, 285-296.

Lee, J., Bang, K., Ketchum, L., Choe, J., & Yu, M. (2002). First flush analysis of urban storm

runoff. *Science of the Total Environment*, 293:163-175.

Lee, S.W., Hwang, S.J., Lee, S.B., Hwang, H.S., & Sung, H.C. (2009). Landscape ecological approach to the relationship of land use patterns in watersheds to water quality characteristics. *Landscape Urban Plan*. 92: 80-89.

Lewis, D.B., & Grimm, N.B. (2007). Hierarchical regulation of nitrogen export from urban catchments: interactions of storms and landscapes. *Ecological Applications*, 17: 2347–2364.

Li, D., Wan, J., Ma, Y., Wang, Y., Huang, M., & Chen, Y. (2015). Stormwater runoff pollutant loading distributions and their correlation with rainfall and catchment characteristics in a rapidly industrialized city. *PLoS ONE*, 10(3).

Li, H., Liu, Z., Qin, Y., & Du, G., (2012) Characteristics of snowmelt runoff pollution and comparison with rainfall runoff pollution in Xi'an City. *Acta Scientiae Circumstantiae*, 32(11): 2795-2802.

Li, H.M., Tang, H.J., Shi, X.Y., Zhang, C.S., & Wang, X.L. (2014). Increased nutrient loads from the Changjiang (Yangtze) River have led to increased harmful algal blooms. *Harmful Algae*, 39 (0), 92-101.

Li, L.Q. (2007). First flush of storm runoff pollution from an urban catchment in China. *Journal of Environmental Sciences*, 19(3): p. 295-299.

Li, L.Q., Shan, B.Q., & Yin, C.Q., (2012). Stormwater runoff pollution loads from an urban catchment with rainy climate in China. Front. *Environmental Science Engineering*, 6(5): 672-677.

Li, T., & Kim, G. (2019). Impacts of climate change scenarios on non-point source pollution in the Saemangeum watershed, South Korea. *Water*, 11, 1982.

Littlewood, I., & Marsh, T. (2005). Annual freshwater river mass loads from Great Britain, 1975–1994: estimation algorithm, database and monitoring network issues. *Journal of Hydrology*, 304(1–4), 221-237.

Litwin, Y.J., & Donigian Jr, A.S., (1978). Continuous simulation of nonpoint pollution. *Journal of Water Pollution Control Federation*, 50, 2348-2361.

Liu, A., Egodawatta, P., Kjølby, M. J., & Goonetilleke, A. (2010). Development of pollutant build-up parameters for MIKE URBAN for Southeast Queensland, Australia. *Proceedings of the International MIKE by DHI Conference*, Modelling in a World of Change. DHI, CD Rom, pp. 1-15.

Liu, A., Egodawatta, P., & Goonetilleke, A., (2011). Variability of input parameters related to pollutants build up in stormwater quality modelling. In: E. M. Valentine, ed. *Proceeding of the 66 34th International Association for Hydro Environment Engineering and Research (IAHR) World Congress*, 26 June – 1 July. Brisbane, Queensland: Brisbane Convention and Exhibition Centre.

Liu, H., Jeong, J., Gray, H., Smith, S., & Sedlak, D.L. (2011). Algal uptake of hydrophobic and hydrophilic dissolved organic nitrogen in effluent from biological nutrient removal municipal wastewater treatment systems. *Environmental Science and Technology*, 46:713-721.

Liu, N.N., Rui, X.F., & Feng, J. (2016). Jinan urban rainstorm model based on Lattice

Boltzmann method. *Water Resource Power*, 34, 48-52.

Liu, X., Duan, L., Mo, J., Du, E., Shen, J., Lu, X., Zhang, Y., Zhou, X., He, C., & Zhang, F., (2011). Nitrogen deposition and its ecological impact in China: An overview. E*nvironmental Pollution*, 159: 2251-2264.

Liu, X., Ju, X., Zhang, Y., He, C., Kopsch, J., & Fusuo, Z. (2006). Nitrogen deposition in agroecosystems in the Beijing area. *Agricultural Ecosystem Environment*, 113: 370-377.

Liu, Z., Yang, J., Yang, Z., & Zou, J. (2012). Effects of rainfall and fertilizer types on nitrogen and phosphorus concentrations in surface runoff from subtropical tea fields in Zhejiang, China. *Nutrient Cycling in Agroecosystems*, 93: 297-307.

Liu, Z.Z., Wang, H., Li, N., Zhu, J., Pan, Z.W., & Qin, F. (2020). Spatial and Temporal Characteristics and Driving Forces of Vegetation Changes in the Huaihe River Basin from 2003 to 2018. *Sustainability*, 12, 2198.

Liu. A., Goonetilleke, A., & Egodawatta. P. (2012). Inherent errors in pollutant build-up estimation in considering urban land use as a lumped parameter. *Journal of Environmental Quality*, 41: 5, 1690-1694.

Lewis Jr., W.M., Melack, J.M., Mcdowell, W.H., McClain, & M., Richey, J.E., (1998). Nitrogen yields from undisturbed watersheds in the Americas. *Biogeochemistry*, 46, 149-162.

Long, T., Wellen, C., Arhonditsis, G., & Boyd, D. (2014). Evaluation of stormwater and snowmelt inputs, land use and seasonality on nutrient dynamics in the watersheds of Hamilton Harbour, Ontario, Canada. *Journal of Great Lakes Research*, 40 (4), 964-979.

Lucke, T., Drapper, D., & Hornbuckle, A., (2018). Urban stormwater characterization and nitrogen composition from lot-scale catchments - New management implications. *Science of the Total Environment*, 619-620, 65-71.

Luo, Z.X., Wang, T., Gao, M.R., Tang, J.L., & Zhu, B., (2012). Stormwater Runoff Pollution in a Rural Township in the Hilly Area of the Central Sichuan Basin, China. *Journal of Mountain Science*, 9: 16-26.

Lusk, M.G., & Toor, G.S. (2016). Dissolved organic nitrogen in urban streams: biodegradability and molecular composition studies. *Water Research*, 96:225-35.

Lyu, R., Zhang, J., Xu, M., & Li, J. (2018). Impacts of urbanization on ecosystem services and their temporal relations: A case study in Northern Ningxia, China. *Land Use Policy*, 77, 163-173.

Ma, Y.K., Wang, S.H., Zhang, X.Y., & Shen, Z.Y. (2021). Transport process and source contribution of nitrogen in stormwater runoff from urban catchments. *Environmental Pollution*, 289. 117824.

Mahbub, P., Ayoko, G.A., Goonetilleke, A., & Egodawatta, P., (2011). Analysis of the build-up of semi and non-volatile organic compounds on urban roads. *Water Research*, 45 (9), 2835-2844.

Mander, U., Kull, A., Kuusemets, V., & Tamm, T., (2000) Nutrient runoff dynamics in a rural catchment: influence of land-use changes, climatic fluctuations and ecotechnological measures. *Ecological Engineering*, 14, 405-417.

Mangimbulude, J.C., van Breukelen, B.M., Krave, A.S., van Straalen, N.M., & Roling, W. F.M.

(2009). Seasonal dynamics in leachate hydrochemistry and natural attenuation in surface run-off water from a tropical landfill. *Waste Management*, 29, 829-838.

Marchetti, R., & Verna, N., (1992). Quantification of the phosphorus and nitrogen loads in the minor rivers of the Emilia-Romagna coast (Italy). A methodological study on the use of theoretical coefficients in calculating the loads. *Science of the Total Environment* (Supplement), 315-336.

McCarthy, D. T. (2009). A traditional first flush assessment of E. coli in urban stormwater runoff. *Water Science and Technology*, 60(11), 2749-2757.

McDowell, W.H., & Asbury, C.E., (1994). Export of carbon, nitrogen, and major ions from three tropical montane watersheds. *Limnology and Oceanography*, 39, 111-125.

McKee, L.J., & Eyre, B.D., (2000). Nitrogen and phosphorus budgets for the sub-tropical Richmond River catchment, Australia. *Biogeochemistry*, 50, 207-239.

McKergow, L.A., Weaver, D.M., Prosser, I.P., Grayson, R.B., & Reed, A.E.G., (2003). Before and after riparian management: sediment and nutrient exports from a small agricultural catchment, Western Australia. *Journal of Hydrology*, 270, 253-272.

McLeod, S.M., Kells. J.M., & Putz, G.J. (2007). Urban Runoff Quality Characterization and Load Estimation in Saskatoon, Canada. *Journal of Environmental Engineering*, 132(11): 1470-1481.

Miguntanna, N. P., Goonetilleke A., Egodowatta, P., & Kokot, S. (2010). Understanding nutrient build-up on urban road surfaces. *Journal of Environmental Sciences*, 22(6) 806-812.

Miguntanna, N.P., Egodawatta, P., Goonetilleke, A., & Liu, A. (2013). Characterising nutrients wash-off for effective urban stormwater treatment design. *Journal of Environmental* Management, 120, 61-67.

Miller, J.E., (1984). Basic concepts of Kinematic-Wave models, U.S. *Geological Survey Professional Paper*, 1302.

Morgan, D., Johnston, P., Gill, L., & Osei, K., (2017), Sediment build-up on roads and footpaths of a residential area. *Urban Water Journal*, 14 (4), 378-385.

Montes, F., Rotz, C.A., & Chaoui, H. (2009). Process modeling of ammonia volatilization from ammonium solution and manure surfaces: a review with recommended models. *American Society of Agricultural and Biological Engineers*, 52(5):1707-1719.

Moss, A.J., Rayment, G.E., Reilly, N., & Best, E.K., (1992). A Preliminary Assessment of Sediment and Nutrient Exports from Queensland Coastal Catchments. Queensland Department of Environment and Heritage, Brisbane.

Mosello, R., Barbieri, A., Brizzio, M.C., Calderoni, A., Marchetto, A., Passera, S., Rogora, M., & Tartari, G., (2001). Nitrogen budget of Lago Maggiore: the relative importance of atmospheric deposition and catchment sources. *Journal of Limnology*, 60, 27-40.

Mueller, C., Zink, M., Samaniego, L., Krieg, R., Merz, R., & Rode, M. (2016). Discharge driven nitrogen dynamics in a mesoscale river basin as constrained by stable isotope patterns. *Environmental Science and Technology*, 50: 9187–9196.

Muthusamy, M., Tait, S., Schellart, A., & Beg, M.N.A., (2018). Improving understanding of the underlying physical process of sediment wash-off from urban road surfaces. *Journal*

of Hydrology, 557, 426-433.

Nakic´enovic´, N., & Swart, R. (2000). Special report on emission scenarios. *In Emissions Scenarios; Cambridge University Press: Cambridge, UK*, p. 570.

Narsimlu, B., Gosain, A.K., & Chahar, B.R. (2013). Assessment of future climate change impacts on water resources of Upper Sind River Watershed, India using SWAT model. *Water Resource Management*, 27, 3647-3662.

Nash, J.E., & Sutcliffe, J.V. (1970). River flow forecasting through conceptual models part I—A discussion of principles. *Journal of Hydrology*, 10, 282-290.

Nazari-Sharabian, M., Taheriyoun, M., & Karakouzian, M. (2019). Surface runoff and pollutant load response to urbanization, climate variability, and low impact developments – a case study. *Water Supply* (in press).

Newbold, J.D., Sweeney, B.W., Jackson, J.K., & Kaplan, L.A., (1995). Concentrations and export of solutes from six mountain streams in Northwestern Costa Rica. *Journal of the North American Benthological Society*, 14, 21-37.

Nguyen, H.H., Recknagel, F., & Meyer, W. (2019). Effects of projected urbanization and climate change on flow and nutrient loads of a Mediterranean catchment in South Australia. *Ecohydrology and Hydrobiology*. Vol. 19, Issue. 2: 279-288.

Nguyen, H.H., Recknagel, F., Meyer, W., Frizenschaf, J., Ying, H., & Gibbs, M.S. (2019). Comparison of the alternative models SOURCE and SWAT for predicting catchment streamflow, sediment and nutrient loads under the effect of land use changes. *Science of the Total Environment*, 662, 254-265.

Nhapi, I., Hoko, Z., Siebel, M.A., & Gijzen, H.J., (2002). Assessment of the major water and nutrient flows in the Chivero catchment area, Zimbabwe. *Physics and Chemistry of the Earth*, 27, 783-792.

Oyarzun, C.E., Godoy, R., & Sepulveda, A., (1998). Water and nutrient fluxes in a cool temperate rainforest at the Cordillera de la Costa in southern Chile. *Hydrological Processes*, 12, 1067-1077.

Peng, H., Liu, Y., Wang, H., Gao, X., Chen, Y., & Ma, L. (2016). Urban stormwater forecasting model and drainage optimization based on water environmental capacity. *Environmental Earth Sciences*, 75, 1094.

Pennino, M.J, Kaushal, S.S., Murthy, S.N., Blomquist, J.D., Cornwell, J.C., & Harris, L.A. (2016). Sources and transformations of anthropogenic nitrogen along an urban river-estuarine continuum. *Biogeosciences*, 13:6211-28.

Pettitt, A.N. (1979). A non-parametric approach to the change-point problem. *Applied Statistics*, 28 (2), 126-135.

Phan, L., Herremans, L., Delaplace, D., & Blanc, D., (1994). Modelling urban stormwater pollution: a comparison between British (MOSQITO) and French (FLUPOL) approaches. *The First International Conference on Hydroinformatics*, Delft, Netherlands.

Poelmeans, L. (2010). Coupling urban expansion models and hydrological models: How important are spatial patterns? *Land Use Policy*, 27 (3), 965-975.

Refsgaard, J.C., Auken, E., Bamberg, C.A., Christensen, B.S.B., Clausen, T., Dalgaard, E., Effersø, F., Ernstsen, V., Gertz, F., Hansen, A.L., He, X., Jacobsen, B.H., Jensen, K.H.,

Jørgensen, F., Flindt Jørgensen, L., Koch, J., Nilsson, B., Petersen, C., De Schepper, G., Schamper, C., Sørensen, K.I., Therrien, R., Thirup, C., & Viezzoli, A. (2014). Nitrogen reduction in geologically heterogeneous catchments: a framework for assessing the scale of predictive capability of hydrological models. *Science of the Total Environment*, 468-469, 1278-1288.

Ren, Y.F., Wang, X.K., Ouyang, Z.Y., Zheng, H., Duan, X.N., & Miao, H. (2008). Stormwater runoff quality from different surfaces in an urban catchment in Beijing, China. *Water Environment Research*, 80, 719.

Riha, K.M., Michalski, G., Gallo, E.L., Lohse, K.A., Brooks, P.D., & Meixner, T. (2014). High atmospheric nitrate inputs and nitrogen turnover in semi-arid urban catchments. *Ecosystems*,17:1309-1325.

Rotz, C.A. (2004). Management to reduce nitrogen losses in animal production. Journal of Animal *Science*, 82:119-137.

Russell, M.A., Walling, D.E., Webb, B.W., & Bearne, R., (1998). The composition of nutrient fluxes from contrasting UK river basins. *Hydrological Processes*, 12, 1461-1482.

Russo, B., Sunyer, D., Velasco, M., & Djordjevic, S. (2015). Analysis of extreme flooding events through a calibrated 1D/2D coupled model: The case of Barcelona (Spain). *Journal of Hydroinformatics*, 17, 473-491.

Salles, C., Tournoud, M. G., & Chu, Y. (2008). Estimating nutrient and sediment flood loads in a small Mediterranean river. *Hydrological Processes: An International Journal*, 22(2), 242-253.

Santhi, C., Arnold, J.G., Williams, J.R., Dugas, W.A., Srinivasan, R., & Hauck, L.M. (2001). Validation of the SWAT model on a large river basin with point and nonpoint sources. *Journal of the American Water Resource Association*, 37, 1169-1188.

Schiff, K., Tiefenthaler, L., Bay, S., & Greenstein, D. (2016). Effects of rainfall intensity and duration on the first flush from parking lots. *Water*. 8: 320.

Schneiderman. E., Jarvinen. M., Jennings, E., May, L., Moore, K., Nadan, P., Pierson, D. (2010). Modeling the Effects of Climate Change on Catchment Hydrology with the GWLF Model. In: George G. (eds) The Impact of Climate Change on European Lakes. *Aquatic Ecology Series*,Vol 4. Springer, Dordrecht.

Selbig, W. (2016). Evaluation of leaf removal as a means to reduce nutrient concentrations and loads in urban stormwater. *Science of the Total Environment*, 571: 12-33.

Skop, E., & Sørensen, P.B., (1998). GIS-based modelling of solute fluxes at the catchment scale: a case study of the agricultural contribution to the riverine nitrogen loading in the Vejle Fjord catchment, Denmark. *Ecological Modelling*, 106, 291-310.

Sharma, S., Khan, S.A., Kumar, A., Jha, P.W., & Jindal, T. (2020). Eutrophication risk assessment by estimation of denitrification rate in Yamuna River sediments. *Transaction of the Indian National Academy of Engineering*, 5: 51-60.

Shi, H.Y., Li, T.J., & Wang, G.Q. (2017). Temporal and spatial variations of potential evaporation and the driving mechanism over Tibet during 1961–2001. *Hydrological Sciences Journal*, 62 (9), 1469-1482.

Smith, S.V., Swaney, D.P., Talaue-mcmanus, L., Bartley, J.D., Sandhei, P.T., Mclaughlin, C.J.,

Dupra, V.C, Crossland, C.J., Buddemeier, R.W, Maxwell, B.A., & Wulff, F. (2003). Humans, Hydrology, and the Distribution of Inorganic Nutrient Loading to the Ocean. *Biological Science*, Vol. 53, No. 3, pp. 235-245.

Smith, S.V., Swaney, D.P., Buddemeier, R.W., Scarsbrook, M.R., Weatherhead, M.A., Humborg, C., Eriksson, H., & Hannerz, F., (2005). River nutrient loads and catchment size. *Biogeochemistry*, 75, 83-107.

Smith, V.H., Joye, S.B., & Howarth, R.W. (2006). Eutrophication of freshwater and marine ecosystems. *Limnology and Oceanography*, 51:351-355.

Soller, J., Stephenson, J., Olivieri, K., Downing, J., & Olivieri, A. W. (2005). Evaluation of seasonal scale first flush pollutant loading and implications for urban runoff management. Journal of Environmental Management, 76(4), 309-318.

Statistics Canada. (2021). Canada's population estimates: Sub provincial areas, July 1, 2020. The Daily. https://www150.statcan.gc.ca/n1/daily-quotidien/210114/dq210114a-eng.htm.

Taebi, A., & Droste, R.L. (2004). First flush pollution load of urban stormwater runoff. *Journal of Environmental Engineering and Science*, 3: 301-309.

Tatli, H. (2015). Detecting persistence of meteorological drought via the Hurst exponent. *Meteorological Applications*, 22 (4), 763-769.

Taylor, G.D., Fletcher, T.D., Wong, T.H.F., Breen, P.F., & Duncan, H.P. (2005). Nitrogen composition in urban runoff - implications for stormwater management. *Water Research*, 39:1982-1989.

Tian, H.Y., Xu, R.T., Pan, S.F., Yao, Y.Z., Bian, Z.H., Cai, W.J., Hopkinson, C.S., Justic, D.,

Lohrenz, S., Lu, C.Q., Ren, W., & Yang, J. (2020). Long-term trajectory of nitrogen loading and delivery from Mississippi river basin to the Gulf of Mexico. *Global Biogeochemical cycles*, 34(5).

Tomasko, D.A., Bristol, D.L., & Ott, J.A. (2001). Assessment of Present and Future Nitrogen Loads, Water Quality, and Seagrass (Thalassia testudinum) Depth Distribution in Lemon Bay, Florida. *Estuaries*. Vol. 24, No. 6A, p. 926-938.

Tong, S.Q., Li, Q., Zhang, J.Q., Bao, Y.H., Lusi, A., Ma, Q.Y., Li, X.Q., & Zhang, F. (2018). Spatiotemporal drought variability on the Mongolian Plateau from 1980–2014 based on the SPEI-PM, intensity analysis and Hurst exponent. *Science of the Total Environment*, 615, 1557-1565.

Toor, G.S., Occhipinti, M.L., Yang, Y.Y., Majcherek, T., & Haver, D.O. (2017). Managing urban runoff in residential neighborhoods: nitrogen and phosphorus in lawn irrigation driven runoff. *PLoS ONE*, 12: e0179151.

Treilles, R., Gasperi, J., Saad, M., Tramoy, R., Breton, J., Rabier, A., & Tassin, B. (2021). Abundance, composition and fluxes of plastic debris and other microliter in urban runoff in a suburban catchment of Greater Paris. *Water Research*, 192, 116847.

Turner, R.E. (2002). Element ratios and aquatic food webs. Estuaries, 25: 694–703.

Ullrich, A., & Volk, M. (2010). Influence of different nitrate–N monitoring strategies on load estimation as a base for model calibration and evaluation. *Environmental Monitoring and Assessment*, 171(1–4), 513-527.

USQS data: data.ecology.su.se/models/bed.htm

Valtanen, M., Sillanpaa, M., & Setala, H. (2014). The effects of urbanization on runoff pollutant concentrations, loadings and their seasonal patterns under cold climate. *Water Air Soil Pollution*, 225:1977.

Vanderbilt, K.L., Lajtha, K., & Swanson, F.J., (2002). Biogeochemistry of unpolluted forested watersheds in the Oregon Cascades: temporal patterns of precipitation and stream nitrogen fluxes. *Biogeochemistry*, 62, 87-117.

van der Sterren, M., Rahman, A., & Dennis, G.R. (2012). Implications to stormwater managements as a result of lot scale rainwater tank systems: a case study in Western Sydney, Australia. *Water Science Technology*, 65:1475–82.

Van Liew. M., Feng. S., & Pathak, T. (2013). Assessing climate change impacts on water balance, runoff, and water quality at the field scale for four locations in the heartland. *Transactions of the ASABE*, 56: 833-900.

Van, D. G., Bouwman, A.F., Harrison. J., & Knoop. J.M. (2009). Global nitrogen and phosphate in urban wastewater for the period 1970 to 2050. *Global Biogeochemical Cycle,* 23: 1-19.

Van, L.M.W., Arnold, J.G., Garbrecht, J.D. (2003). Hydrologic simulation on agricultural watersheds: Choosing between two models. *American Society of Agricultural and Biological Engineers*, 46, 1539-1551.

Vaze, J., & Chiew, F.H.S. (2004). Nutrient loads associated with different sediment sizes in urban stormwater and surface pollutants. *Journal of Environmental Engineering ASCE*, 130: 391-396.

Victoria (Australia) data: www.vicwaterdata.net/vicwaterdata

Voutsa, D., Manoli, E., Samara, C., Sofoniou, M., & Stratis, I., (2001). A study of surface water quality in Macedonia, Greece: speciation of nitrogen and phosphorus. *Water, Air, and Soil Pollution*, 129, 13-32.

Wakida, F. T., & Lerner, D. N. (2005). Non-agricultural sources of groundwater nitrate: A review and case study. *Water Research*, 39, 3-16.

Wall, D. (2013). Nitrogen in waters: forms and concerns. nitrogen in minnesota surface waters. *Minnesota Pollution Control Agency.*

Wang, B.D. (2006). Cultural eutrophication in the Changjiang (Yangtze River) plume: history and perspective. *Estuarine, Coastal and Shelf Science*, 69, 471-477.

Wang, H., Yan, H.Y., Zhou, F.N., Li, B., Zhuang, W., & Shen, Y.H. (2020). Changes in nutrient transport from the Yangtze River to the East China Sea linked to the Three-Gorges Dam and water transfer project. *Environmental Pollution*, 256: 113376.

Wang, L., Stuart, M.E., Lewis, M.A., Ward, R.S., Skrivin, D., Naden, P.S., Collins, A.L., & Ascott, M.J. (2016). The changing trend in nitrogen concentrations in major aquifers due to historical nitrogen loading from agricultural land across England and Wales from 1925 to 2150. *Science of the Total Environment*, 542, 694-705.

Wang, M., Zhang, D.Q., Su, J., Trzcinski, A.P., Dong, J.W., & Tan, S.K. (2017). Future scenarios modeling of urban stormwater management response to impacts of climate change and urbanization. *Clean-Soil, Air, Water*, 45, 1700111.

Wang, Y., Luan, Q., Wang, H., Liu, J., & Ma, J., (2019). Risk assessment of rainstorm waterlogging in new district based on MIKE Urban, in: Dong, W., Lian, Y., Zhang, Y.

(Eds.), Sustainable development of water resources and hydraulic engineering in China. *Springer*, Cham, Switzerland, pp. 29-40.

Warwick, J.J., & Wilson, J.S., (1990). Estimating uncertainty of stormwater runoff computations. *Journal of Water Resources Planning and Management*, 116 (2), 187-204.

Waschbusch, R.J., Selbig, W.R., & Bannerman, R.T. (1999). Sources of phosphorus in stormwater and street dirt from two urban residential basins in Madison, Wisconsin, 1994–95: U.S. *Geological Survey Water-Resources Investigations Report*, 99-4021. p. 47.

Wijesiri, B., Egodawatta, P., McGree, J., & Goonetilleke, A., (2015). Process variability of pollutant build-up on urban road surfaces. *Science of the Total Environment*, 518, 434-440.

Williams, M.R., & Melack, J.M., (1997). Atmospheric deposition, mass balances, and processes regulating stream water solute concentrations in mixed- conifer catchments of the Sierra Nevada, California. *Biogeochemistry*, 37, 111-144.

Wu, J., & Malmstrom, M.E. (2015). Nutrient loadings from urban catchments under climate change scenarios: case studies in Stockholm, Sweden. *Science of the Total Environment*, 518–519, 393-406.

Xia, H., Peng, Y., Yan, W., & Ning, W. (2014). Effect of snow depth and snow duration on soil N dynamics and microbial activity in the alpine areas of the eastern Tibetan plateau. *Russian Journal of Ecology*, 45(4): 263-268.

Yan, W., Zhang, S., Chen, X., & Tang, Y., (2005). Nitrogen export by runoff from agricultural plots in two basins in China. *Nutrient Cycling in Agroecosystems*, 71, 121-129.

Yang, W., Wang, Z., Hua, P., Zhang, J., & Krebs, P. (2021). Impact of green infrastructure on the mitigation of road-deposited sediment induced stormwater pollution. *Science of the Total Environment*, 770, 145294.

Yang, X.Y., Liu, Q., Fu, G.T., He, Y., Luo, X.Z., & Zheng, Z. (2016). Spatiotemporal patterns and source attribution of nitrogen load in a river basin with complex pollution sources. *Water Research*, 94: 187-199.

Yang, Y.Y., & Lusk, M.G. (2017). Nutrients in urban stormwater runoff: Current state of the science and potential mitigation options. *Current Pollution Reports*, 4: 112-127.

Yang, Y.Y., & Toor, G.S. (2016). $\delta^{15}N$ and $\delta^{18}O$ reveal the sources of nitrate nitrogen in urban residential stormwater runoff. *Environment Science and Technology*, 50: 2881-2889.

Yazdi. M. N., Sample, D. J., Scott. D., Wang. X. X., & Ketabchy, M. (2021). The effects of land use characteristics on urban stormwater quality and watershed pollutant loads. *Science of the Total Environment*, 773. 145358

Yi, Q., Chen, Q., Hu, L., & Shi, W. (2017). Tracking nitrogen sources, transformation, and transport at a basin scale with complex plain river networks. *Environment Science and Technology*, 51: 5396-5403.

Zafra, C.A., Temprano, J., & Tejero, I., (2008). Particle size distribution of accumulated sediments on an urban road in rainy weather. *Environmental Technology*, 29, 571-582.

Zhang, A.J., Zheng, C.M., Wang, S., & Yao, Y.Y. (2015). Analysis of streamflow variations in the Heihe River Basin, northwest China: Trends, abrupt changes, driving factors and ecological influences. *Journal of Hydrology: Regional Studies*, 3, 106-124.

Zhang, J., Qiao, R.R., Song, Y.Y., & Lai, Y.Q. (2021). Assessing runoff and pollutant loading upstream of the Miyun Reservoir for sustainable water resources management. *Water and Environment Journal*, 1-17.

Zhang, L., Lu, W., An, Y., Li, D., & Gong, L. (2012). Response of Non-Point Source Pollutant Loads to Climate Change in the Shitoukoumen Reservoir Catchment. *Environmental Monitoring and Assessment*, 184, 581-594.

Zhang, Q.Q., Wang. X.K., Hou, P.Q., Wan, W.X., Ren, Y.F., & Ouyang, L.Y. (2013). The temporal changes in road stormwater runoff quality and the implications to first flush control in Chongqing, China. *Environmental Monitoring Assessment*, 185:9763-9775.

Zhang, W., Yan, Y.X., Zheng, J.H., Li, L., Dong, X., & Cai, H.J. (2009). Temporal and spatial variability of annual extreme water level in the Pearl River Delta region, China. *Global and Planetary Change*, 69: 35-47.

Zhang, W.S., Swaney, D.P., Hong, B.H., Howarth, R.W., & Li, X.Y. (2017). Influence of rapid rural-urban population migration on riverine nitrogen pollution: perspective from ammonia-nitrogen. *Environmental Science and Pollution Research*, 24, 27201-27214.

Zhang, X., Wu, Y., & Gu, B. (2015). Urban rivers as hotspots of regional nitrogen pollution. *Environmental Pollution*, 205:139-144.

Zhao, H., Jiang, Q., Ma, Y., Xie, W., Li, X., & Yin, C., (2018). Influence of urban surface roughness on build-up and wash-off dynamics of road-deposited sediment. *Environmental Pollution,* 243, 1226-1234.

Zhang, Z., Fukushima, T., Onda, Y., Gomi, T., Fukuyama, T., Sidle, R., Kosugi, K., &

Matsushige, K., (2007). Nutrient runoff from forested watersheds in central Japan during typhoon storms: implications for understanding runoff mechanisms during storm events. *Hydrological Processes*, 21: 1167-1178.

Zhou, Z. Q., Shi, H. Y., Fu, Q., Li, T. X., Gan, T. Y., & Liu, S. N. (2020). Assessing spatiotemporal characteristics of drought and its effects on T climate-induced yield of maize in Northeast China. *Journal of Hydrology*, 588: 125097.

Zoppou, C., (2001). Review of urban storm water models. Environmental *Modeling and Software*, 16, 195-231.

Appendix

Chapter 2

Tables:

Table A2.1. Worldwide stormwater nitrogen EMC

Country	City	Catchment type/name	Land use	Study time	Sample type	TN (mg/L)	TKN (mg/L)	NO_2-N (mg/L)	NO_3-N (mg/L)	NH_4-N (mg/L)	reference
China	Beijing	Campus road		2005	Stormwater EMC	7.4					(Ren et al. 2008)
		Ring road				13.62					
				2018	Snowmelt EMC	52.23					(Chen et al. 2018)
	Chongqing			2010/6/7	Stormwater EMC	7.03			0.95	1.31	(Zhang et al. 2014)
				2010/6/19		1.98			0.28	0.53	
				2010/7/4		5			1.04	1.4	
				2010/7/9		2.07			1.59	1.31	
				2010/9/13		6.36			3.08	0.31	
				2011/5/30		9.03			4.67	5.14	

		2011/6/5		2.09	1.04	0.75	
		2011/7/11		4.54	3.03	1.26	
		2011/8/4		4.5	2.31	2.07	
Wuhan	road		Stormwater	4.9-6.04			(Li et al. 2012)
	Shilipu	2003/6/23	Stormwater EMC	6.43			
		2003/7/6		10.12			
		2004/6/14		14.63			
		2004/6/23		6.93			
		2005/4/8		56.35			
		2005/5/1		33.58			
		2005/5/17		16.36			
		2005/6/10		27.77			
		2005/6/26		14.62			
		2005/7/10		22.49			

		2005/7/22		13.52				
		2005/8/3		24.09				
Shanghai	Traffic	2004/2/21	Stormwater EMC		0.16	0.23	2.7	(Ballo et al. 2009)
	Industrial				0.31	0.36	4.05	
	Commercial				0.15	0.18	3	
	Residential				0.15	0.37	2.38	
	Traffic	2004/3/21			0.43	0.87	2.05	
	Industrial				0.09	0.25	1.04	
	Commercial				0.17	0.45	0.82	
	Residential				0.24	0.62	2.64	
	Traffic	2004/6/24			0.23	0.34	2.32	
	Industrial				0.17	0.71	1.54	
	Commercial				0.05	0.34	3.34	
	Residential				0.14	0.23	1.09	
Linshan, Sichuan		2006/6-2007/7	Stormwater EMC	21.31				(Luo et al. 2012)
Guangzhou	Highway	2008	Stormwater EMC	7.32				(Huang et al. 2007)
Macau	road	2007	Stormwater EMC	3.58				(Gan et al. 2008)

	Xi’an		road	2012	Snowmelt EMC	0.7			(Li et al. 2012)
Canada	Saskatoon, SK	Sturgeon		2001	Baseflow		0.99		(McLeod et al. 2007)
		Silverwood					1.4		
		Taylor street					1.8		
		Ave B					4		
		Ave B		2001	Stormwater SMC		2.2		
		Taylor street					2.5		
		Silverwood					0.73		
	Broadview, SK			2013	Snowmelt EMC	4.39			(Cade-Menun et al., 2013)
	Assiniboine River Watershed, MB			1996-2003	Snowmelt EMC	2.91			(Henry et al. 2020)
					Stormwater EMC	1.52			
	Vancouver, BC			2003	Stormwater SMC		0.8		(El-Khoury et al. 2015)
	Edmonton, AB			2007-2018	Snowmelt EMC	4.40	3.54	0.97	(This study)
					Stormwater EMC	3.97	3.00	0.50	
Australia	Melbourne		Residential	2004	Stormwater	2.12			(Lucke et al. 2015)

			Commercial	2005		3.44					
					Baseflow	2.17	1.3				
					Stormflow	2.13	1.39				
Iran	Isfahan	Siosepol catchment		1999-2001	Stormwater EMC	6.65					(Taebi and Droste et al. 2004)
Malaysia	Skudai, johor		Commercial	2008/8/12	Stormwater EMC			0.006	1.1	0.2	(Chow et al. 2011)
				2008/8/22				0.004	1.9	1.3	
				2008/8/27				0.008	2	1.3	
				2008/10/10				0.008	0.8	0.6	
				2008/11/12				0.006	0.7	0.7	
				2008/12/31				0.003	2.5	7.2	
South Korea	Soro, Chungbuk			2006	Stormwater EMC	0.71					(Kim et al. 2006)
Japan	Kamihara, Taiki			2007	Stormwater EMC	0.76					(Zhang et al. 2007)
USA	Tampa, FL		Residential	2016	Stormwater	0.96			0.24		(Yang et al. 2016)
				2017		0.42			0.1		
	Tucson Basin, AZ		Urban watershed	2014	Stormwater				0.3-1.1	0.02-0.6	(Riha et al. 2014)
	Phoenix, AZ		Urban watershed	2014	Stormwater EMC				0.16-1.65	0.006-10.13	(Hale et al. 2014)
	Saint Paul, MN		Residential	2017	Stormwater EMC	2.36				0.26	(Janke et al. 2017)

				Snowmelt	4.3					(Bratt et al. 2017)
	Madison, WI	Residential	2016	Stormwater	1.9-3.6					(Selbig et al. 2016)
	Pittsburgh, PA	Urban stream	2014	Stormwater				0.6-1.0		(Divers et al, 2014; Collins et al, 2010)
		Residential		Stormwater	4.84	2.43	0.44	1.71	0.84	
		Commercial			2.91	1.85	0.21	0.52	1.48	
		Industrial			2.23	6.3	0.07	0.92	0.73	
		Institutional			2.25	1.66	0.17	0.37	1.38	
		Freeways			1.7	3.21	0.3	1.85	1.63	
		Open space			1.59	1.64	0.04	0.75	0.73	
Finland	Lahti		2014	Snowmelt EMC	2.92					(Valtanen et al. 2014)
				Stormwater EMC	1.31					
Sweden	Ostersund		2012-2014	Snowmelt EMC	1.63					(Galfi et al. 2016)
				Stormwater EMC	1.15					

Table A2.2. Annual TN and NO_3-N loadings in different countries (unit: kg N/km^2 yr^{-1})

Continent	Country	n (number of observations)	TN range	TN average	NO_3-N range	NO_3-N average	Reference
Oceania	Australia	75	1-4758	361	0.02-3937	177	(Victoria; Smith et al. 2005; Caraco and Cole, 1999; McKergow et al. 2003; Moss et al. 1992; McKee and Eyre, 2000)
	Nauru	1			2	2	(Smith et al. 2005)
	New Zealand	6	180	180	45-643	246	(Smith et al. 2005)
North America	USA	361	1-11147	803	0.23-10645	490	(USGS)
	Canada	35	58-90	71	0.45-758	35	(Smith et al. 2005; Caraco and Cole, 1999; Behrendt and Opitz, 2000; Cooke and Prepas, 1998; Clair et al. 1994)
	Mexico	10			8-104	29	(Smith et al. 2005)
This study	Canada	28	24-945	348	5-396	118	
South America	Argentina	3	50	50	31	31	(Smith et al. 2005; Caraco and Cole, 1999),
	Brazil	27	147-4667	1236	0.14-254	101	(Smith et al. 2005; McDowell and Asbury, 1994; Filoso et al. 2003]
	Chile	2			36-69	53	(Smith et al. 2005; Oyarzun et al. 1998)
	Colombia	5	235-860	547.5	16-204	123	(Smith et al. 200; Lewis et al. 1998)
	Costa Rica	8			8-610	369	(Newbold et al. 1995)
	Ecuador	2			37-114	76	(Smith et al. 2005)
	Puerto Rico	4	360-556	486.5	75-140	109	(Lewis et al. 1998; McDowell and Asbury, 1994]

	New Guinea	1			38	38	(Smith et al. 2005)
Europe	Austria	7			60-2500	1406	(Behrendt and Opitz, 2000)
	Denmark	25	900-3800	241	1068	1068	(Anderson et al. 2001; Kronvang et al. 1999; Skop and Sorensen, 1998; Krug, 1993)
	Estonia	6	114-1800	983.2	8-1567	364.5	(NEST; Smith et al. 2005; Mander et al. 2000)
	Finland	41	168-.3494	640	6-623	93	(NEST; Behrendt and Opitz, 2000, Arheimer et al. 1996)
	France	7	491-727	609	189-1443	1028.4	(Smith et al. 2005; Caraco and Cole, 1999; Behrendt and Opitz, 2000)
	Germany	24	153-1520	864	244-3062	1375	(Smith et al. 2005; Caraco and Cole, 1999; Behrendt and Opitz, 2000)
	Greece	2	75	75	43	43	(Smith et al. 2005; Voutsa et al. 2001)
	Ireland	2			30-697	363.5	(Smith et al. 2005)
	Italy	36	587-4550	2057	4-2716	998	(Smith et al. 2005; Marchetti and Verna, 1992; Mosello et al. 2001)
	Latvia	4	371-695	503	44-104	70	(NEST)
	Lithuania	4	167-581	362	19-90	40	(NEST; Smith et al. 2005)
	Norway	8	73-4870	1462			(Caraco and Cole, 1999; Hoyas et al. 1997)
	Poland	11	531-553	542	67-628	265	(NEST; Smith et al. 2005; Behrendt and Opitz, 2000)
	Russia	10	3-230	123	0.41-17	4.8	(NEST; Smith et al. 2005; Caraco and Cole, 1999)
	Spain	56	5-20630	1553	5-3667	542	(Alvarez-Cobelas et al. 2008)
	Sweden	57	8-692	229	3-596	44.5	(NEST; Smith et al. 2005; Behrendt and Opitz,

							2000, Arheimer et al. 1996)
	Switzerland	9			683-3150	1422	(Behrendt and Opitz, 2000)
	Ukraine	5			5-54	28.4	(Smith et al. 2005)
	United Kingdom	21	300-5173	2224	4-3404	1783	(Smith et al. 2005; Caraco and Cole, 1999; House et al. 1997; Russell et al. 1998; Jones et al. 2005)
Asia	China	13	235-4220	1352	5-184	95	(Smith et al. 2005; Caraco and Cole, 1999; Yan et al. 2005; Gao et al. 2004; Cao et al. 2006)
	India	3	198	198	9-160	73	(Smith et al. 2005; Caraco and Cole, 1999)
	Indonesia	5			6-2220	501.2	(Smith et al. 2005)
	Taiwan, China	3			39-1848	690	(Smith et al. 2005)
	Thailand	7			6-272	55	(Smith et al. 2005)
	Japan	5			761-3590	2042	(Smith et al. 2005)
	South Korea	2			250-746	498	(Smith et al. 2005)
	Malaysia	1			104	104	(Smith et al. 2005)
	Philippines	10			8-512	150	(Smith et al. 2005)
Africa	Cameroon	2			21-44	33	(Smith et al. 2005)
	Ghana	1			4	4	(Smith et al. 2005)
	Kenya	2			0.32-14	7.16	(Smith et al. 2005)
	Morocco	1			153	153	(Smith et al. 2005)
	Nigeria	1	21	21	68	68	(Smith et al. 2005)

	South Africa	8	4	4	0.21-180	29	(Smith et al. 2005; Caraco and Cole, 1999)

Figures

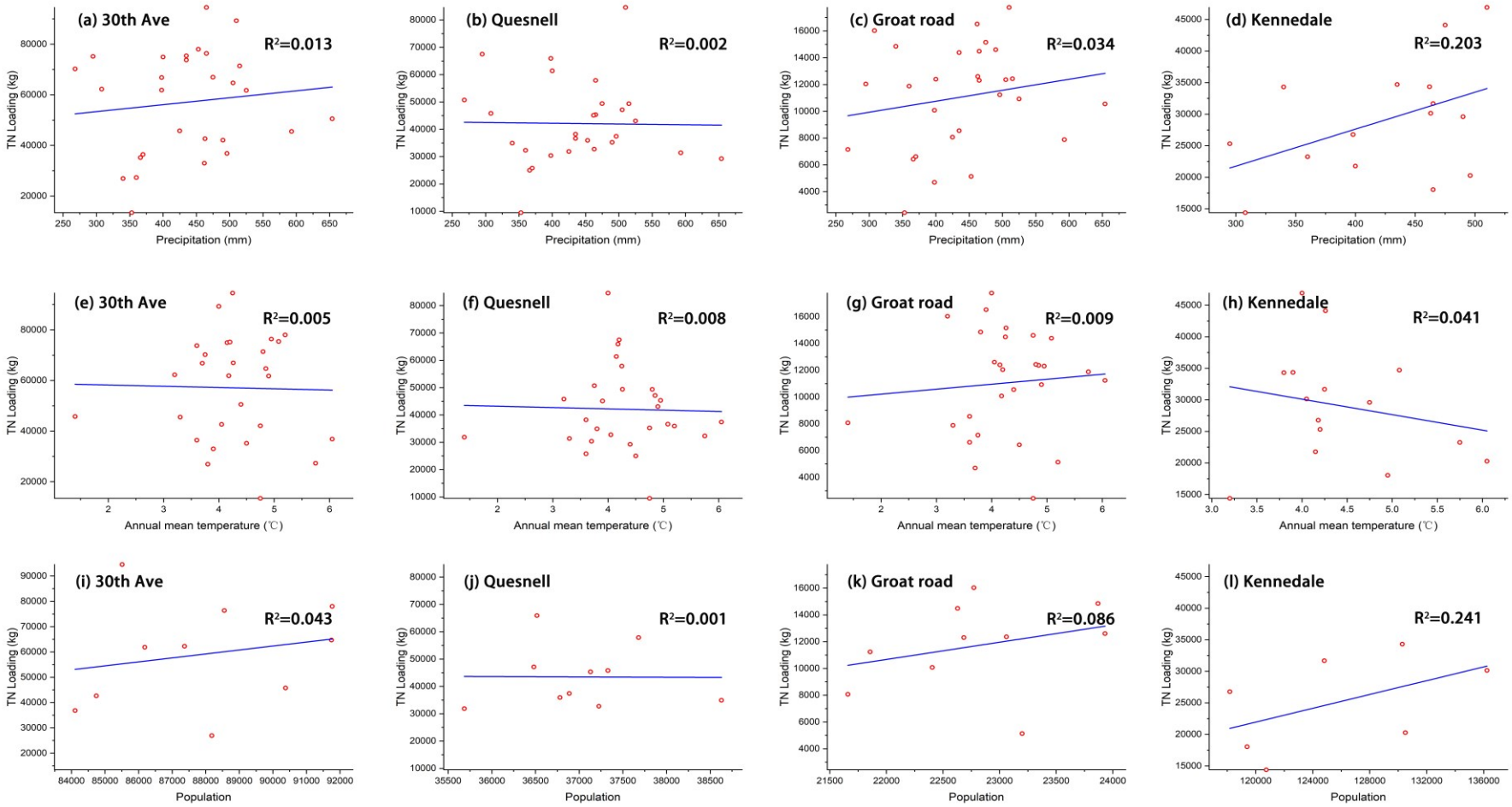

Figure A2.1 Correlation between precipitation, temperature and population with TN loading at four outfalls.

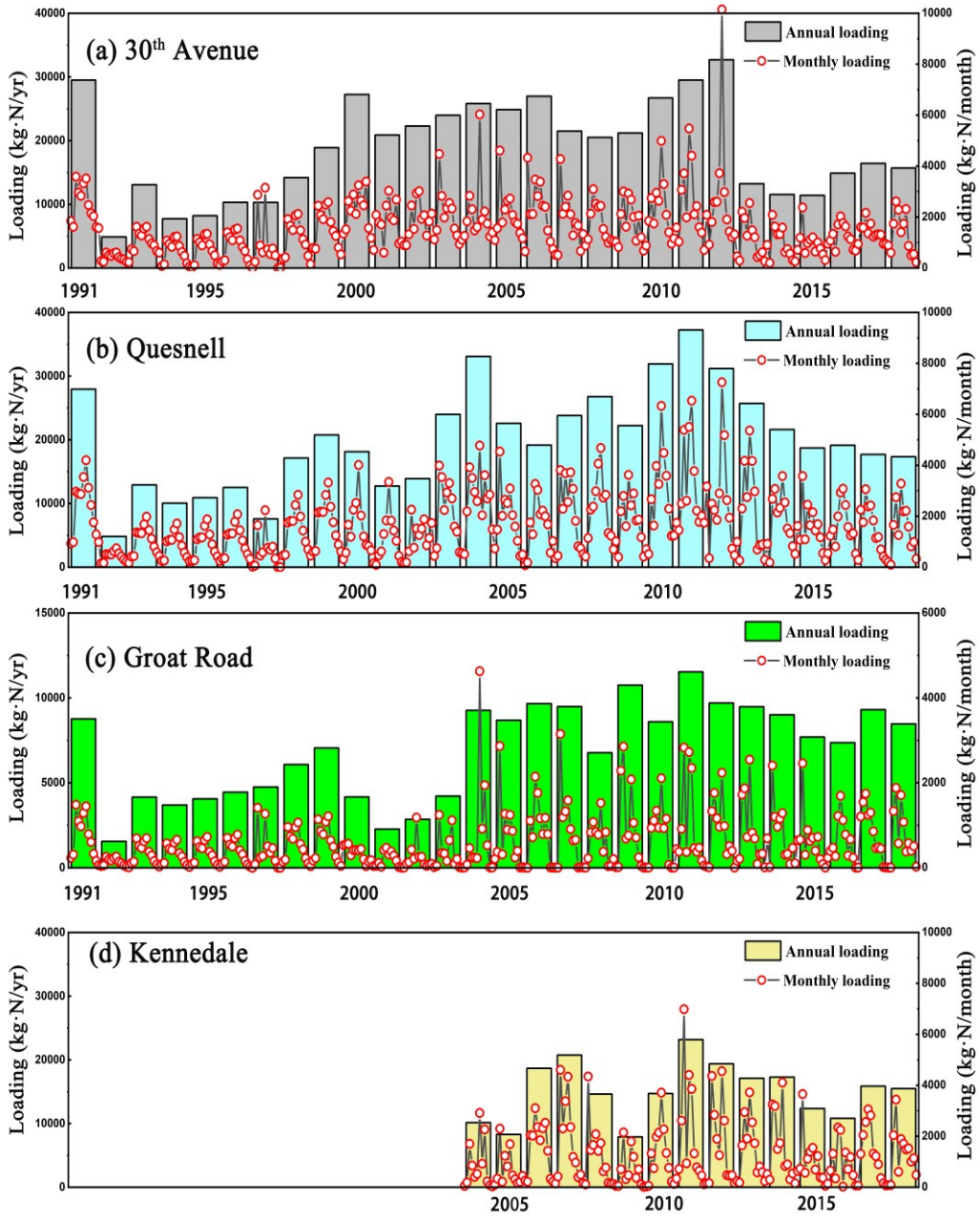

Figure A2.2 Annual and monthly total organic nitrogen (TON) loadings at the four storm outfalls: **(a)** the 30th avenue outfall; **(b)** the Quesnell outfall; **(c)** the Groat Road outfall; **(d)** the Kennedale outfall.

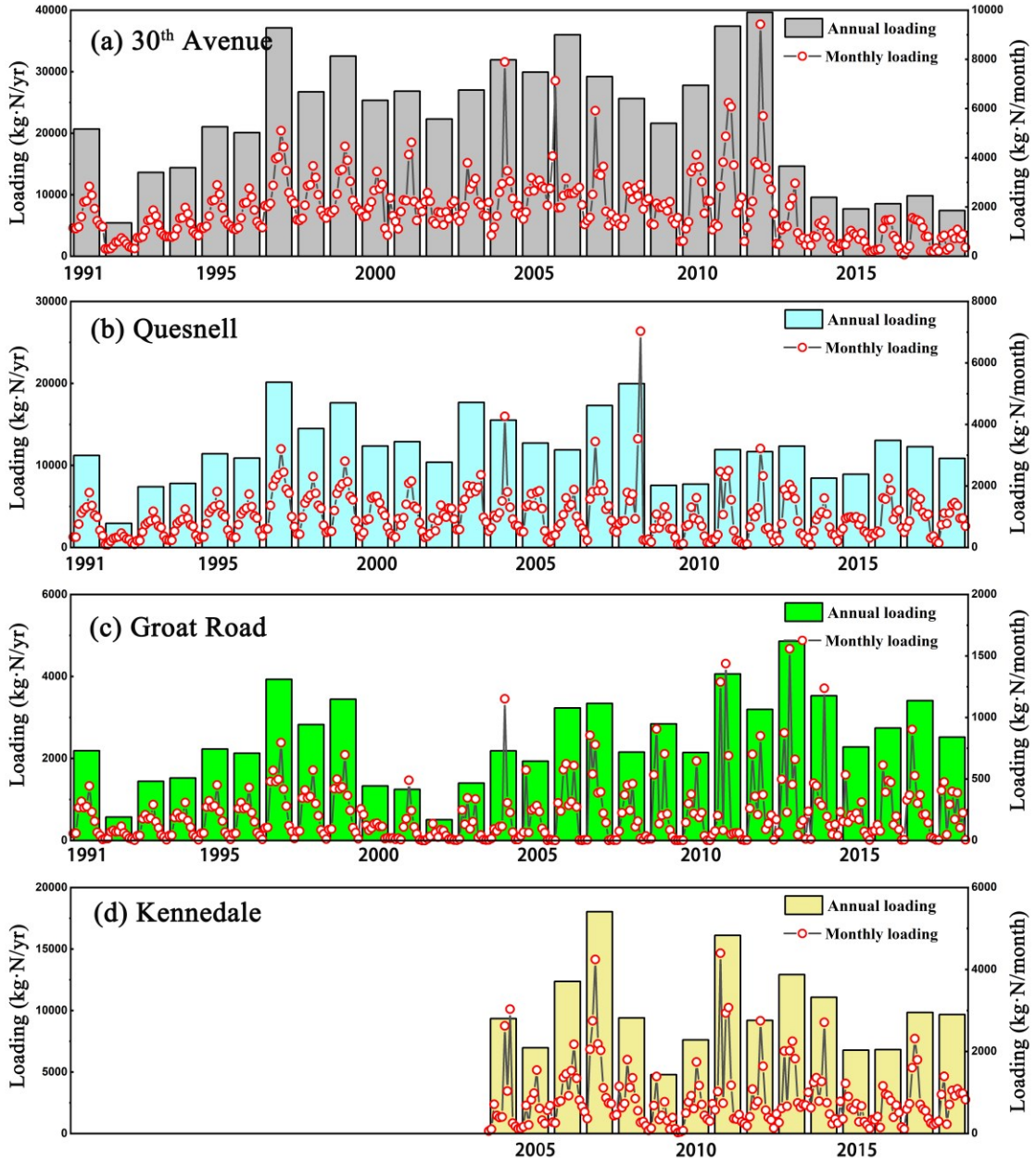

Figure A2.3 Annual and monthly nitrite and nitrate (NO_x-N) loadings at the four storm outfalls: **(a)** the 30th avenue outfall; **(b)** the Quesnell outfall; **(c)** the Groat Road outfall; **(d)** the Kennedale outfall.

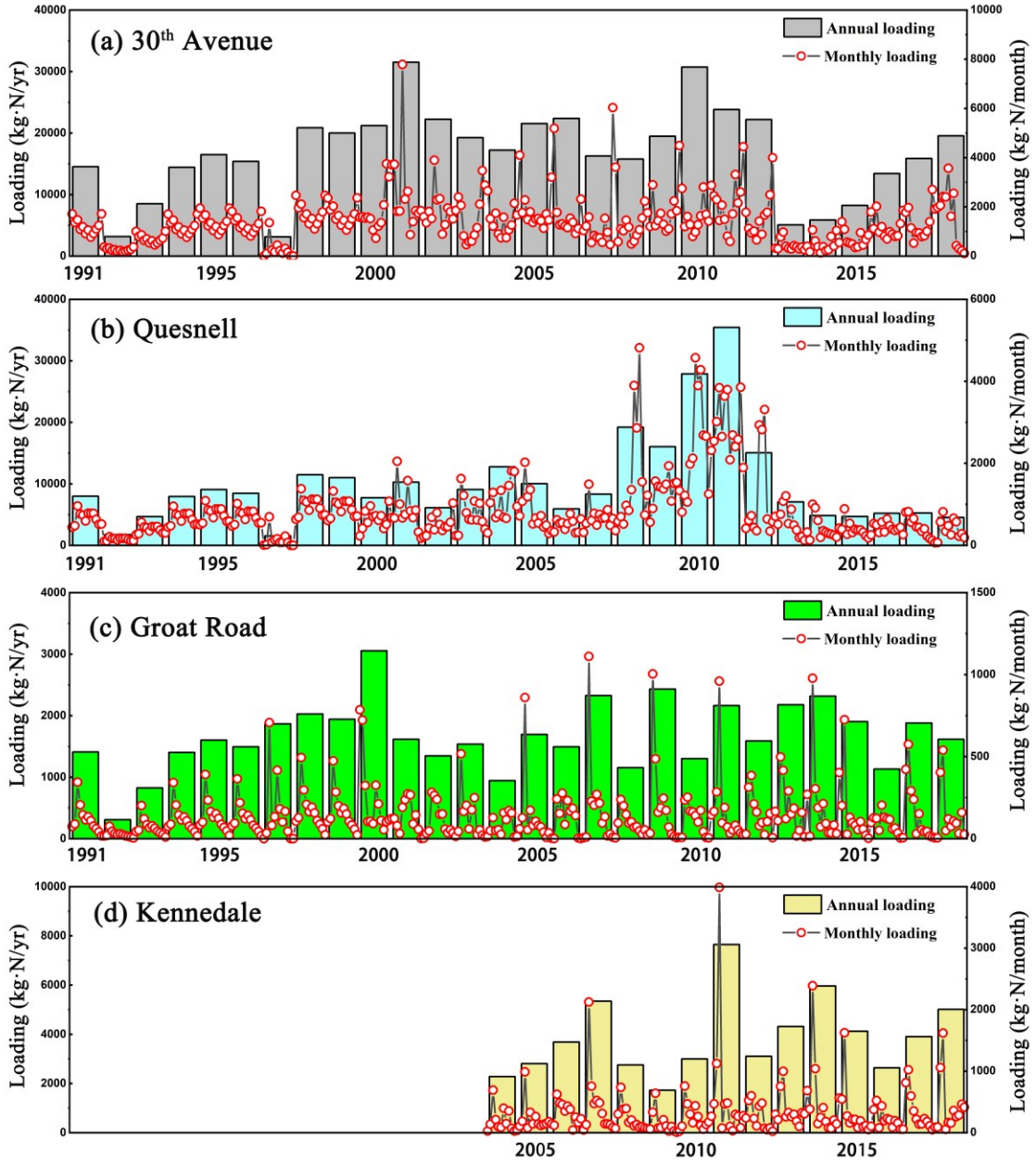

Figure A2.4 Annual and monthly ammonium (NH_4-N) loadings at the four storm outfalls: **(a)** the 30th avenue outfall; **(b)** the Quesnell outfall; **(c)** the Groat Road outfall; **(d)** the Kennedale outfall.

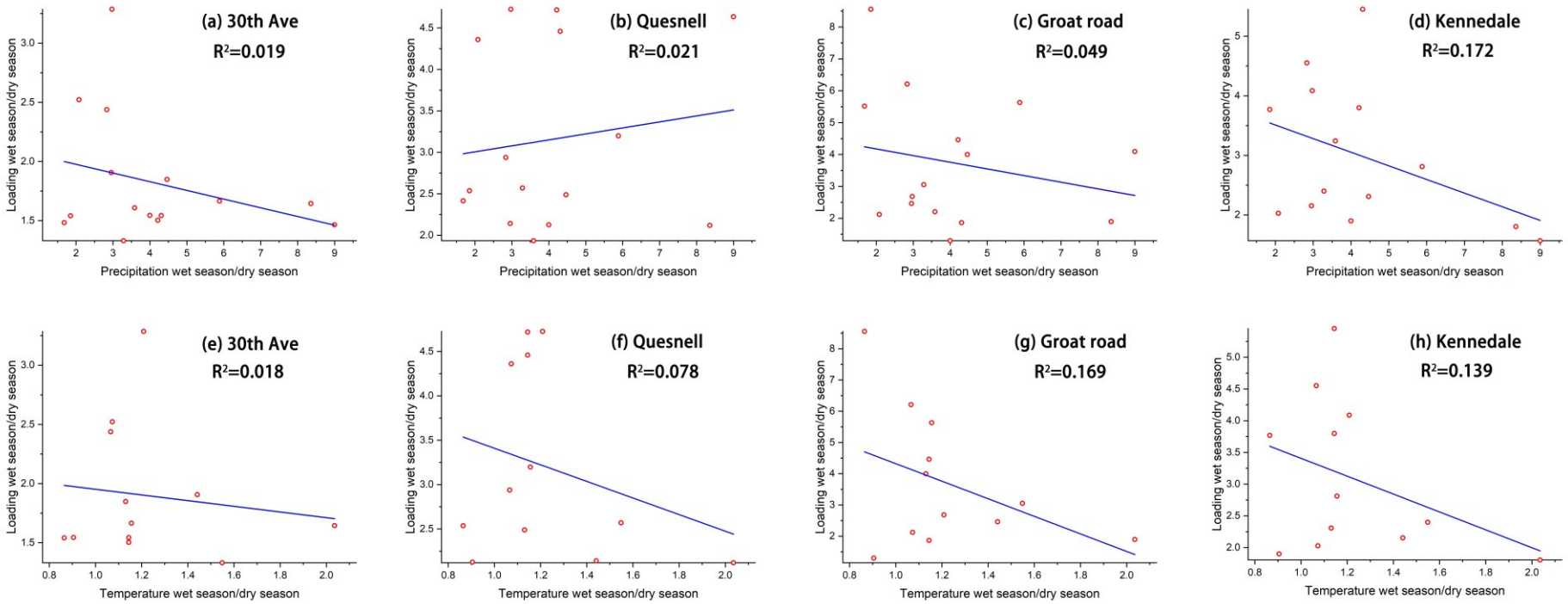

Figure A2.5 Correlation between ratios of precipitation and temperature in wet season to dry season with loading ratio**.**

Algorithms:

Codes for the three test methods are developed in MATLAB.

Algorithms 1.1 Code for Mann-Kendall test

```
function [UF,UB]=KendallRS(x,TIME)
time=(0:length(x)-1);
n=length(x);
[rows,cols]=size(x);
%---------JUDGEMENT OF TIME SERIES------------
if rows==1
    error('x should be a column vector')
end
if cols~=1
    error('x should be a column vector')
end
% -----------------COMPUTATION IN NORMAL SEQUENCY--------------------
for k=2:n
    count1=0;
    for j=1:k-1
      if x(k)>x(j)
         count1=count1+1;
      end
      %mean=k*(k-1)/4;
     %variance=k*(k-1)*(2*k+5)/72;
      %z(1,1)=0;
     % z(k,1)=(count1-mean)/sqrt(variance);
    end
      ES1(k,1)=k*(k-1)/4;
      VAR1(k,1)=k*(k-1)*(2*k+5)/72;
      zonghe1(1,1)=0;
      zonghe1(k,1)=count1;
```

```
end
%------------------COMPUTATION IN ADVERSE SEQUENCY----------------
x1=flipud(x);
for m=2:n
    count2=0;
    for i=1:m-1
      if x1(m)>x1(i)
        count2=count2+1;
      end
      %mean=m*(m-1)/4;
      % variance =m*(m-1)*(2*m+5)/72;
      %z(1,2)=0;
      %z(m,2)=(count-mean)/sqrt(variance);
    end
      ES2(m,1)=m*(m-1)/4;
      VAR2(m,1)=m*(m-1)*(2*m+5)/72;
      zonghe2(1,1)=0;
      zonghe2(m,1)=count2;
end
%-----------------------autocorrelation analysis-----------------------
kkk = fix(n/3);
for ii = 0:kkk;
    rr(ii+1) = sum(((x(1:n-ii,1)-mean(x))/std(x)).*((x(1+ii:n,1)-mean(x))/std(x)))/(n-ii);
end
%---------------confidence level for autocorrelation coefficient--------
for jj = 0:kkk
    pk(jj+1) = length(x(1:n-jj));
end
lower = (-1-1.96*(pk-2).^0.5)./(pk-1);
upper = (-1+1.96*(pk-2).^0.5)./(pk-1);
%----------calculate adjustment factor----------------
adjust=1+2*(rr(2)^(n+1)-n*rr(2)^2+(n-1)*rr(2))/(n*(rr(2)-1)^2);
```

```
%-----------the adjustment factor is calculated-----------
if rr(2)>upper(2)
%-------------------- Z2 and Z1 value computation ----------------
ES1(1,1)=0;
VAR1(1,1)=0;
UF(1,1)=0;
zonghe1=cumsum(zonghe1);
UF(2:n,1)=(zonghe1(2:end)-ES1(2:end))./sqrt(VAR1(2:end)*adjust);
%%      UB value      %%
UB(1,1)=0;
ES2(1,1)=0;
VAR2(1,1)=0;
zonghe2=cumsum(zonghe2);
UB(2:n,1)=(zonghe2(2:end)-ES2(2:end))./sqrt(VAR2(2:end)*adjust);
else
ES1(1,1)=0;
VAR1(1,1)=0;
UF(1,1)=0;
zonghe1=cumsum(zonghe1);
UF(2:n,1)=(zonghe1(2:end)-ES1(2:end))./sqrt(VAR1(2:end));
%%      UB value      %%
ES2(1,1)=0;
VAR2(1,1)=0;
UB(1,1)=0;
zonghe2=cumsum(zonghe2);
UB(2:n,1)=(zonghe2(2:end)-ES2(2:end))./sqrt(VAR2(2:end));
end
UB(2:n,1)=flipud(UB(2:n,1));
UB(:,1)=-UB(:,1);
%----------------PLOT------------------
figure(1)
plot(time,UF(:,1),'o-r','linewidth',1,'MarkerSize',3) ;
```

```
hold on
plot(time,UB(:,1),'o-b','linewidth',1,'MarkerSize',3) ;
hold on
plot(time,ones(size(time))*1.96, ':','linewidth',1) ;
xr=[min(time):365:max(time)];
xt=[ 1991 1992 1993 1994 1995 1996 1997 1998 1999 2000 2001 2002 003 2004 2005 2006
2007 2008 2009 2010 2011 2012 2013 2014 2015 2016 2017 2018];
xt=TIME;
set(gca,'xtick',xr);
set(gca,'XTickLabel',xt);
axis([min(time) ,max(time)+2 ,-4 ,5]);
title('NH4-N 的 Mann-Kendall 分析');
legend('UF statistic value','UB statistic value ','0.05 significance level',4);
plot(time,zeros(size(time)),'-.','linewidth',1) ;
plot(time,ones(size(time))*1.96, ':','linewidth',1) ;
plot(time,-1.96*ones(size(time)), ':','linewidth',1) ;
hold off
xlabel('Time (year)','FontSize',12) ;
ylabel('statistical result','FontSize',12) ;
```

Algorithms 1.2 Code for Pettitt test

```
% This code is used to find the change point in a univariate continuous time series
% using Pettitt Test.
% The test here assumed is two-tailed test. The hypothesis are as follow:
% H (Null Hypothesis): There is no change point in the series
% H (Alternative Hypothesis): There is a change point in the series
% Input: univariate data series
% Output:
% The output of the answer in row wise respectively,
% loc: location of the change point in the series, index value in
% the data set
% K: Pettitt Test Statistic for two tail test
% pvalue: p-value of the test
%Reference: Pohlert, Thorsten. "Non-Parametric Trend Tests and Change-Point Detection." (2016).
function a=pettitt_changeplot(data)
[m n]=size(data);
for t=2:1:m
      for j=1:1:m
         v(t-1,j)=sign(data(t-1,2)-data(j,2));
         V(t-1)=sum(v(t-1,:));
      end
end
U=cumsum(V);
loc=find(abs(U)==max(abs(U)));
K=max(abs(U));
pvalue=2*exp((-6*K^2)/(m^3+m^2));
a=[loc; K ;pvalue];
pvalue2=exp((-3*K^2)/(m^3+m^2));
figure('color',[1 1 1])
hold on
plot(data(2:m,1),U,'k-','linewidth',1.5);
```

```
plot([data(loc+1,1),data(loc+1,1)],[-K,K],'r--','linewidth',1.5);
plim = 0.5;
klim = sqrt(log(plim/2)*(m^3+m^2)/-6);
plot([data(1,1),data(m,1)],[-klim,-klim],'b-.');
plot([data(1,1),data(m,1)],[klim,klim],'b-.');
plim = 0.05;
klim = sqrt(log(plim/2)*(m^3+m^2)/-6);
plot([data(1,1),data(m,1)],[-klim,-klim],'b--');
plot([data(1,1),data(m,1)],[klim,klim],'b--');
plim = 0.01;
klim = sqrt(log(plim/2)*(m^3+m^2)/-6);
plot([data(1,1),data(m,1)],[-klim,-klim],'b:');
plot([data(1,1),data(m,1)],[klim,klim],'b:');
legend('UT','T0','p<0.5','p<0.05','p<0.01');
hold off
return
```

Algorithms 1.3 Code for Rescale Range

```
X=xlsread;
X=X';
dd=ceil(length(X));
n=2:5:dd;
N=max(size(X));
A=floor(N./n);
for i=1:max(size(A) )
    RR=X(:,1:A(i)*n(i));
    XX{i}=reshape(RR,n(i),A(i));
    pjz{i}=mean(XX{i},1);
end
for k=1:1:max(size(A) )
    [m,n]=size(XX{k});
    for i=1:m
        for j=1:n
            LC{k}(i,j)=XX{k}(i,j)-pjz{k}(1,j);
        end
    end
    Z{k}=cumsum(LC{k},1);
    R{k}=max(Z{k})-min(Z{k});
    SD{k}=std(XX{k},1,1);
for k=1:max(size(A))
    [p,q]=size(SD{k});
    for i=1:p
        for j=1:q
            R_S{k}(i,j)=R{k}(i,j)/SD{k}(i,j);
            R_S{k}=R{k}./SD{k};
        end
    end
end
```

```
for k=1:max(size(A))
    R_S_mean(k)=mean(R_S{k});
end
count=1;
for k=1:max(size( R_S_mean))
    if isnan(R_S_mean(k))~=1
        R_S_average(count)=R_S_mean(k);
        nn(count)=k;
        count=count+1;
    end
end
k=1;
while k<=max(size(R_S_average))
    LOG_R_S(k)=log(R_S_average(k));
    LOG_n(k)=log(nn(k));
    k=k+1;
end
RC=polyfit(LOG_n,LOG_R_S,1);%Regression Coefficient
%[B,BINT,R,RINT,STATS] = regress(LOG_R_S',LOG_n')
H=RC(1);
if H>=1
    H=floor(H)
end
plot(LOG_n,LOG_R_S,'bo')
hold on
fc=polyval(RC,LOG_n);
plot(LOG_n,fc,'r-');
xlabel('log10(N)');
ylabel('log10(R/S)');
title('R/S method');
legend('Calculated Value','Fitting Result',4)
text(LOG_n(floor(count*1/4)),fc(floor(count*1/2)),.....
```

```
        sprintf('y=%.4f+%.4f*x',RC(2),H), 'interpreter',.....
        'latex','FontSize', 15,'FontWeight','bold')
[B,BINT,R,RINT,STATS] = regress(LOG_R_S',LOG_n');
text(LOG_n(floor(count*1/2)),fc(floor(count*1/2)),.....
        sprintf('R^2=%0.4f',STATS(1)), 'interpreter',.....
        'latex','FontSize', 15,'FontWeight','bold')
```